

INVESTIGATION OF EFFECTS OF HYPERLIPIDEMIA ON IRE1 α AND
INSULIN SIGNALING PATHWAY IN THE CEREBRAL CORTEX OF APOE^{-/-}
MICE

A THESIS SUBMITTED TO
THE GRADUATE SCHOOL OF NATURAL AND APPLIED SCIENCES
OF
MIDDLE EAST TECHNICAL UNIVERSITY

BY

DENİZ AK

IN PARTIAL FULFILLMENT OF THE REQUIREMENTS
FOR
THE DEGREE OF MASTER OF SCIENCE
IN
MOLECULAR BIOLOGY AND GENETICS

JANUARY 2022

Approval of the thesis:

**INVESTIGATION OF EFFECTS OF HYPERLIPIDEMIA ON IRE1 α AND
INSULIN PATHWAY IN THE CEREBRAL CORTEX OF APOE^{-/-} MICE**

submitted by **DENİZ AK** in partial fulfillment of the requirements for the degree of
**Master of Science in Molecular Biology and Genetics, Middle East Technical
University** by,

Prof. Dr. Halil Kalıpçılar
Dean, Graduate School of **Natural and Applied Sciences** _____

Prof. Dr. Ayşe Gül Gözen
Head of the Department, **Molecular Biology and Genetics** _____

Assoc. Prof. Dr. Tülin Yanık
Supervisor, **Molecular Biology and Genetics, METU** _____

Examining Committee Members:

Assoc. Prof. Dr. Çağdaş Devrim Son
METU, Biological Sciences _____

Assoc. Prof. Dr. Tülin Yanık
Molecular Biology and Genetics, METU _____

Prof. Dr. Michelle Adams
Psychology, Bilkent University _____

Date: 20.01.2022

I hereby declare that all information in this document has been obtained and presented in accordance with academic rules and ethical conduct. I also declare that, as required by these rules and conduct, I have fully cited and referenced all material and results that are not original to this work.

Name Last name : Deniz Ak

Signature :

ABSTRACT

INVESTIGATION OF EFFECTS OF HYPERLIPIDEMIA ON IRE1 α AND INSULIN PATHWAY IN THE CEREBRAL CORTEX OF APOE^{-/-} MICE

Ak, Deniz
Master of Science, Molecular Biology and Genetics
Supervisor: Assoc. Prof. Dr. Tülin Yank

January 2022, 90 pages

Obesity prevalence increases worldwide. The most crucial reason for obesity is high-fat diet (HFD). Serum fatty acid levels are increased with HFD, inducing inflammation and glucose homeostasis disruption, leading to insulin signaling impairment linked to metabolic and neurodegenerative disorders in the brain. Glucose uptake of the cells is regulated by insulin through insulin receptor substrate (IRS) proteins, and disruption of this pathway results in insulin resistance. Hyperlipidemia, a lipid metabolism disorder associated with obesity, is the risk factor for neurodegenerative disorders. Therefore, it is crucial to elucidate the underlying cellular mechanisms of hyperlipidemia.

Cellular stress and inflammatory response were accompanied by obesity. Although the stress origin has not been revealed yet, endoplasmic reticulum (ER) is linked with the stress response. The association between HFD and ER stress activation in rodents is well studied: moreover, ERS and insulin signaling impairment was substantially investigated in the hippocampus and frontal cortex of obese rats.

In this study, the effects of high cholesterol diet along with HFD were examined on the activation of the IRE1 α and insulin signaling pathway through the JNK/IRS/Akt

pathway in the cortex of both C57BL/6 and ApoE^{-/-} mice using Western blot analysis. Results indicated that there was not any statistically significant change in the insulin receptor- β (IR- β) expression in both groups. However, IRE1 α /JNK/IRS-1/Akt pathway activation was increased in ApoE^{-/-} mice with chow diet. Although IRE1 α activation and stress status of the cells increased with impaired IRS-1 activation in ApoE^{-/-} mice, there was no direct conclusion for the insulin signaling impairment.

Keywords: Hyperlipidemia, ApoE^{-/-} mice, cortex, ERS, IRE1 α

ÖZ

HİPERLİPİDEMİNİN APOE^{-/-} FARELERİNİN SEREBRAL KORTEKSİNDE IRE1 α VE İNSÜLİN SİNYALİ YOLAKLARINA ETKİSİNİN ARAŞTIRILMASI

Ak, Deniz

Yüksek Lisans, Moleküler Biyoloji ve Genetik
Tez Yöneticisi: Doç. Dr. Tülin Yanık

Ocak 2022, 90 sayfa

Obezite prevalansı dünya çapında artmaktadır. Yüksek yağlı diyet (YYD) obezite oluşumunda en önemli nedendir. YYD ile serum yağ asidi seviyeleri yükseldiğinde inflamasyonun indüklenmesi ve glikoz dengesinin bozulması, insülin yolaklarının bozukluğuna neden olur. İnsülin sinyal yolaklarının bozulması, beyinde metabolik ve nörodejeneratif hastalıklarla ilişkilidir. Hücrelere glikoz alımı, insülin tarafından insülin reseptör substrat (IRS) proteinleri aracılığıyla düzenlenir. Bu yolağın bozulması insülin direnci ile sonuçlanır. Obeziteyle ilişkili bir lipit metabolizması bozukluğu olan hiperlipidemi, nörodejeneratif bozukluklar için risk faktörüdür. Bu nedenle, hiperlipideminin altında yatan mekanizmaların aydınlatılması önemlidir.

Hücrel stres ve inflamatuvar yanıtta obezite eşlik eder. Stresin kaynağı henüz ortaya çıkarılmamış olsa da endoplazmik retikulum (ER) stres yanıtıyla bağlantılıdır. Kemirgenlerde, YYD ve ER stres aktivasyonu arasındaki ilişki iyi çalışılmıştır; ayrıca, obez sıçanların hipokampus ve kortekslerinde ER stres ve insülin yolağı bozukluğu önemli ölçüde gösterilmiştir. Bu çalışmamızda, yüksek yağ/yüksek kolesterol (YY/YK) diyetin C57BL/6 ve ApoE^{-/-} farelerin korteksinde IRE1 α aktivasyonuna ve JNK/IRS/Akt sinyali üzerinden insülin yolağına etkisi

gösterilmiştir. Sonuçlarımıza göre kortekste insülin reseptör β (IR- β) ifadesinde istatistiksel bir deęişiklik gözlemlenmiştir. Bununla birlikte, ApoE^{-/-} farelerinde standart diyet ile IRE1 α /JNK/IRS-1/Akt aktivasyonunun arttığı gösterilmiştir. ApoE^{-/-} farelerinde IRE1 α aktivasyonu ve hücrelerde stres statüsü ile bozulmuş IRS-1 aktivasyonu artmış olmasına rağmen, insülin sinyal bozukluğu için doğrudan bir sonuç yoktur.

Anahtar Kelimeler: Hiperlipidemi, ApoE^{-/-} fareleri, korteks, ERS, IRE1 α

To my family

ACKNOWLEDGMENTS

I would like to express my deepest gratitude to my supervisor, Assoc. Prof. Dr. Tülin Yanık for her guidance, advise, useful criticism, and encouragement throughout the study.

I would like to thank the members of my thesis committee, Prof. Dr. Michelle Adams, and Assoc. Prof. Dr. Çağdaş Devrim Son, for their valuable time, comments, and contributions as members of my thesis jury. I would like to further thank Prof. Dr. Michelle Adams for her experimental support for this study.

I would like to thank Assoc. Prof. Dr. Ebru Erbay for this project and her financial support from European Molecular Biology Organization (EMBO). I would like to express my gratitude to her lab members; Begüm Kocatürk, İnci Ona, Aslı Ekin Doğan, and Zehra Yıldırım for the maintenance of animals and their technical support.

I would like to express my heartfelt gratitude to Naz Mengi for her patience, continued advise and friendship. You have my most sincere appreciation for your contributions to my thesis. I would like to thank the members of Yanık Lab; Didem Mimirolu, Seyda Durhan and Orhan Ekşi for their endless support and memorable memories throughout my time in the lab.

Finally, I cannot thank enough to my parents for their love, understanding, patience, and endless support. Additionally, I wish to thank my lovely friends; Eda Akyıldız, Didem Mimirolu, Naz Mengi, Merve Akkulak, Özlem Durukan, Büşra Bınarcı for their friendship. You are always there for me for the good times and the bad times. I would like to thank my old but gold friends Tuğçe Şengül, Melike Can, Hande Basırlı, Tuğçe Kızılırmak for their friendship and support. Lastly, I would like to thank Deniz Çabuk for his patience, support, and endless love. I am very lucky to have you.

TABLE OF CONTENTS

ABSTRACT.....	v
ÖZ	vii
ACKNOWLEDGMENTS	x
TABLE OF CONTENTS.....	xi
LIST OF TABLES	xiv
LIST OF FIGURES	xv
LIST OF ABBREVIATIONS.....	xvii
CHAPTERS	
INTRODUCTION	1
1.1 Obesity	1
1.2 Hyperlipidemia.....	3
1.2.1 Hyperlipidemia Model: ApoE ^{-/-} Mice.....	5
1.2.2 High Fat/Cholesterol (HF/HC) Diet Effect on Brain.....	6
1.3 The brain as an Insulin Sensitive Organ.....	7
1.4 Insulin Transport to the Brain	7
1.5 Insulin Activity in Central Nervous System	9
1.6 Insulin Receptor	10
1.6.1 Insulin Receptor Signaling.....	11
1.6.2 Impairment in Insulin Signaling in CNS	13
1.7 Endoplasmic Reticulum Stress (ERS).....	16
1.7.1 Unfolded Protein Response (UPR)	18
1.8 Activation of IRE1 α	21
1.9 IRE1 α Effects on Chronic Metabolic Diseases.....	23

1.10	c-Jun N-terminal Kinases (JNK)	25
1.11	The Aim of this Study	26
MATERIALS AND METHODS		29
2.1	Ethics, Animal Subjects and Diets	29
2.2	Dissections	30
2.3	Homogenization of Cortex Tissues	31
2.4	Protein Isolation from Cortex Tissues	31
2.5	Bradford Assay	32
2.6	Western Blot	33
2.6.1	Protein Samples Preparation	33
2.6.2	SDS-PAGE Gel Preparation	34
2.6.3	Running SDS-PAGE Gels	35
2.6.4	Blotting: Transfer of Proteins to PVDF Membranes	35
2.6.5	Blocking, Primary and Secondary Antibody Detection	36
2.6.6	Chemiluminescent Detection	37
2.6.7	Band Intensity Quantification	38
2.6.8	Statistical Analysis	38
RESULTS		39
3.1	Bradford Assay Result	39
3.2	Effects of high fat/cholesterol diet on IR- β protein levels	40
3.3	Effects of high fat/cholesterol diet on p-IRE1 α protein levels	42
3.4	Effect of high fat/high cholesterol diet on SAPK/JNK protein levels	44
3.5	Effect of high fat/high cholesterol diet on p-SAPK/JNK protein levels	46
3.6	Effect of high fat/high cholesterol diet on p-IRS-1 protein levels	49

3.7. Effect of high fat/high cholesterol diet on p-Akt protein levels.....	51
3.8. The Working Model	53
DISCUSSION	55
CONCLUSION AND FUTURE DIRECTION	67
REFERENCES	69
APPENDICES	
A. Chemicals, Brands and Product Numbers.....	85
B. Solutions and Their Preparations for Western Blotting	86
C. Whole Western Blot Images for Each Marker.....	88

LIST OF TABLES

TABLES

Table 2.1 BSA Standards and Dilutions.....	32
Table A.1. Chemical Names, Their Brands and Product Numbers.....	85

LIST OF FIGURES

FIGURES

Figure 1.1. Insulin receptor signaling and JNK activity	15
Figure 1.2. Insulin signaling inhibition through serine phosphorylation of IRS protein	16
Figure 1.3. ER Stress and Unfolded Protein Response	21
Figure 1.4. In the presence of acute and chronic ERS, IRE1 α effects on insulin signaling	22
Figure 1.5. Unfolded protein response, metabolism and inflammation	24
Figure 2.1. Schematic representation of animal subjects experimental design in this study	29
Figure 2.2. Representative structure of transfer sandwich system of Western blot	36
Figure 3.1. BSA Standard Calibration Curve.....	39
Figure 3.2. Western blot analysis of anti-IR- β levels in the cerebral cortex. (A) Representative immunoblot of anti-IR- β (B) the quantification of immunoblots ..	41
Figure 3.3. Western blot analysis of anti-p-IRE1 α level in cerebral cortex. (A) Representative immunoblot of anti-p-IRE1 α (B) the quantification of immunoblots	43
Figure 3.4. Western blot analysis of anti-SAPK/JNK in cerebral cortex. (A) Representative immunoblot of anti-SAPK/JNK. The quantification of immunoblots of (B) the SAPK/JNK upper band, (C) the SAPK/JNK lower band, and (D) total bands	45
Figure 3.5. Western blot analysis of anti-p-SAPK-JNK in the cerebral cortex. (A) Immunoblot image of anti-p-SAPK/JNK. The quantification of immunoblots of (B) p-SAPK/JNK upper band, (C) lower band, and (D) total bands.....	48
Figure 3.6. Western blot analysis of anti-p-IRS-1 levels in cerebral cortex. (A) Representative immunoblot of anti-p-IRS-1 (B) the quantification of immunoblots.	50

Figure 3.7. Western blot analysis of anti-p-Akt protein levels in cerebral cortex. (A) Representative immunoblot of anti-p-Akt (B) the quantification of immunoblots.	52
Figure 3.8. The Working model of this study.....	53
Figure C.1. Western blot image of anti-IR- β as whole blot	88
Figure C.2. Western blot image of anti-p-IRE1 α as whole blot.....	88
Figure C.3. Western blot image of anti-SAPK/JNK as whole blot.....	89
Figure C.4. Western blot image of anti-p-SAPK/JNK as whole blot.....	89
Figure C.5. Western blot image of anti-p-IRS-1 as whole blot.....	90
Figure C.6. Western blot image of anti-p-Akt as whole blot	90

LIST OF ABBREVIATIONS

ABBREVIATIONS

- AD: Alzheimer's Disease
- AgRP: Agouti-related peptide
- APOE: Apolipoprotein E
- ApoE^{-/-}: Apolipoprotein E knockout mice
- ATF6: Activating transcription factor 6
- ATF4: Activating transcription factor 4
- BBB: Blood brain barrier
- BiP: Binding immunoglobulin protein
- BSA: Bovine serum albumin
- CHOP: C/ERB homologous protein
- CNS: Central nervous system
- CSF: Cerebrospinal fluid
- eIF2 α : Eukaryotic initiation factor 2 alpha
- ER: Endoplasmic reticulum
- ERAD: ER associated degradation
- ERS: Endoplasmic reticulum stress
- FFA: Free fatty acids
- FOXO: Forkhead box protein O1

GADD34: Growth arrest and DNA damage-inducible 34

GLUT: Glucose transporter

GTP: Guanosine triphosphate

HC/HFD: High cholesterol/ high fat diet

HDL: High density lipoprotein

HFD: High fat diet

HRP-conjugated: Horseradish peroxidase

IGF-1: Insulin-like growth factor 1

IGF-1R: Insulin-like growth factor 1 receptor

IKK β : Inhibitor of nuclear factor kappaB kinase subunit beta

IL-1 β : Interleukin 1 beta

IL-6: Interleukin 6

IP: Intraperitoneal

IRE1 α : Inositol-requiring enzyme 1

IR: Insulin receptor

IRS-1: Insulin receptor substrate 1

IRS 2: Insulin receptor substrate 2

JNK: c-Jun N-terminal protein kinase

LDL: Low density lipoprotein

MAM: Mitochondria-associated ER membrane

ME: Median eminence

MBH: Mediobasal hypothalamus

mTOR: Mammalian target of rapamycin

PBS: Phosphate buffered saline

PK1: Phosphoinositide-dependent kinase 1

PERK: Protein kinase RNA-like endoplasmic reticulum kinase

PI3K: Phosphatidyl inositol 3 kinase

PKB/Akt: Protein kinase B

POMC: Proopiomelanocortin

PVDF: Polyvinylidene fluoride

RIPA: Radioimmunoprecipitation assay

ROS: Reactive oxygen species

SDS-PAGE: Sodium dodecyl sulfate polyacrylamide gel electrophoresis

T2DM: Type 2 diabetes mellitus

TAG: Triacylglyceride

TBS: Tris buffered saline

TBS-T: Tris buffered saline-Tween 20

TLR4: Toll-like receptor 4

TNF- α : Tumor necrosis factor alpha

TORC1: Target of rapamycin complex 1

UPR: Unfolded protein response

VLDL: Very low-density lipoprotein

CHAPTER 1

INTRODUCTION

1.1 Obesity

Extreme and aberrant accumulation of fat or adipose tissue in the body is called obesity. Accumulation of fats occurs due to an imbalance between energy intake and expenditure in the body. (Panuganti et al., 2021). As a polygenic condition, obesity interests the public concern with increasing global prevalence (Rogerero & Calder, 2018). Overweight and obesity are crucial health problems worldwide since by 2030, 1.35 billion people are expected to be overweight, and 573 million people are expected to be obese (Kelly et al., 2008). Turkey is also affected by the increasing prevalence of obesity despite raising awareness, knowledge, and education about obesity and nutrition. It was reported that approximately 35% of the population was overweight in Turkey in 2010 (Yuksel, n.d.).

The main reason for overweight and obesity is a high-fat diet (HFD). With HFD, free fatty acids (FFAs) are elevated chronically in the blood, and it can lead to many detrimental issues like low-grade inflammation in the body, which can cause insulin resistance, impaired insulin signaling, and disruption of molecules that have a role in energy homeostasis (Gökhan S Hotamisligil, 2006; H.-M. Lee et al., 2013; Lumeng & Saltiel, 2011). FFA metabolism is vigorously controlled in healthy individuals. Fatty acids are converted into triacylglycerides (TAGs) in adipocytes for energy storage and are found as phospholipids found in the cell membrane. FFAs are transferred into the mitochondria for the beta-oxidation process, leading to ATP production from fatty acids (Pilz & März, 2008). FFAs are found in the bloodstream due to hydrolysis of TAGs, de novo synthesis of FFA, and dietary intake of FFAs (Pilz & März, 2008). When FFA levels are excessive in the blood, overwhelmed adipocytes cannot convert

FFAs into TAGs, and they accumulate as lipid droplets in other organs and subsequently lead to lipotoxicity (A. B. Engin, 2017; Saponaro et al., 2015). Also, those FFAs result in the production of inflammatory cytokines, directly and indirectly, leading to inflammation (Fritsche, 2015). Inflammation caused by obesity is observed in many organs like adipose, skeletal muscle, liver, heart, pancreas, and brain (Saltiel & Olefsky, 2017). Studies are showing the entrance of FFAs into the brain. When it enters, it can accumulate in the brain of animal models with metabolic syndrome (Karmi et al., 2010).

Glucose homeostasis is crucial for the proper functioning of the body. On the other hand, change in glucose levels due to glycogen and lipid metabolism, food intake, body weight perpetuation, inflammation, cell growth, and reproduction lead to significant outcomes in the body (IS Sobczak et al., 2019). It is known that starvation and malnutrition can disrupt immune function, so balanced energy flow and well-disposed metabolic homeostasis need an immune system that works properly (Gökhan S Hotamisligil & Erbay, 2008).

It was shown that obesity has been risen to risk for developing dementia (Whitmer et al., 2008), insulin resistance, type 2 diabetes (T2DM), hypercholesterolemia, fatty liver disease, atherosclerosis, and some cancers (Semenkovich, 2006). Genetic, metabolic, behavioral, and environmental factors effectively affect obesity. However, unhealthy eating habits and lack of exercise are the main elements for developing obesity. In modern societies, diet is mainly converged to high carbohydrate and high-fat contained Western diet which ameliorates the development of obesity (Amuna & Zotor, 2008). As a result of a high-fat diet, elevated fat molecules in the blood threaten the individual's health, eventually may cause death. One of the common obesity-related disorders is hyperlipidemia.

1.2 Hyperlipidemia

Hyperlipidemia is defined as a high level of plasma lipids such as triglycerides, cholesterol, cholesterol esters and phospholipids, very-low-density lipoprotein (VLDL), and low-density lipoprotein (LDL) with a low level of high-density lipoprotein (HDL) in the circulating blood (Shattat, 2015). Hyperlipidemia is linked to many life-threatening disorders. For example, one of the significant risk factors for developing cardiovascular diseases (CVDs) is hyperlipidemia (Jørgensen et al., 2013). It is well-known that CVDs cause one-third of the total deaths worldwide. More than 17 million people died in 2015 due to CVDs, which means 31% of human deaths globally (Organization, 2017). In addition to CVDs, hyperlipidemia has a role in developing hypertension, some cancer types, type 2 diabetes (T2DM), and heart and kidney disorders (Rai et al., 2021). Therefore, molecular mechanisms underlying hyperlipidemia and its related disorders should be elucidated to overcome the development of these diseases by targeting and inhibiting the signaling pathways that lead to disease development.

For proper brain functioning, cholesterol homeostasis is critical. Approximately 25% of all body cholesterol is present in the brain, even if the brain is composed of nearly 2% of the total body weight (Dietschy & Turley, 2001). Cholesterol and triglycerides are transported in the bloodstream with the help of lipoproteins since they are insoluble in plasma (Nelson, 2013). Lipoproteins are spherical molecules, and their core is composed of cholesterol esters and triglycerides, which are encompassed by free cholesterol, phospholipids, and apolipoproteins. According to the size, lipid composition, and apolipoproteins, there are seven classes of lipoproteins which are chylomicrons, chylomicron remnants, VLDL, intermediate-density lipoproteins (IDL), LDL, HDL, and lipoprotein a (Lp (a)) present in plasma (Feingold & Grunfeld, 2015).

Almost all lipids taken by the nutrients are absorbed by the intestine and packaged into chylomicrons to secrete into the bloodstream. They are hydrolyzed into glycerol and

non-esterified fatty acids by endothelial lipoprotein lipase. Apolipoprotein E (APOE) is a glycoprotein with a 34 kDa size. In both the liver and brain, APOE is synthesized, and it is integrated into lipoprotein particles (Mahley, 1988). Chylomicron remnants, rich in cholesterol esters, acquire ApoE, are taken into the liver, forming VLDL with cholesterol, cholesterol esters, and ApoB100. When these VLDL are secreted into the bloodstream, with the help of lipoprotein lipase and hepatic lipase, they are converted into IDL, which subsequently hydrolyzed by hepatic lipase to form LDL (Shattat, 2015). ApoE on the chylomicron is important in its clearance in hepatocytes, and any mutations in ApoE can lead to impaired clearance of chylomicron and increased plasma cholesterol and lipid molecules (Feingold & Grunfeld, 2015). The significance of APOE in lipid/cholesterol transport and the metabolism was shown with the study of ApoE^{-/-} mice. In that mice, severe hypercholesterolemia and atherosclerosis were observed (S. H. Zhang et al., 1992). Most of the cholesterol in the bloodstream is carried by pro-atherogenic LDL molecules. On the other hand, HDL is responsible for reverse cholesterol transport, where the transport occurs from the periphery to the liver, and they are anti-atherogenic. The hepatocytes take up LDL molecules carrying cholesterol with the help of LDL receptors (Feingold & Grunfeld, 2015).

Cholesterol and lipid metabolism is carried out independently from the periphery in the brain. The blood-brain barrier (BBB) inhibits the entrance and exit of cholesterol and plasma lipoproteins in the CNS. Cholesterol is produced by astrocytes, oligodendrocytes, microglia, and to a lesser extent neurons in the CNS. ApoE-mediated lipoprotein system is necessary for the recycling and distribution of cholesterol in the CNS (Mahley, 2016).

As stated, obesity is defined as the accumulation of fat molecules in the body, which leads to permanent inflammation where proinflammatory cytokines are produced by white adipose tissue. Also, reactive oxygen species (ROS) are produced along with the proinflammatory cytokines (Tabas & Bornfeldt, 2016). With HFD and ROS exposure, LDL burden in the blood due to insufficient levels of LDL-receptors in hepatocytes or excessive amount of LDL may cause the oxidation of LDL molecules (Ox-LDL) taken

up by the macrophages called foam cells. Those cells accumulate in the artery and subsequently result in plaque formation. These plaques are the reason for cardiovascular disorders, which make the blood-brain barrier more permeable (FERENCE et al., 2017). Thus, the brain becomes more susceptible to lipid metabolism and more prone to neurodegenerative disorders.

1.2.1 Hyperlipidemia Model: ApoE^{-/-} Mice

Different animal models have been used to mimic human atherosclerosis (Russell & Proctor, 2006). The mouse is the most studied animal model, but it uses almost only HDL to transport cholesterol in the bloodstream. On the other hand, cholesterol is mostly transported by LDL in humans. The difference is due to the absence of cholesterol ester transfer protein (CETP) in mice, which is present in humans (Vergeer et al., 2010). CETP is responsible for transferring cholesteryl esters from HDLs (antiatherogenic) to proatherogenic lipoproteins such as VLDLs, VLDL remnants, IDLs, and LDLs. Lack of CETP is linked with high HDL levels and low LDL levels, an antiatherogenic profile (Barter et al., 2003). Due to this difference, typically, mice are not prone to develop atherosclerosis. However, genetic and dietary manipulations are applied to mouse models to develop and mimic human disease: atherosclerosis (Vergeer et al., 2010).

C57BL/6 mice are used in human disease mimicking studies since they are prone to developing obesity, hyperglycemia, and insulin resistance when fed with HFD. Also, they are susceptible to developing atherosclerosis in feeding with HFD containing cholesterol and bile salts (Schreyer et al., 1998). It was shown that a chow diet that includes low levels of lipids and cholesterol was not enough to develop hyperlipidemia in C57BL/6 mice (Almeida-Suhett et al., 2019). Thus, the high fat/high cholesterol diet called the Western diet is used to enhance hyperlipidemia in mouse models. Mild hypercholesterolemia with approximately 200 mg/dL plasma cholesterol levels is developed in C57BL/6 mice fed with HFD (Schreyer et al., 1998). Also, in

hyperlipidemia studies, a genetically modified ApoE^{-/-} mice model is used. When ApoE^{-/-} mice were fed with low fat, low cholesterol diet, it was concluded that their plasma cholesterol levels were 494 mg/dL with respect to control mice which had 60 mg/dL plasma cholesterol levels. On the other hand, when both ApoE^{-/-} and control mice groups were fed with the high-fat Western diet, their plasma cholesterol levels were measured as 1821 mg/dL and 132 mg/dL in ApoE^{-/-} and control mice groups, respectively (Plump et al., 1992). In ApoE^{-/-} mice, plasma lipoprotein clearance is impaired. It means that severe hypercholesterolemia is observed in ApoE^{-/-} mice with approximately 400 mg/dL plasma cholesterol levels (Plump & Breslow, 1995). Furthermore, when they were fed with HFD, accelerated plasma cholesterol levels increased atherosclerosis lesion development (Plump et al., 1992).

1.2.2 High Fat/Cholesterol (HF/HC) Diet Effect on Brain

According to clinical and epidemiological studies, metabolic syndrome is mainly based on dietary factors. In developing many metabolic disorders, the ‘Western diet’, which includes a high amount of saturated fat and cholesterol, has a significant impact (Pasinetti & Eberstein, 2008). To understand the underlying molecular mechanisms behind hyperglycemia, hyperlipidemia, and atherosclerosis, experimental and diet-induced animal models of the metabolic disorders are used (G S Hotamisligil, 2008).

Early animal studies showed severe cognitive function impairment was observed in high-fat diet (HFD) fed rats for three months (Winocur & Greenwood, 2005). This impairment was linked with hippocampal synaptic plasticity alteration and brain-derived neurotrophic factor downregulation (Stranahan et al., 2008; A. Wu et al., 2004). In transgenic mice studies, HFD-Alzheimer Disease’s (AD) association was demonstrated with increasing amyloidosis, tau phosphorylation, and behavioral default, which are the hallmarks of AD by feeding mice with HF/HC diet (Refolo et al., 2000). HFD caused memory loss by inducing neuroinflammation, which was related again to AD pathology (Thirumangalakudi et al., 2008). Although the

mechanism behind this interaction is complex, some evidence indicates that impaired insulin signaling may be responsible for diet-induced AD pathology (Pasinetti & Eberstein, 2008). Also, it was known that metabolic disorders such as obesity and T2DM are caused by impaired insulin signaling within the central nervous system (CNS) (Liang et al., 2015). Therefore, it is crucial to understand molecular mechanisms behind the interaction of HF/HC diet and insulin signaling pathway in both C57BL/6 and ApoE^{-/-} mice cortex samples.

1.3 The brain as an Insulin Sensitive Organ

The brain needs high energy, and glucose is the primary energy source in energy metabolism. Proper functioning insulin signaling has a vital function as insulin signaling directs the uptake and usage of glucose into the brain. On the other hand, it is well-known that improper insulin signaling in the brain is associated with many metabolic and neurodegenerative diseases (An et al., 2018; Zhao et al., 2018). Early studies proved that the brain uses approximately 20% of the body's glucose, and it was considered a glucose-insensitive organ. Identifying widespread expression of insulin receptors (IR) throughout the brain and their higher expression in various brain regions like the cerebellum, hippocampus and cortex confirmed it as a critical point for an insulin-sensitive organ. Today, both IR and insulin-like growth factor 1 (IGF-1) are known to have a role in brain metabolism and cellular function (Milstein & Ferris, 2021).

1.4 Insulin Transport to the Brain

As a peptide hormone, insulin is synthesized and secreted from pancreatic beta cells, and its function is to maintain the blood glucose level within an optimal range (Petersen & Shulman, 2018). For the mature form of insulin, cleavage of C-peptide from pancreatic preproinsulin is carried out in the endoplasmic reticulum with the help

of multiple endopeptidases. When the mature form is obtained in the secretory granules, it is exocytosed from beta cells in response to increased blood glucose levels. A single gene encodes for insulin in humans and rabbits, but in rodents, there are two (Milstein & Ferris, 2021). Previously thought that insulin would be produced only by pancreatic beta cells, but today, low insulin concentrations are also detected in specific neurons (Csajbók & Tamás, 2016). However, most insulin present in the brain is obtained from pancreatic insulin through the bloodstream. It must be carried out through the blood-brain barrier (BBB) and/or blood-cerebrospinal fluid (CSF) barrier (Milstein & Ferris, 2021). Since insulin is a 51-amino acid peptide, active transport mechanisms are necessary for its transportation into the brain (Gray & Barrett, 2018). Peripheral insulin is taken into the brain in a concentration-dependent manner (Banks et al., 1997). Although the exact mechanism is not well elucidated, according to the radiolabeling studies, peripheral insulin is taken into the brain via IR-dependent manner (Gray & Barrett, 2018; Meijer et al., 2016).

The BBB is an interface between the periphery and the central nervous system (CNS) and facilitates the transport and intake of blood into the brain. Paracellular movement is limited by the tight junctions formed by endothelial cells forming BBB (Ballabh et al., 2004; Hawkins & Davis, 2005). Radiolabeling studies showed that insulin is placed in brain endothelial cells, then vesicles are formed to take insulin inside with the help of endothelial cell-specific IR on BBB. In endothelial cell-specific IR-knock out mice, BBB permeability is changed, and insulin signaling is damaged in the hypothalamus, hippocampus, and prefrontal cortex (King & Johnson, 1985; Konishi et al., 2017). Insulin transport to the brain can occur in an IR-independent way as well. Under the mediobasal hypothalamus (MBH), a circumventricular organ, median eminence (ME) is present in the brain, which lacks fully protected BBB, allowing passive diffusion of insulin into the brain (Banks et al., 1997; Blasberg et al., 1983). Insulin is also detected in CSF in very low concentrations. Insulin transport from CSF to the brain is performed by tanycytes which are specialized ependymal cells, with the help of receptor-mediated endocytosis (Mullier et al., 2010; Rodríguez et al., 2005).

1.5 Insulin Activity in Central Nervous System

Many physiological and behavioral functions and cellular metabolism in CNS are affected by insulin signaling (Beddows & Dodd, 2021). Insulin has a crucial role in differentiation, proliferation, and neurite growth in the developing nervous system (Apostolatos et al., 2012). Brain growth is also induced by insulin action (Wozniak et al., 1993). Detrimental effects of ischemia, beta-amyloid toxicity, oxidative stress, and apoptosis are inhibited by insulin action. Thus, dementia may be prevented. However, when insulin signaling is disrupted, its protective effects might decrease, leading to neuropsychiatric and neurodegenerative diseases (Agrawal et al., 2021).

Studies show that insulin is also necessary for regulating anxiety and depression in the brain. For example, depressive and anxiety-like behaviors have been seen in IR knockdown in the hypothalamus of the animals (Grillo et al., 2011).

If the body's response to insulin (endogenous or exogenous) is lower than usual, this situation is called insulin resistance. Many factors like age, weight, ethnicity, body fat, physical activity, diet, medication, and gut microbiota can affect insulin resistance (M. White & Kahn, 2021). Downregulation of IRs, lower capacity of IRs to bind its ligand, or defective activity of insulin signaling pathway may initiate insulin resistance (Arnold et al., 2018). Insulin deficiency and/or reduced insulin activity in the brain may lead to obesity, type 2 diabetes (T2DM), and Alzheimer's disease (AD) (Kullmann et al., 2016). Hyperphosphorylation of tau protein (Schubert et al., 2004) and amyloid-beta (Chua et al., 2012) accumulation are the hallmarks of AD, and it has been shown that disruption in brain insulin signaling led to a rise in these neuropathological hallmarks. Diabetic patients are more prone to develop AD (Chatterjee & Mudher, 2018). Moreover, systemic insulin resistance or high insulin levels in the bloodstream disrupts the BBB permeability to insulin since it downregulates the endothelial IRs on the BBB, which may result in reduced insulin levels in the brain and lower insulin-mediated neural and glial action (Heni et al., 2014).

In both diabetes (Suzuki et al., 2010) and AD (Vance, 2012), brain cholesterol metabolism alteration has been detected, which may be another possible interaction between these metabolic and cognitive dysfunctions. It is well-known that cholesterol is a crucial molecule in the cell membrane and functions in cell physiology and signaling (Korinek et al., 2020). Studies show that with the help of enhanced insulin activity in the brain, disrupted cholesterol biosynthesis in the brain of diabetic patients can be repaired. Not only neurons but also glial cells (mostly astrocytes) are the sites where brain cholesterol metabolism is affected by insulin action (Suzuki et al., 2010).

A well-known function of insulin is to control body weight and feeding behavior. In both energy and glucose homeostasis, agouti-related peptide (AgRP) and proopiomelanocortin neurons (POMC) located in the arcuate nucleus (ARC) of the hypothalamus have significant roles. These neurons express IRs and affect insulin signaling to the brain. In other words, insulin can change the expression of these neurons (Varela & Horvath, 2012). AgRP neurons are orexigenic, and they are responsible for enhanced food intake, raised body weight, and diminished energy consumption. On the other hand, POMC neurons are anorexigenic, and they promote reduced food intake, diminished body weight, and raised energy consumption (Millington, 2007).

1.6 Insulin Receptor

Although the highest IR density is obtained from the olfactory bulb, hippocampus, hypothalamus, cerebral cortex, and cerebellum, it is widely expressed and distributed throughout the brain (Havrankova et al., 1978). As a transmembrane protein, it is a tyrosine receptor kinase that has two disulfide-linked alpha at the (extracellular region) and two transmembrane beta subunits inside the cell. Ligand binding occurs at alpha subunits, and beta subunits have the cytoplasmic protein tyrosine kinase (PTK) domain (Dodd & Tiganis, 2017). In humans, the IR gene is found on chromosome 19 and comprises 22 exons. IR-A and IR-B are the isoforms of IR according to the alternative

splicing of exon 11 (Belfiore et al., 2017; Siddle, 2011). IR-A isoform does not have exon 11, while IR-B has (Cai et al., 2017). The other ubiquitously expressed receptor in the brain is IGF-1R, where insulin can bind (Adem et al., 1989). Insulin and IGF-1 receptors can form homodimers or heterodimers, which influence the affinity of insulin and IGF-1 to the receptor (Kleinridders, 2016). The higher affinity of the heterodimers is toward IGF-1. On the other hand, homodimers of IR and IGF-1R have a higher affinity to their endogenous ligands, insulin and IGF-1, respectively (Slaaby et al., 2006).

1.6.1 Insulin Receptor Signaling

When insulin enters the brain, it binds to the alpha subunit of IR and results in autophosphorylation in the beta subunit at Y¹¹⁴⁶, Y¹¹⁵⁰, and Y¹¹⁵¹ residues (Wilden et al., 1992). This autophosphorylation recruits insulin receptor substrates 1 and 2 (IRS-1 and IRS-2), which are cytoplasmic adaptor proteins and cause tyrosine phosphorylation of IRS proteins for the insulin signal transduction (Arnold et al., 2018). Among the IRS proteins, IRS-1 and 2 are the best-characterized ones, and in skeletal muscle, adipose tissue, and cerebral cortex, IRS-1 is more crucial, while in the hypothalamus and liver, IRS-2 is more significant (Arnold et al., 2018). Downstream activators of the IRS proteins are phosphatidylinositol 3-kinase (PI3K), protein kinase B (PKB, also known as Akt), and mammalian target of rapamycin (mTOR) (Kleinridders et al., 2014; Kwon & Pessin, 2020). Many cellular functions like synaptic plasticity, neuronal survival, cholesterol synthesis, and neurotransmitter trafficking are influenced by this PI3K/Akt/mTOR pathway (GOODNER et al., 1980).

In most cell types, insulin-dependent mitogenesis and glucose metabolism regulation are mediated by IRS proteins ubiquitously expressed (M. F. White, 2002). They transmit signals from IR/IGF-1R to cellular response, and they do not have intrinsic enzymatic activity (Sun et al., 1991). In their N-termini, PH and PTB domains help them to be recruited to the activated receptors (Voliovitch et al., 1995). Additional

domain, kinase regulatory loop binding domain (KRLB) on IRS-2 restricts tyrosine phosphorylation of IRS-2 by tyrosine kinase domain of IR. However, this domain does not prevent phosphorylation by IGF-1R. It shows that signaling through IRS-2 may be dominated by IGF-1R or IR/IGF-1R heterodimer (J. Wu et al., 2008).

When they are phosphorylated on their tyrosine residues located in C-termini, binding sites are formed to recruit downstream molecules (Sun et al., 1993). In IR/IGF-1R signaling cascade, the primary role of IRS proteins is to exaggerate the PI3K signaling for the activation of AKT, a serine-threonine kinase (Okada et al., 1994). Src-homology (SH) 2-carrying proteins like PI3K distinguishes tyrosine-phosphorylated IRS proteins, and PI3K causes the production of phosphoinositides to recruit Akt to the membrane, and Akt is activated when it is phosphorylated at T308 by phosphoinositide-dependent kinase 1 (PDK1) (Alessi et al., 1997; M. F. White, 2002). When target of rapamycin complex 2 (TORC2) additionally phosphorylates Akt on its S473 residue, its activity is improved (Sarbasov et al., 2005). Substrates of Akt are Akt Substrate of 160 kD (AS160), mTORC1, and the forkhead box protein O1 (FOXO) transcription factors (Manning & Cantley, 2007).

Glucose uptake to the cells and its usage in both energy production and macromolecule synthesis are regulated by IRS proteins through insulin-regulated glucose homeostasis. Glucose transporter proteins (GLUT proteins) are responsible for glucose and, in some cases, fructose uptake to the cells (Dong et al., 2006). GLUT4 is the major one, and in response to glucose, both IRS1 and 2 regulate glucose uptake upon GLUT4 (Zaid et al., 2008). When AKT is activated through the IRS pathway, it phosphorylates Rab-GAP AS160 by preventing its GAP activity and the GTP-bound (active) form of Rab proteins which mediates GLUT4 movement to the cell surface to facilitate glucose transport into the cells (W. Zhang et al., 2006). Akt has many cellular functions. When activated, it prevents glycogen and fatty acid synthesis by inhibiting the functions of the glycogen synthase and ATP-citrate lyase enzymes and supports protein synthesis by inactivating mTORC1. By suppressing the proapoptotic pathway, the cell survival is interceded by Akt (Haeusler et al., 2018; Saltiel, 2021). On the other hand, GLUT4

expression is restricted to only the hypothalamus and hippocampus in the brain, leading to differences in glucose transport in the periphery and brain. GLUT1 expressed by endothelial cells and astrocytes at BBB is responsible for circulation in the brain. GLUT3 and GLUT1 are insulin insensitive transporters; they are extensively expressed in neurons and glial cells, respectively. However, according to some evidence, insulin can indirectly have a function for the glucose uptake to the brain (Milstein & Ferris, 2021).

1.6.2 Impairment in Insulin Signaling in CNS

IR signaling is regulated through a negative feedback loop. In this loop, receptor affinity to insulin reduces, and translocation of IR to the target cell surface is diminished. This negative feedback loop negatively affects the IR and its downstream activators (W. Chen et al., 2017). There are two heterogeneous binding sites on IR for insulin to bind. However, even though the first insulin binds with high affinity, the second binding can be at low affinity (Meyts, 1976). In other words, in increased insulin levels, affinity to insulin reduces since the receptor is highly occupied, which is known as negative cooperativity (De Meyts et al., 1973). When insulin concentration increases, IR levels on the cell membrane reduce by internalization and degradation of IRs, which are occupied with excess insulin (Gavin et al., 1974). Also, a chronic excessive amount of insulin may cause IR desensitization, and the disruption of insulin signaling subsequently results in insulin resistance (Rask-Madsen et al., 2012).

Under normal conditions, changes in glucose and insulin levels are tightly controlled by the feedback mechanisms to maintain cellular homeostasis (M. F. White, 2002). Evidence indicates that the function of IR/IGF-1R signaling pathways can be disrupted by microenvironmental issues like oxidative stress, inflammatory cytokines, and free fatty acids linked to obesity and metabolic disorders. In the end, the disruption can result in insulin resistance, hyperglycemia, and hyperinsulinemia (Gual et al., 2005).

IRS proteins are crucial in the maintenance of metabolic homeostasis because these proteins have a role in the feedback mechanism of IR/IGF-1R signaling pathways. Serine phosphorylation of IRS proteins can positively or negatively affect insulin activity. A Positive-feedback loop for insulin activity is obtained when IRS proteins are phosphorylated at serine residues by protein kinase B through IR signaling (Gual et al., 2005; Patti et al., 1998). On the other hand, many downstream molecules, which can phosphorylate IRS proteins from their serine residues, interrupt their function and cause inactivation and/or proteasomal degradation of these adaptor proteins (Gual et al., 2005). For instance, IRS-1 phosphorylation at serine 302 and 307 residues prevents the fundamental interaction between IRS-1 and IR since serine phosphorylation causes a conformational change in the PTB domain of IRS-1, and thus signaling pathway is disrupted. If serine phosphorylation occurs in the PI3K binding site of the IRS proteins, the downstream signaling pathway is impeded since the interaction between IRS proteins and PI3K is disturbed. Hence, serine phosphorylated IRS proteins are directed to ubiquitination and degradation in proteasomes. This is called negative feedback and mediated by mTORC1. As a result, the extent and continuance of insulin signaling can be restricted, and insulin sensitivity and glucose homeostasis maintenance are held. If this negative feedback loop is dysregulated, it might lead to insulin resistance and diabetes (Gual et al., 2005).

Toll-like receptors (TLRs) are the transmembrane proteins expressed in different cell compartments like adipocytes and liable for a function in the innate immune system (F. A. Carvalho et al., 2012). In humans, TLR4 is the first reported receptor, and it is expressed in many cell types like adipocytes, macrophages, and muscle cells (Dobrovolskaia & Vogel, 2002). Evidence indicates that TLR4 can be activated by binding of saturated FAs, and inflammatory response is initiated to produce proinflammatory cytokines like tumor necrosis factor-alpha (TNF- α), interleukin 6 (IL-6), and IL-1 β (D. Hwang et al., 2012; D. H. Hwang et al., 2016). TNF- α can activate c-Jun N-terminal kinases (JNK), which subsequently phosphorylates IRS-1 at its serine 307 residues. Inactivation of IRS-1 in this way may inhibit insulin signaling

(Gökhan S Hotamisligil et al., 1996) and result in insulin resistance. Again, IR/IGF-1R pathway can be disrupted in the presence of increased free FFAs and oxidative stress since they can lead to negative serine phosphorylation (Shaw, 2011). It has been shown that overexpression of TNF- α , a proinflammatory cytokine, was seen in adipose tissue of obese mice. It was the first obvious clue for the association between obesity, diabetes, and chronic inflammation (Wellen, 2005). Abnormal cytokine production and inflammatory signal activation are the indicators of chronic inflammation (Gokhan S Hotamisligil et al., 1993). In the absence of TNF- α in obese mouse models, glucose homeostasis and insulin sensitivity are enhanced, confirming the inflammatory response's inhibitory role on insulin signaling in obesity (Uysal et al., 1997; Ventre et al., 1997).

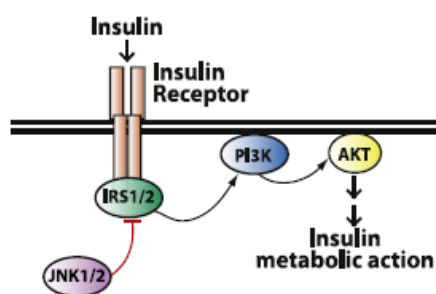


Figure 1.1. Insulin receptor signaling and JNK activity (Solinas & Becattini, 2017)

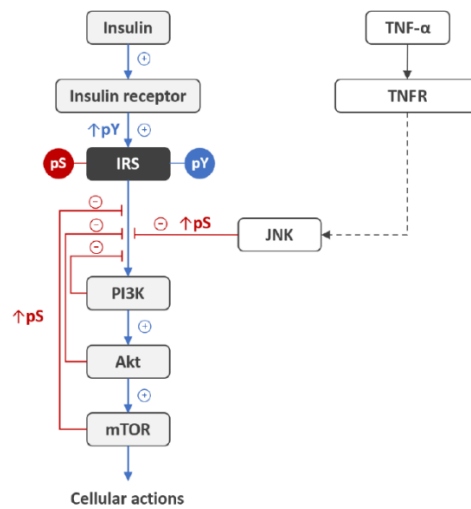


Figure 1.2. Insulin signaling inhibition through serine phosphorylation of IRS protein (Pomytkin & Pinelis, 2021)

1.7 Endoplasmic Reticulum Stress (ERS)

The endoplasmic reticulum (ER) is the largest organelle in eukaryotes which includes the nuclear envelope, sheet-like cisternae, and a polygonal array of tubules. It is classified into rough ER (rER) and smooth ER (sER) according to the membrane structure (Shibata et al., 2006). Protein synthesis and folding into their 3D conformation, lipid synthesis (like cholesterol, glycerophospholipids, and ceramide), and calcium homeostasis are carried out in ER (Mukherjee et al., 2015). The environment in the ER lumen is extremely oxidizing to accomplish the folding and maturation of the proteins (Shibata et al., 2006). In addition to that, ER requires a high amount of calcium, enzymes, and chaperons for proper functioning (Back & Kaufman, 2012).

ER and mitochondria have interacted with mitochondria-associated ER membrane (MAM), where ions, lipids, and metabolites are exchanged between ER and mitochondria (Back & Kaufman, 2012). MAM is rich in cholesterol and ceramides in

structure (Teruo Hayashi & Fujimoto, 2010). Since MAM is important in calcium stability (T Hayashi et al., 2009), dysregulated MAM causes the impairment in calcium homeostasis and leads to oxidative stress in obesity (Arruda et al., 2014). Also, glucose metabolism is highly influenced by calcium signaling. For instance, fasting can result in elevated calcium levels in the cytosol in a way that IP3R is phosphorylated and activated indirectly by increased levels of glucagon. Increased cytosolic calcium is related to gluconeogenesis, which is the main cause of hyperglycemia, resulting in insulin resistance. Also, it is stated that in diabetes, gluconeogenesis is improved by increased IP3R activity, resulting in increased blood glucose (Herzig, 2001; Wang et al., 2012). Oppositely, calcium homeostasis is also influenced by insulin signaling. Calcium influx can be stimulated by active AKT to the cytosol, and increased levels of cytosolic calcium induce ER channels for transportation to the mitochondria. Moreover, IP3R activity can be blocked by phosphorylation of AKT, and at the end, ER calcium release is attenuated, and cytosolic calcium levels are decreased (Cheng et al., 2020; Marchi et al., 2012). Due to the importance of calcium signaling in glucose metabolism, obesity and T2DM may be the result of disruption in calcium signaling, which is affected by oxidative and ER stresses. Oxidative stress, hyperlipidemia, and calcium imbalance are the main factors that impair ER homeostasis and the reason for ERS (Dandekar et al., 2015; L Ozcan & Tabas, 2016).

Saturated FAs in mitochondria can promote inflammation in different ways. For instance, elevated β -oxidation of FFAs can cause the production of reactive oxygen species (ROS) and oxidative stress. JNK and IKK β , which are related to inflammation, are generated by ROS (Sears & Perry, 2015). They both disrupt insulin signaling by phosphorylating IRS-1 protein on its serine residue (Gökhan S Hotamisligil, 2006). Also, ROS can result in ERS, which contributes to inflammation (Legrand-Poels et al., 2014). The ultimate result of both ERS and mitochondrial stress is apoptosis which is seen in the later stage of T2DM in the loss of β -cells (IS Sobczak et al., 2019).

Fatty acid composition in the cell membrane can also be affected by saturated FFAs since they influence the passage of ions and molecules through the membrane by

altering the fluidity and permeability of the membrane (Pilon, 2016). Studies show a strong interaction between T2DM and membrane phospholipids with elevated saturated FFAs that gives rigidity to the membrane, and it is thought that it subsequently results in insulin signaling disruption (Kröger et al., 2015; Pilon, 2016). ER is an organelle where elongation, desaturation, and esterification of FFAs occur (Legrand-Poels et al., 2014). In the presence of excess FFAs, ER morphology and function change then trigger ERS (Borradaile et al., 2006).

The folding mechanism in rER is a complex, error-prone folding mechanism which is accomplished by chaperons and enzymes may not allow all newly synthesized proteins to fold into their 3D conformations (Dandekar et al., 2015; Hampton, 2002; Kruse et al., 2006; L Ozcan & Tabas, 2016). Those unfolded proteins accumulate in the rER lumen and lead to ERS (Dandekar et al., 2015; L Ozcan & Tabas, 2016). Inflammatory response and apoptotic signaling are the pathophysiologies of the ERS, and chronic ERS can result in atherosclerosis development (Kruzliak et al., 2015). For the maintenance of ER homeostasis, unfolded protein response (UPR), ER-associated degradation (ERAD), and autophagy are required (Hampton, 2002; Kruse et al., 2006).

1.7.1 Unfolded Protein Response (UPR)

Unfolded and misfolded proteins are the main cause of ERS (Kruzliak et al., 2015). UPR, an evolutionarily preserved signaling cascade, is stimulated in the presence of ERS to preserve the functional unity of ER and cellular homeostasis (Schröder, 2008). Before ERS, cells try to solve unfolded/misfolded protein problems by raising the chaperon protein levels such as binding immunoglobulin protein (BiP), also known as 78 kDa glucose-regulated protein (GRP78), which is only found in rER lumen and is sensitive to the glucose level in the cell (Adamopoulos et al., 2014; Liu et al., 2010). Three transmembrane mediators regulate UPR in rER, which are RNA-dependent protein kinase (PKR)-like ER kinase (PERK, protein kinase), inositol-requiring enzyme 1 α (IRE1 α , protein kinase-endoribonuclease), and activating transcription

factor 6 (ATF6, membrane bound-transcription factor) (Yoshida et al., 2000). When ERS is not present, these proteins are in an inactive form where they are bound to BiP. Under ERS conditions, BiP and sensor proteins are separated, and the UPR cascade is activated. IRE1 α and PERK are activated via dimerization and autophosphorylation. On the other hand, ATF6 is activated through intramembrane proteolysis at the Golgi network (Ghemrawi et al., 2018). There is no clear evidence about the first activated sensor proteins, but in one study, it is reported that PERK is the first activated UPR protein (Hu et al., 2017). When UPR is activated, all three proteins are generally influenced (Ron & Walter, 2007).

When UPR is activated as a response to ERS, the first reaction is to stop protein translation, then chaperon protein production is upregulated to enhance the folding, and lastly, if the correct conformation is not held, degradation of misfolded proteins are stimulated (F. Engin & Hotamisligil, 2010).

Upon ERS, PERK dissociates from BiP, and after dimerization and autophosphorylation processes, it phosphorylates eukaryotic initiation factor 2 α (eIF2 α) (Ron & Walter, 2007). Therefore, it inactivates eIF2 α and downregulates mRNA translation. As a result, the accumulation of unfolded proteins into ER lumen is inhibited. However, even if eIF2 α activity is restricted, the 5' untranslated region of some mRNA molecules with a short open reading frame (ORF) can be translated preferentially for encoding ATF4, a transcription factor. C/ERP homologous protein (CHOP) and growth arrest and DNA damage-inducible 34 (GADD34) are activated by ATF4. CHOP is a transcription factor responsible for apoptosis. Although the PERK arm of the UPR is preservative, it can also induce apoptosis (Walter & Ron, 2011). GADD34 dephosphorylates eIF2 α by protein phosphatase 1 (PP1) activity. Dephosphorylation of eIF2 α is the negative feedback mechanism regulated by ATF4 when the cell is relieved from ERS, and it is time to restore the protein production (Mustapha et al., 2021).

The other UPR sensor protein is IRE1, expressed as IRE1 α and IRE1 β . While IRE1 β is expressed in intestinal epithelial cells and airway mucous cells, IRE1 α 's expression is ubiquitous (Bertolotti et al., 2001; Martino et al., 2013). Their lumenol domain amino acid sequences are different; thus, their substrate specificity and functions are discrete (Imagawa et al., 2008). IRE1 α is a bifunctional transmembrane protein with kinase and endoribonuclease functions (Tirasophon et al., 1998). Upon ERS, accumulated unfolded proteins activate the kinase domain through oligomerization and autophosphorylation, then RNase activity is evoked. RNase activity is necessary for splicing the 26-nucleotide sequence of X-box binding protein 1 (XBP1) mRNA; then, it is translated to have an active form of XBP1 protein (Rojas-Rivera et al., 2018). XBP1 expression is responsible for the activation of genes which are amenable for protein translocation, folding and secretion in rER and degradation of unfolded/misfolded proteins (Basseri & Austin, 2012). According to the early studies, IRE1 and PERK are inactive when they bind to BiP, but there is competition between unfolded proteins and lumenol UPR sensor proteins for BiP. All proteins are unfolded when they enter rER lumen, so there should be an activation threshold for these sensor proteins. When unfolded proteins win the competition, sensor proteins are dissociated from BiP and are oligomerized (Ron & Walter, 2007). In an IRE1 mutant yeast, it has been shown that UPR is activated even if it cannot bind to BiP (Kimata et al., 2004; Pincus et al., 2010). In the following studies, it has been supported that there is a direct interaction between IRE1 and unfolded protein and, subsequently, oligomerization of IRE1, which indicates UPR can directly be sensed by IRE1 (Gardner & Walter, 2011; Kawaguchi & Ng, 2011). Also, precursor microRNAs and mRNAs can be degraded by IRE1 α in the process of regulated IRE1-dependent decay (RIDD); thus, protein load can be inhibited. Chaperon protein expressions are upregulated, and CHOP is prevented for cell survival by IRE1 α , but in the presence of chronic stress, IRE1 α causes the activation of c-Jun N-terminal kinase (JNK) to induce cell death (Urano et al., 2000). JNK activation is carried out in mitochondria. When it is active, it starts cell death by resulting in the phosphorylation of proapoptotic markers while preventing the antiapoptotic ones (Lei & Davis, 2003). Also, apoptosis signal-regulating kinase

(ASK1) (Nishitoh et al., 2002) and caspase 12 (Nakagawa et al., 2000) are activated when IRE1 α and tumor necrosis factor TNF receptor associated factor 2 (TRAF2) are interacted.

Another UPR protein, ATF6, is a transmembrane transcription factor. When activated by ERS, it is released from BiP and sent to Golgi, undergoing proteolytic cleavage (X. Chen et al., 2002). Then ATF6 is imported into the nucleus where adaptive stress response elements GRP78 (BiP) and XBP1 are expressed (Rutkowski & Kaufman, 2004). As an ERS-associated apoptosis marker, CHOP can be expressed by the association of ATF4, ATF6, and XBP1 (Oyadomari & Mori, 2004). If ER homeostasis is interrupted and chronic ERS continues, ERS-activated apoptosis and inflammation can occur in cells (Yang et al., 2020).

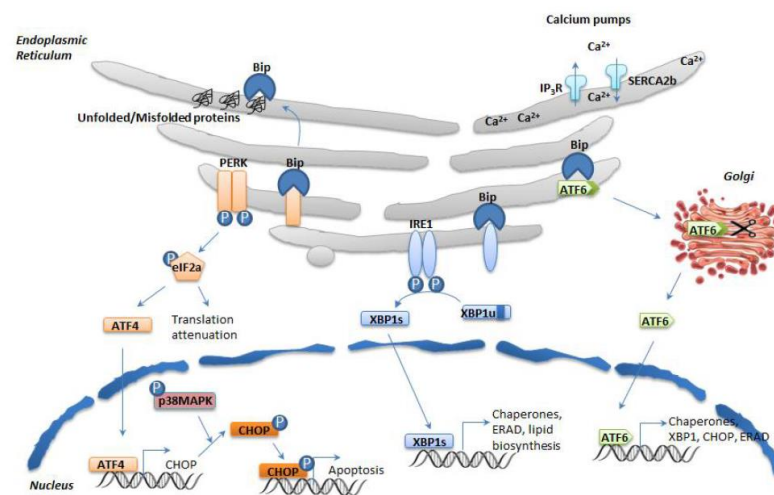


Figure 1.3. ER Stress and Unfolded Protein Response (Ghemrawi et al., 2018)

1.8 Activation of IRE1 α

The molecular weight of human IRE1 α protein is about 110 kDa, and it has a luminal domain where BiP binds, type I transmembrane domain, and cytoplasmic domain where kinase and endoribonuclease domains are found (Ron & Walter, 2007). There are six phosphorylation sites on the IRE1 α cytoplasmic domain distributed throughout

the linker region, kinase activation loop region, and RNase domain region. The most critical region is the kinase domain, and phosphorylation of it at serine 724, 726, and 729 residues significantly contribute its activity (Prischi et al., 2014). Phosphorylation in the kinase activation loop is crucial for the UPR activation through IRE1 α (Li et al., 2010).

IRE1 α activation and inactivation must be suitably controlled since extended activation leads to apoptosis. For example, it is carried out transiently in adaptable stress conditions but causes increased proapoptotic marker expressions in prolonged stress conditions (Riaz, Junjappa, Handigund, et al., 2020). When IRE1 α interacts with TRAF2 and Ask1, they cause phosphorylation of JNK. When its activity is prolonged, apoptosis is induced. Also, the expression of nuclear factor kappa B (NF- κ B) through IRE1 α -TRAF2 interaction results in TNF α expression. Once again, under ERS, apoptosis is regulated by MTORC1 since it downregulates Akt and upregulates IRE1-JNK interaction (Estornes et al., 2014; Kato et al., 2012).

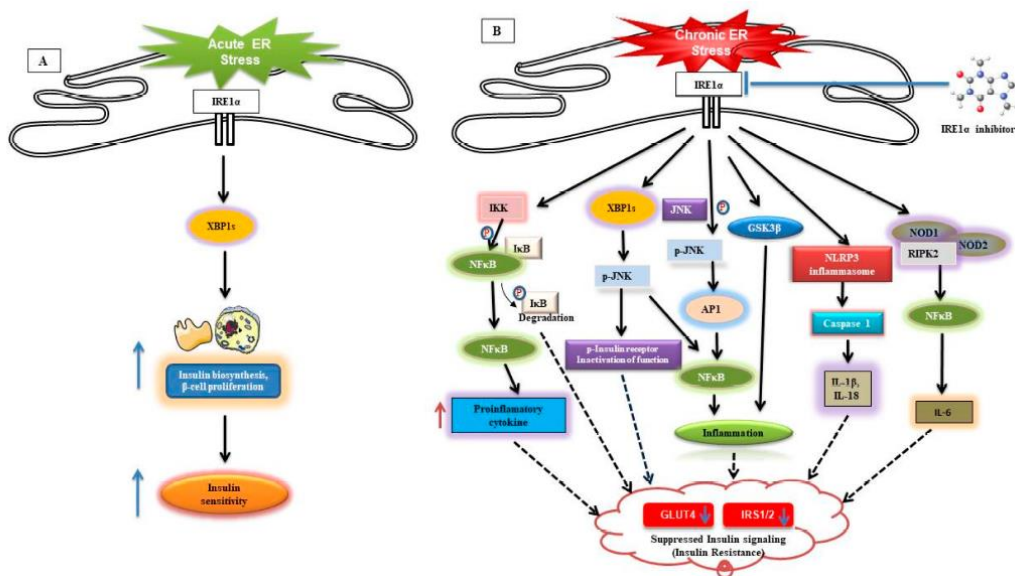


Figure 1.4. In the presence of acute and chronic ERS, IRE1 α effects on insulin signaling (Riaz, Junjappa, Hadigund, et al., 2020)

1.9 IRE1 α Effects on Chronic Metabolic Diseases

Insulin and glucagon are the main hormones that regulate metabolic glucose intake into the tissues. According to the blood glucose levels, rER in pancreatic beta cells works intensively to meet the need for secretory protein folding. In type 1 diabetes (T1DM) auto immune system attacks beta cells, and there is an inadequate amount of insulin. On the other hand, in T2DM, both the beta cell death and impairment in insulin-sensing cells lead to insulin resistance, it means tissues cannot be sensitive to insulin. In both cases, ERS has an effect (Kanekura et al., 2015).

High glucose levels in the bloodstream induce beta cells to synthesize and secrete insulin. In physiological adaptive stress conditions, rER occurs to meet the insulin demand and fold it into the correct folding structure. However, if the stress is persistent, pathological conditions occur since rER capacity becomes full and unfolded proteins accumulate, beta-cell homeostasis is impaired, and UPR is activated (Lipson et al., 2006). In insulin biosynthesis and oxidative balance, IRE1 α has essential functions (Hassler et al., 2015). In short-term transient ERS, the IRE1 α -XBP1s arm is amenable for cell survival by means of enhanced insulin sensitivity. On the other hand, under chronic ERS, IRE1 α associates with TRAF2, ASK1, and receptor-serine/threonine protein kinase 1 (RIPK1) to phosphorylate and activate JNK, which subsequently activates activator protein 1 (AP-1) as a transcription factor to induce cytokine production like IL-6 and TNF α (Riaz, Junjappa, Handigund, et al., 2020). Activated JNK can phosphorylate IRS-1 from its serine residues, impair insulin signaling, and cause insulin resistance, which is the indicator of T2DM and obesity (Mishra et al., 2017).

IRE1 α is again crucial in both diet-induced and genetically obese models in which FFAs, proinflammatory cytokines, and the excessive amount of blood glucose are the indicators (Olefsky & Glass, 2010). In obesity, accumulated fat induces low-grade inflammation, and the chronic burden of ER results in ERS in adipocytes, pancreatic beta cells, hepatocytes, and neurons (Riaz, Junjappa, Handigund, et al., 2020). Again,

IRE1 α leads to the production of JNK and I κ B, both having a role in insulin signaling disruption and glucose homeostasis impairment (Nie et al., 2012).

IRE1 α also causes the activation of glycogen synthase kinase 3 beta (GSK-3 β), which induces proinflammatory cytokine production like IR-1 β and TNF- α in metabolic disorders. However, GSK-3 β activation prohibits XBP-1 splicing, and thus TNF- α expression is downregulated (Kim et al., 2015).

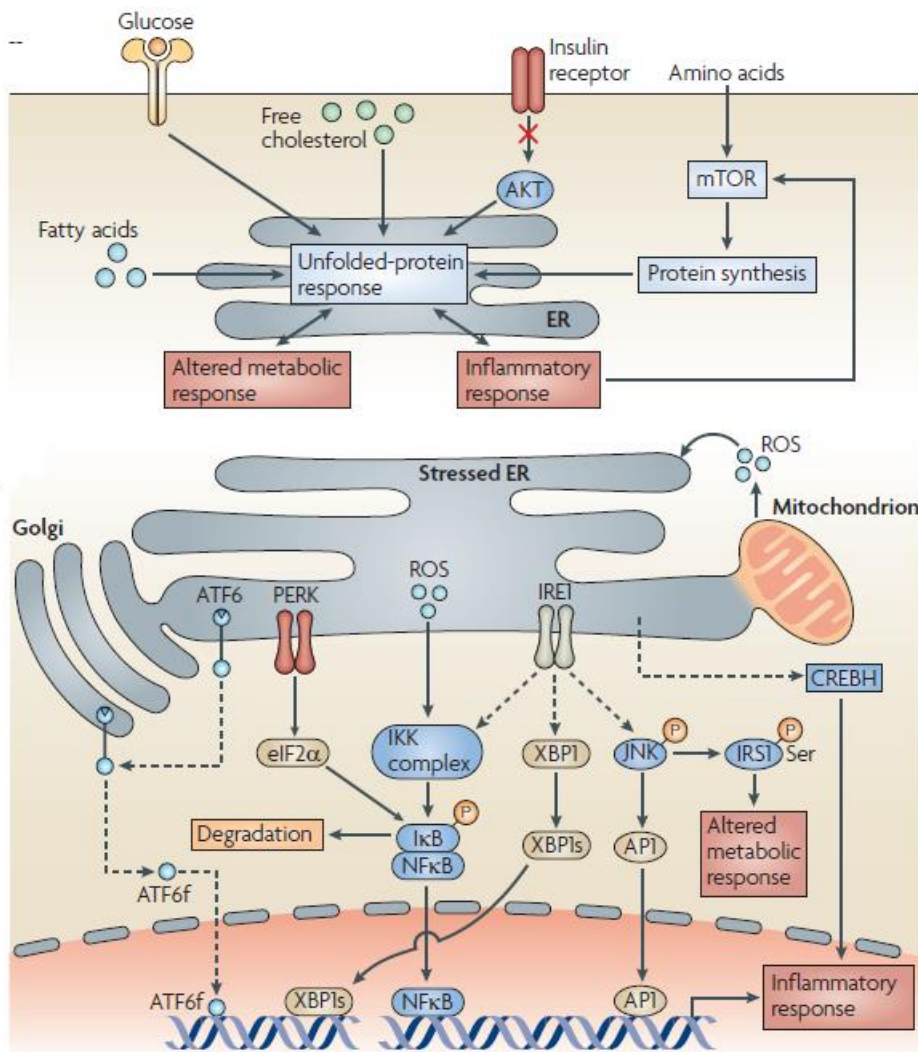


Figure 1.5. Unfolded protein response, metabolism and inflammation (Gökhan S Hotamisligil & Erbay, 2008)

1.10 c-Jun N-terminal Kinases (JNK)

c-Jun N-terminal kinases (JNK) are one of the mitogen-activated protein kinases (MAPK) family members (serine-threonine kinases). They are also known as stress-activated kinases (SAPK) (Chang & Karin, 2001). It is different from the other MAPK family members because cellular stress instead of mitogens activates them. Mitogen-activated protein kinase kinase (MAP2K), MKK4, and MKK7 are responsible for the activation of JNKs. For the full activation of JNK, dual phosphorylation of threonine (Thr183) and tyrosine (Tyr185) residues on the activation loop is necessary. MKK4 preferentially phosphorylates tyrosine residue, while MKK7 phosphorylates threonine residue (Thévenin et al., 2011). JNK's name comes from the fact that they phosphorylate and activate one of the AP-1 transcription factor components, c-Jun (Hibi et al., 1993). c-Jun, Fos, Maf, and ATF are the components of AP-1 transcription factor (Behrens et al., 1999), and JNKs can phosphorylate ATF2, ATF3, and c-Jun to improve AP-1 function (Shaulian & Karin, 2001).

Three JNK genes encode for three JNK isoforms which are JNK1, JNK2, and JNK3. While JNK1 and JNK2 expressions are ubiquitous, JNK3 is expressed only in pancreatic beta cells, brain, and testis (Chang & Karin, 2001; Solinas & Karin, 2010). Expression of each JNK isoform occurs as one short (46 kDa) and one long (54 kDa) version (Pulverer et al., 1991). Differentially expressed three isoforms can bind and activate different mediators (Gupta et al., 1996).

JNKs activation is observed in IR signaling inhibition, obesity, and inflammatory pathways (Hirosumi et al., 2002). In response to FFAs, proinflammatory cytokines, reactive oxygen species (ROS), pathogens, and pathogen-associated proteins, JNK activation is carried out. Afterward, the cytokine production and inflammation are further raised by JNK activation along with IRS-1 serine phosphorylation. It is well-known that in the development of metabolic diseases, JNK activation is crucial (Gökhan S Hotamisligil & Erbay, 2008). On the other hand, in the JNK1^{-/-} mice model, insulin resistance and T2DM development are reduced (Gökhan S Hotamisligil, 2005).

With the help of JNK1^{-/-} mice, adiposity is reduced, HFD resistance is gained, insulin sensitivity is ameliorated, and IR signaling cascade is improved (Hirosumi et al., 2002).

1.11 The Aim of this Study

As a result of changes in diet and lifestyle, the prevalence of obesity increases exponentially. Consumption of HFD increases the serum FFA levels in the blood, inducing low-grade inflammation and impairment in glucose homeostasis, leading to insulin resistance and insulin signaling disruption. High glucose consumption makes the brain highly affected by changes in glucose homeostasis, so insulin signaling should work properly. Insulin performs glucose uptake into the cells through the signal pathway delivered through the IRS-1 and IRS-2 adaptors, disruption of this pathway can damage glucose metabolism in the cells and cause insulin resistance. Furthermore, because of HFD and obesity, a high level of plasma lipids called hyperlipidemia is observed which is the primary reason for CVDs affecting one-third of people's death. Therefore, underlying mechanisms of hyperlipidemia need to be solved.

Obesity have been associated with cellular stress and inflammatory response activation in mammalian cells. Even though the stress origin has not been elucidated yet, ER is the central organelle responsible for stress response. Therefore, analyzing ERS and subsequent activation of UPR pathways became critical that their activation was revealed in the HFD fed mice brains. ERS in the hypothalamus had a role in peripheral insulin and leptin resistance, also in the hippocampus and frontal cortex. ERS and insulin signaling impairment was demonstrated in obese rats' models.

In this study, the effect of HF/HC diet on the activation of the IRE1 α pathway as one of the UPR pathways and its relationship with the insulin signaling pathway through JNK activation was investigated in the cerebral cortex of C57BL/6 (WT) and ApoE^{-/-} mice. In this study, we aimed to study the insulin signaling pathway when animals were exposed to high cholesterol along with HFD (HC/HF diet). The insulin signaling

pathway was assessed via determining the IRE1 α /JNK/IRS-1/Akt pathway. Assessing this pathway using ApoE^{-/-} a transgenic mice model, and a different diet composition were novel in this study.

CHAPTER 2

MATERIALS AND METHODS

2.1 Ethics, Animal Subjects and Diets

All animal subjects (male C57BL/6 (WT) and ApoE^{-/-} mice) were obtained from Charles River, Wilmington, Massachusetts. Animal studies were carried on in Bilkent University, Institute of Materials Science and Nanotechnology (UNAM), and mice were supplied by Prof. Dr. Michelle Adams, Bilkent University and Assoc. Prof. Ebru Erbay, Bilkent University. Ethical committees of Bilkent University permitted all procedures used in this study (2018/2). Animal facility conditions were temperature at 20-22°C, humidity at 45-50%, and a 12/12 light-dark cycle. Experiments were started when mice were at 8 weeks of age. They were divided into four groups, randomly (n=7 per group) and fed with standard chow diet (diet composition: 4.5% fat) or Western diet, also known as high cholesterol/high-fat diet (HC/HFD) (diet composition: 0.21% cholesterol, 21% butterfat, cat no: TD.88137/E15721, Ssniff Spezialdiated, Germany) for 16 weeks.

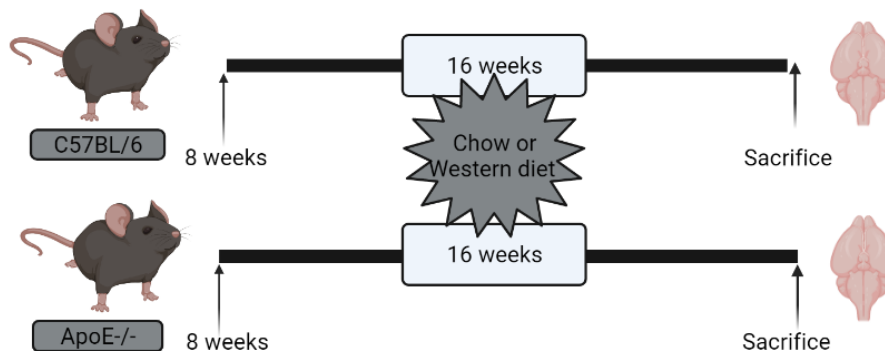


Figure 2.1. Schematic representation of animal subjects experimental design in this study

Animal groups were 1-) C57BL/6 and chow diet (n=7), 2-) C57BL/6 and Western diet (n=7), 3-) ApoE^{-/-} and chow diet (n=7), and 4-) ApoE^{-/-} and Western diet n=7). All mice had free access to both diet and water during the experiment. Schematic representation of animal subjects experimental periods used in the study showed in Figure 2.1.

2.2 Dissections

Dissection procedure was conducted at UNAM, Bilkent University, Ankara. First, at the end of the 16 weeks of diet, fasting was applied to mice for 12 hours before they were sacrificed. Then, intraperitoneal (IP) administration of xylazine (10 mg/kg) and ketamine (100 mg/kg) was administered to mice for anesthesia. Sterile Phosphate-Buffered Saline (PBS) was used to prepare Ketaset (100 mg/mL) and Xylaject (20 mg/mL). After 3-5 minutes of anesthetic, the toes of mice were controlled by pinching them to understand whether they were under the anesthesia. One-two hours of anesthesia can be held by this method. Their abdominal and thoracic cavity was opened when they were under anesthesia, and for the metabolic parameter measurements, nearly 1 mL of blood was obtained from the apex of the heart. After that, 10-20 mL of ice-cold PBS was given from the apex of the heart, and the right atrium of the heart was incised to permit it to drain away both blood and PBS. In this way, both the clot formation and the remaining blood would be eliminated with the help of PBS (Maganto-Garcia et al., 2012). For euthanasia, the cervical dislocation procedure was applied to mice after PBS wash of the vascular system. The decapitation of mice accompanied it. The whole brain was obtained from the head of mice by using scissors, forceps, and spatula without disrupting the brain. The Petri dish, which included 0.1M ice-cold PBS, was on the ice. To get rid of contaminants, extracted intact brains were placed on a Petri dish and washed with ice-cold PBS (C. Carvalho & Moreira, 2017). First, the cerebellum and olfactory bulb were taken off using a scalpel blade. All brains were divided into two cerebral hemispheres for the Western blot experiments. The hippocampi were separated from the cortex by holding two hemispheres' medial

surfaces facing up and placing sterile spatula under the ventral part of the hippocampi. This process was applied to both hemispheres of the brain. After removing the hippocampus, the rest will be the cortex and those cortex tissues were collected into separate 1.5 mL Eppendorf tubes as left and right and snap-frozen into liquid nitrogen. This process should be as fast as possible to inhibit protein degradation. Then, cortex tissues were stored at -80°C until use.

2.3 Homogenization of Cortex Tissues

Cortex tissues were weighed before inserting them into 1.5 mL Eppendorf tubes. Approximately 700 μL of ice-cold homogenization buffer [includes 1 mM EDTA, 10 mM HEPES, 250 mM Sucrose, and Protein Inhibitor Cocktail, pH 7.4] was used per 100 mg tissue (Graham, 2002; Wirths, 2017). Protein samples were obtained from the right hemisphere of the cortex. For homogenization of cortex tissues, dounce glass homogenizer was used. After that, 1 mL of 26-gauge needle was used to pass samples through it 6-8 times on ice until all the particles were gone (Morse et al., 2006).

2.4 Protein Isolation from Cortex Tissues

To get rid of the homogenization buffer, centrifugation at 8000 X g for 6 minutes at 4°C was carried out. Then, supernatant was taken away and pellet of cortex samples was dissolved in 1000 μL of ice-cold radioimmunoprecipitation assay (RIPA) buffer [includes 50 mM Tris-HCl, pH 7.4, containing 150 mM NaCl, 0.25% (w/v) sodium deoxycholate, 1% NP-40, 1.0 mM EDTA and Protein Inhibitor Cocktail]. Sonication was carried out 5-6 times on ice at 50 amp for 0.5-1 cycle. Then, 30 minutes of incubation on ice was followed, but every 10 minutes, sample tubes were gently inverted upside down a few times for mixing. After that, centrifugation at 13000 rpm for 20 minutes at 4°C was done. Proteins were in the supernatant form, so it was

collected and aliquoted. After protein concentrations were measured as in the section of method 2.5, protein samples were stored at -80°C .

2.5 Bradford Assay

Unknown protein concentrations were measured with the help of Bradford protein assay where bovine serum albumin (BSA, A7906, Sigma Aldrich, St. Louis, MO, USA) was used as a standard protein ddH₂O was used as a blank. The procedure was followed according to the manufacturer's instructions on a 96-well plate. First, BSA standard curve was generated using varying concentrations of 2 mg/mL of standard protein, which was obtained from its dilutions given in Table.2.1 below:

Table 2.1 BSA Standards and Dilutions

	ddH ₂ O (μL)	BSA (2 mg/mL stock) (μL)	Final concentration ($\mu\text{g}/\mu\text{L}$)
Blank	5	0	0
Standard 1	4.5	0.5	0.2
Standard 2	4	1	0.4
Standard 3	3	2	0.8
Standard 4	2	3	1.2
Standard 5	1	4	1.6
Standard 6	0	5	2

Unknown protein samples were loaded as 0.5 μL protein and 4.5 μL ddH₂O mixture. Both the BSA standards and unknown proteins were calculated as 1:10 diluted. After all, BSA standards, blanks, and unknown protein samples were loaded into 96-well plate as two repeats, 250 μL Bradford reagent including Coomassie brilliant dye (B6916, Sigma-Aldrich, St. Louis, MO, USA) was added to all wells, including blanks. If there were any bubbles, they would be removed by syringe. Next, a 96-well plate was put on a shaker at 240 rpm for 30 seconds to make them mixed. After that, the plate was covered with aluminum folio and incubated for 10 minutes at RT. The

absorbance values were measured with a multi-plate reader (SpectraMax M5, Molecular Devices, Sunnyvale, CA, USA) at 595 nm when the incubation was over. A standard curve was drawn according to the average blank-subtracted 595 nm measurement of BSA standards versus their concentrations. Using the equation obtained from this curve, unknown protein concentrations were calculated. Since these results were 1:10 diluted, their concentrations were multiplied by 10.

2.6 Western Blot

Western blot is a technique for understanding the presence of certain proteins in a sample, and it uses specific antibodies to detect these certain proteins. Not only the presence of the proteins but also the size and relative amounts of the proteins can be understood from this technique (Mahmood & Yang, 2012).

2.6.1 Protein Samples Preparation

To be able to determine the protein levels of p-IRE1 α , IR- β , p-IRS-1, SAPK/JNK, p-SAPK/JNK, p-Akt in mice cortex tissues, 40 μ g protein samples were used. The amounts of proteins being used were determined with optimization experiments (20, 30, 40, 50 μ g protein samples, data not shown). To obtain 40 μ g proteins for each sample, calculations were obtained with Bradford assay results. Protein samples were loaded into the gels in cohorts. Because 10-well combs were used during Western blot analysis, each cohort of samples (for example, sample numbers 1, 8, 15, 22) would be seen on each side of the gels. Thus, more accurate results would be seen. According to the calculations, samples and dH₂O were mixed with a 2X loading buffer (Appendix B) in a 1:1 ratio to prepare protein samples. After that, these mixtures were vortexed, spin downed, and heated up to 95°C in the heater (mTOPS, DMB-2, Dry Block Heater) for 5 minutes to denature proteins. After the heating step, protein samples were spin downed again and put into an ice box for 5 minutes. Protein samples should be at RT

when they were loaded into gels. Next, protein samples were loaded into the polyacrylamide gels.

2.6.2 SDS-PAGE Gel Preparation

According to the molecular weights of the desired proteins, the percentage of resolving gel was determined as 10% polyacrylamide. Required amounts of chemicals were mixed in their ratios explained in Appendix B. Materials, except APS and TEMED, were mixed and stored at 4°C but for the gel preparation as APS and TEMED should be added fresh and fast one after the other. After a gentle vortex process, it was ready to be poured.

First, the gel casting was set up such that 1 mm glasses were placed into the gel casting apparatus by pushing the green wings outwards. Before pouring the resolving gel, the possibility of leakage should be tested with dH₂O. After that, dH₂O was removed, and 10% resolving gel was poured between the glasses until 0.5 cm space from the endpoint of the comb-line. To be able to prevent bubble formation and have a smooth surface, enough isopropanol was used on the top of the resolving gel. Polymerization of the gel could be checked by observing the remaining resolving gel buffer inside the flask. After the gel was polymerized, isopropanol was removed by pouring it, and the remaining part was moved away with the help of a paper towel. Then, 5% polyacrylamide was prepared as a stacking gel (Appendix B). Again, APS and TEMED were added last, and they were quickly mixed by inverting the flask a few times. After pouring the stacking on the top of the resolving gel, bubbles should be removed quickly if any exist, and the 10-well comb was placed immediately. The gel was left for approximately 20 minutes for the polymerization process, which may be used immediately or stored at 4°C for approximately two weeks.

2.6.3 Running SDS-PAGE Gels

To perform protein gel electrophoresis, the gel placed inside the electrophoresis apparatus chamber, Mini-PROTEAN Tetra Cell System (BioRad, CA, USA) was used for electrophoresis which was filled with fresh 1X SDS buffer (Appendix B) and outside of the gel within the chamber may be filled with used/fresh 1X SDS buffer; if used buffer was utilized, it should not be used more than 2-3 times. Next, the comb was removed slowly without damaging the wells, and then the wells were cleaned using a syringe. Always 1.2 μ L pre-stained protein ladder (26619, Thermo Scientific, 10-250 kDa) was loaded into the first and last wells to assess the molecular masses of proteins in the gel, and 40 μ g protein samples were loaded between the ladder wells as two cohorts. Then, the tank's lid was closed, and the lid was connected to the power source, which is designed to conduct current through the buffer solution. The gels were run at 80 volts for approximately 30 minutes to ensure they were lined up at the resolving gel. When ladder bands started to be separated, voltages were increased to 100 volts for around 120 minutes until the loading dye was seen at the bottom of the gel.

2.6.4 Blotting: Transfer of Proteins to PVDF Membranes

Separated proteins were transferred/blotted to polyvinylidene fluoride (PVDF) membrane labeled from its left and right sides and incubated in 100% methanol for 30 seconds to 3 minutes to activate it. Buffers to be used should be cold unless it is indicated. To equilibrate, the membrane was soaked into 1X transfer buffer (Appendix B) for at least 10 minutes. Before blotting started, sponges, blotting papers, and transfer cassettes were pre-wet in a 1X transfer buffer for 10 minutes. After electrophoresis, glasses were separated from each other with the help of a spatula, and the gel was released into a container filled with transfer buffer, and the stacking gel was cut off. The 'sandwiching assembly' was implemented (Figure 2.2) in an order that the movement of proteins can be transferred onto the PVDF membrane. It should

be noted that there should be no bubbles between the membrane and the gel. PVDF membrane was placed on the side of the positive anode, and the gel should be toward the negative cathode since negatively charged proteins would move from the negative to the positive end. Then, the cassette was placed into the Mini-Trans-blot Electrophoretic Transfer Cell system (BioRad, CA, USA), and the tank was filled with 1X transfer buffer. Blotting was carried out in a cold room or on ice for 90 minutes at 100 V with that electricity proteins were moved from the gel onto the surface of the membrane and become tightly attached. After transfer, the total protein on the membrane is sometimes assessed with a protein stain, Ponceau S, to check the transfer efficiency.

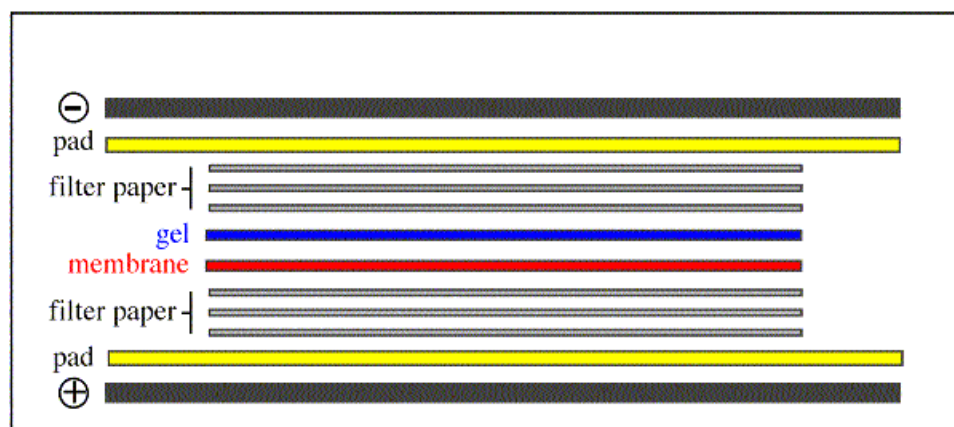


Figure 2.2. Representative structure of transfer sandwich system of Western blot

2.6.5 Blocking, Primary and Secondary Antibody Detection

Next, the membrane was blocked to prevent any non-specific binding of antibodies. After the transfer process, the membrane was removed from the transfer cassette and washed in 0.1% Tris-buffered saline Tween-20 (TBS-T). According to the molecular weights of the desired proteins, the blot was cut horizontally by checking the ladder bands, and the protein side of the membrane should face up. After optimization, the appropriate blocking buffer for every single antibody was TBS-T, including 5% BSA

at RT for 1 hour on a shaker. After the blocking step, membranes were washed with 0.1% TBS-T for 10 minutes. Next, primary antibody incubation on the blocked membrane was carried out at 4°C overnight. Appropriate buffers (using either BSA or milk) and dilutions were determined for primary and secondary antibodies during optimization experiments. Primary antibodies which were used in this study are: anti-IR-beta (Cell Signaling Technologies (CST), cat#3025, 1:1000 BSA), anti-SAPK/JNK (CST, cat#9052, 1:1000 BSA), anti-p-SAPK/JNK (phospho Thr183/Tyr185) (CST, cat#9255, 1:500 BSA), anti-p-IRE1 α (phospho Ser724) (abcam, cat#48187, 1:1000 BSA), anti-p-IRS-1(phospho Ser307) (GeneTex, cat#133848, 1:1000 BSA) , anti-p-Akt (phospho Ser473) (CST, cat#4060, 1:1000 BSA), anti- α -tubulin (Santa Cruz, cat#5286, 1:5000 BSA). After overnight incubation, primary antibodies were collected, and membranes were washed 3x10 minutes with 1X TBS-T at RT on the shaker. Then, membranes were incubated with suitable horseradish peroxidase (HRP)-conjugated secondary antibodies (Santa Cruz, cat#2357, 1:10.000 BSA and Santa cruz, cat#2005, 1:10.000 BSA) for 1 hour at RT, then, secondary antibodies were collected, and membranes were washed three times for 10 minutes at RT.

2.6.6 Chemiluminescent Detection

Since the secondary antibody was HRP-conjugated, when the substrate was given a chemiluminescent signal that would be obtained from the reaction between enzyme and substrate, and light which was emitted from the substrate can be detected by the chemiluminescence imaging system. For the chemiluminescent detection ECL kit (BioRad, #1705061, USA) was used that contained two solutions: luminol/enhancer and peroxide. These two solutions were mixed in a 1:1 ratio, and the membrane was incubated with it for 5 minutes in the dark. Later, the excess mixture was collected, and the membrane was inserted into a transparent plastic file to visualize with ChemiDocTM XRS+ imaging system (BioRad, CA, USA) with the help of ImageLab software (BioRad, CA, USA).

2.6.7 Band Intensity Quantification

The ImageJ program (NIH, Bethesda, MD, USA) was used for the band intensity quantification. First, a rectangular shape was selected to encompass the first band in a row, and the same sized rectangular shape was used to enumerate the following bands in the same row. After selecting all bands, band intensities were measured with the ImageJ program and recorded in an Excel sheet. Next, the average of the intensities was calculated, and each band intensity was divided into the average band intensity in the same blot. The process was called gel normalization. The same procedure was applied to the internal control using anti-Tubulin to obtain tubulin gel normalization. When the gel normalization of each protein was divided into the tubulin normalization, standard normalization values were obtained (Karoglu et al., 2017).

2.6.8 Statistical Analysis

In Western blot analysis, four groups of genotypes (C57BL/6 and ApoE^{-/-}) and diets (Chow and Western diets) and their biological replicates (n=7) were analyzed. To minimize the experimental variations, samples were run at least twice as a technical replica for each antibody (n=2 for the p-Akt, but the rest, n=3). Also, each cohort samples were run on both sides of the gel to get more accurate results. After the band intensity quantification process, the SPSS program was used to test the normality and homogeneity so presumptions for parametric tests would be controlled (IBM Corp. Released 2017, n.d.). Then, a two-way ANOVA test was applied as a statistical analysis to understand the effects of diet (Chow diet and Western diet) and genotype (C57BL/6 mice and ApoE^{-/-} mice) on the protein levels of each individual marker. Statistically significant value was accepted as *p≤0.05.

CHAPTER 3

RESULTS

3.1 Bradford Assay Result

According to the BSA calibration curve, unknown protein concentrations were calculated using the equation obtained from the curve (Figure 3.1). After optimization assays, 40 μg of protein samples were used in all of Western blot analysis.

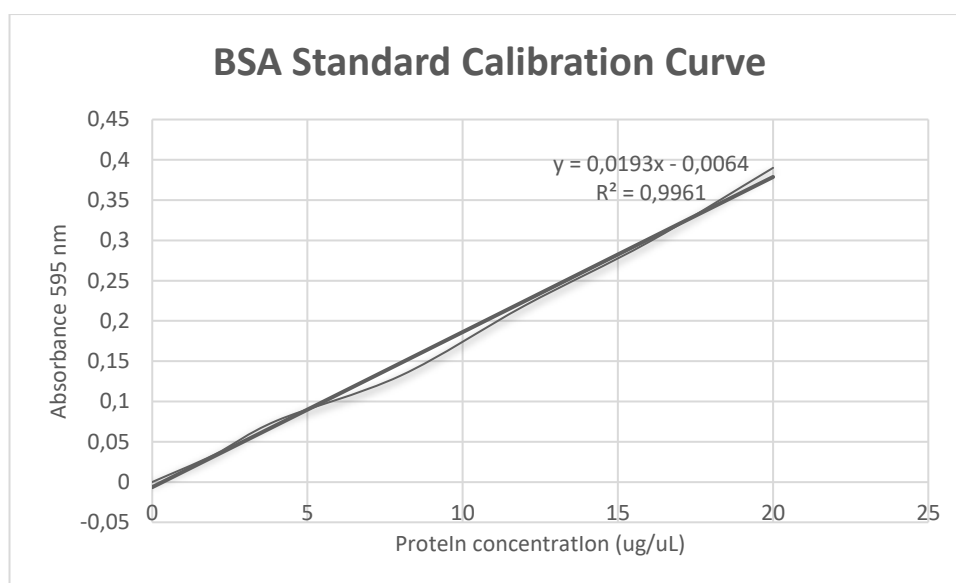


Figure 3.1. BSA Standard Calibration Curve

3.2 Effects of high fat/cholesterol diet on IR- β protein levels

The insulin signaling pathway starts with the ligand binding to IR/IGF-1R. The ligand binds to the alpha subunit of IR, and autophosphorylation occurs at the beta subunit (Wilden et al., 1992). To investigate the effects of high fat/high cholesterol diet on the IR- β protein levels, Western blot analysis was performed in the cerebral cortex of C57BL/6 (WT) and ApoE^{-/-} mice. Mice fed with chow/Western diet for 16 weeks and afterwards they were sacrificed to obtain brain tissues. Proteins were isolated from cortex tissue of C57BL/6 and ApoE^{-/-} mice fed with either chow or Western diet (n=7, biological replicates) and relative IR- β protein levels were quantified. Based on the normalized data, there was no statistically significant difference between both diet ($p>0.05$) and genotype ($p>0.05$) for the IR- β expression levels in the cortex (Figure 3.2). (The whole blot image could be seen in Appendix C, Figure C.1).

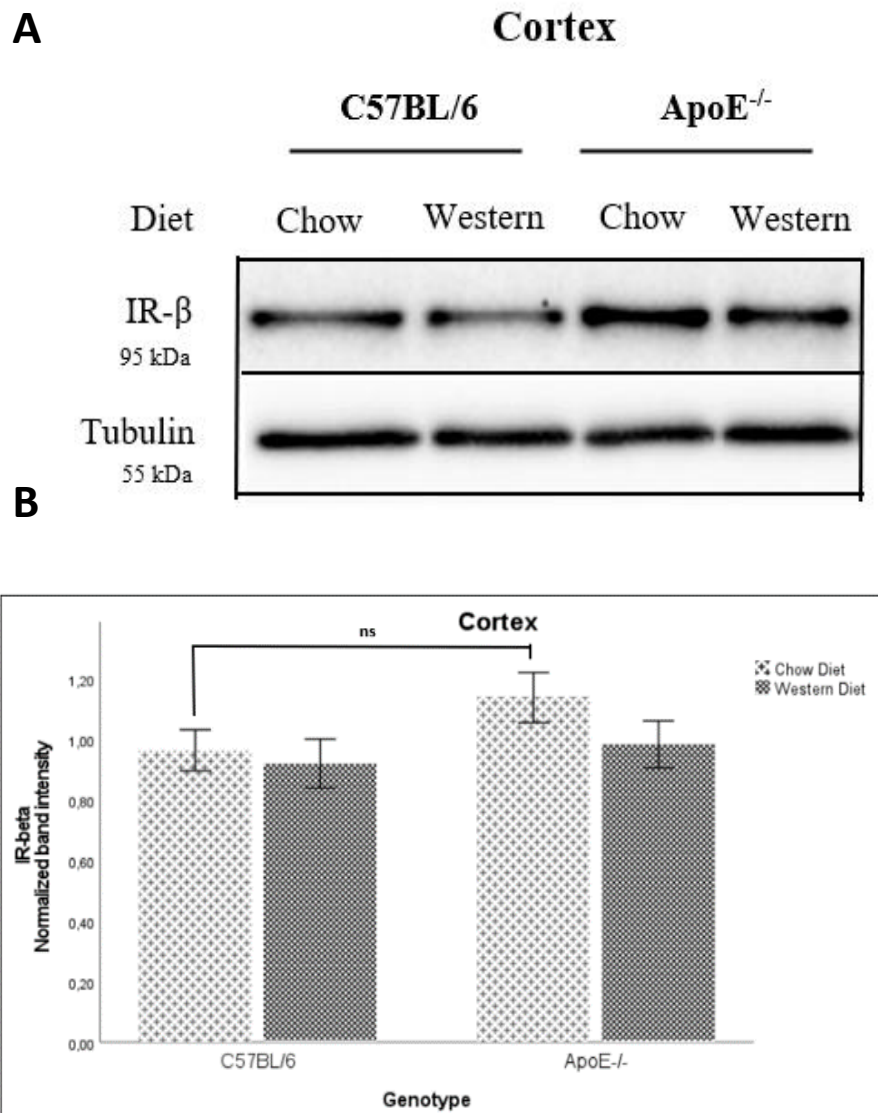


Figure 3.2. Western blot analysis of anti-IR-β levels in the cerebral cortex. Data showed the effects of HF/HC diet on IR-β levels. 40 μg of total cortex protein samples were loaded to the wells. (A) Representative immunoblot indicated that anti-IR-β was at 95 kDa and anti-tubulin as a loading control was at 55 kDa. (B) the quantification of immunoblots (n=3, technical replicates) demonstrated protein level comparison of IR-β among the groups. Tubulin normalization was performed to calculate IR-β levels in the cortex. Two-way ANOVA was used to determine significance values. Each bar indicates the mean ± SEM.

3.3 Effects of high fat/cholesterol diet on p-IRE1 α protein levels

In order to determine UPR activation through the IRE1 α arm, p-IRE1 α protein levels in the cortex were analyzed. The data analysis showed no significant differences between the main effect of chow and Western diet on p-IRE1 α protein levels in the cerebral cortex ($p>0.05$). However, the main genotype was effective on the protein levels of p-IRE1 α in the cortex (** $p<0.01$). p-IRE1 α expression was significantly higher in ApoE^{-/-} mice when they fed with chow diet compared to C57BL/6 mice with chow diet (** $p<0.01$). Even though the decreased protein expression was seen in ApoE^{-/-} mice fed with the Western diet with respect to ApoE^{-/-} mice fed with chow diet, those levels was nearly off the statistically significance ($p=0.052$). The highest p-IRE1 α protein levels were observed in ApoE^{-/-} mice fed with the Western diet with respect to others (Figure 3.3). (The whole blot image could be seen in Appendix C, Figure C.2).

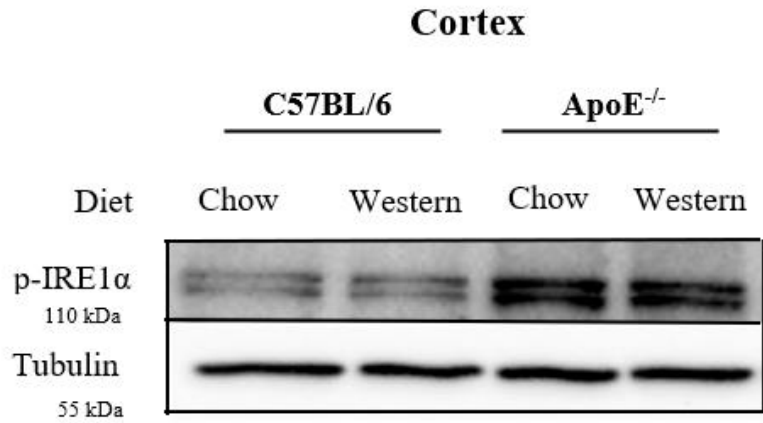
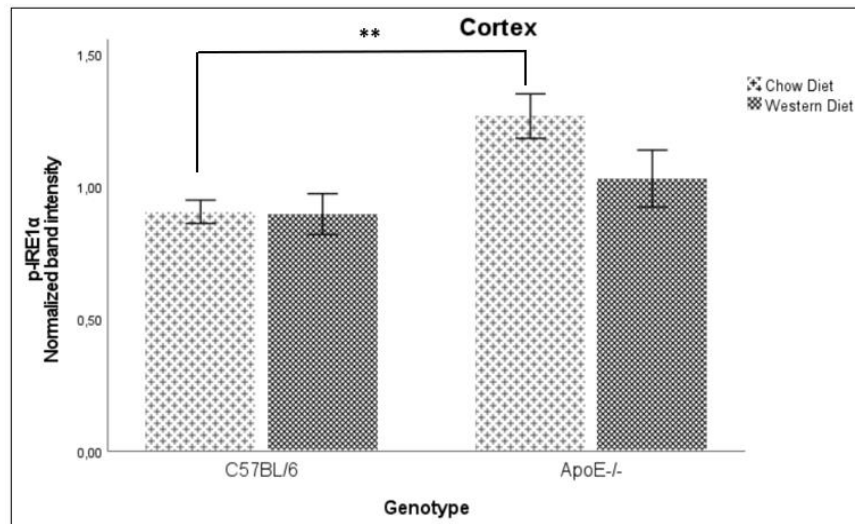
A**B**

Figure 3.3. Western blot analysis of anti-p-IRE1 α level in cerebral cortex. 40 μ g protein samples were used. (A) Representative immunoblot showed that anti-p-IRE1 α were detected at 110 kDa and anti-tubulin at 55 kDa. (B) the quantification of immunoblots (n=3, technical replicates) demonstrates protein level comparison of p-IRE1 α among the groups using tubulin normalization. Two-way ANOVA was used to determine significance values. Each bar indicates the mean \pm SEM, ** p <0.01

3.4. Effect of high fat/high cholesterol diet on SAPK/JNK protein levels

To determine the effect of HF/HC diet on the total SAPK/JNK protein levels and both upper and lower bands of SAPK/JNK were calculated separately since the protein level change in upper and lower bands was different (Figure 3.4). SAPK/JNK protein levels were detected using Western blot data analysis. Main effects of both diet (** $p < 0.01$) and genotype (***) ($p < 0.001$) on the protein levels of SAPK-JNK upper band were significant. The SAPK/JNK upper band levels were significantly increased in ApoE^{-/-} mice compared to C57BL/6 mice with a chow diet (***) ($p < 0.001$). Two-way ANOVA analysis showed that there was statistically significant increase in Western diet of ApoE^{-/-} mice compared to Western diet of C57BL/6 mice (** $p < 0.01$). Additionally, SAPK/JNK upper band levels among ApoE^{-/-} mice were significantly lower in mice fed with the Western diet in respect to that of chow diet (***) ($p \leq 0.001$) (Figure 3.4B).

Western blot analysis revealed that both main diet ($p \leq 0.05$) and genotype (***) ($p < 0.001$) had significant effects on SAPK/JNK lower band protein levels. Normalized data implicated that SAPK/JNK lower band protein levels were significantly increased in the chow diet of ApoE^{-/-} mice compared to C57BL/6 mice (***) ($p < 0.001$). Nevertheless, there was a statistically significant decrease in SAPK/JNK lower band protein levels in the cortex of Western diet-fed ApoE^{-/-} mice compared to the chow diet-fed ApoE^{-/-} group (***) ($p < 0.001$) (Figure 3.4C).

Data indicated that the main diet effect on the total protein amount of SAPK/JNK was not significant ($p > 0.05$). However, genotype affected significantly (***) ($p < 0.001$) on the total protein levels of SAPK/JNK in the cerebral cortex. Further diet-genotype interaction analysis revealed that SAPK/JNK total band protein level was significantly increased in ApoE^{-/-} mice fed with chow diet compared to C57BL/6 mice with the same diet (***) ($p < 0.001$). Moreover, there were statistically significantly lower amounts of SAPK/JNK total band protein levels in ApoE^{-/-} mice fed with Western diet than ApoE^{-/-} mice fed with chow diet (** $p < 0.01$) (Figure 3.4D). (The whole blot image could be seen in Appendix C, Figure C.3).

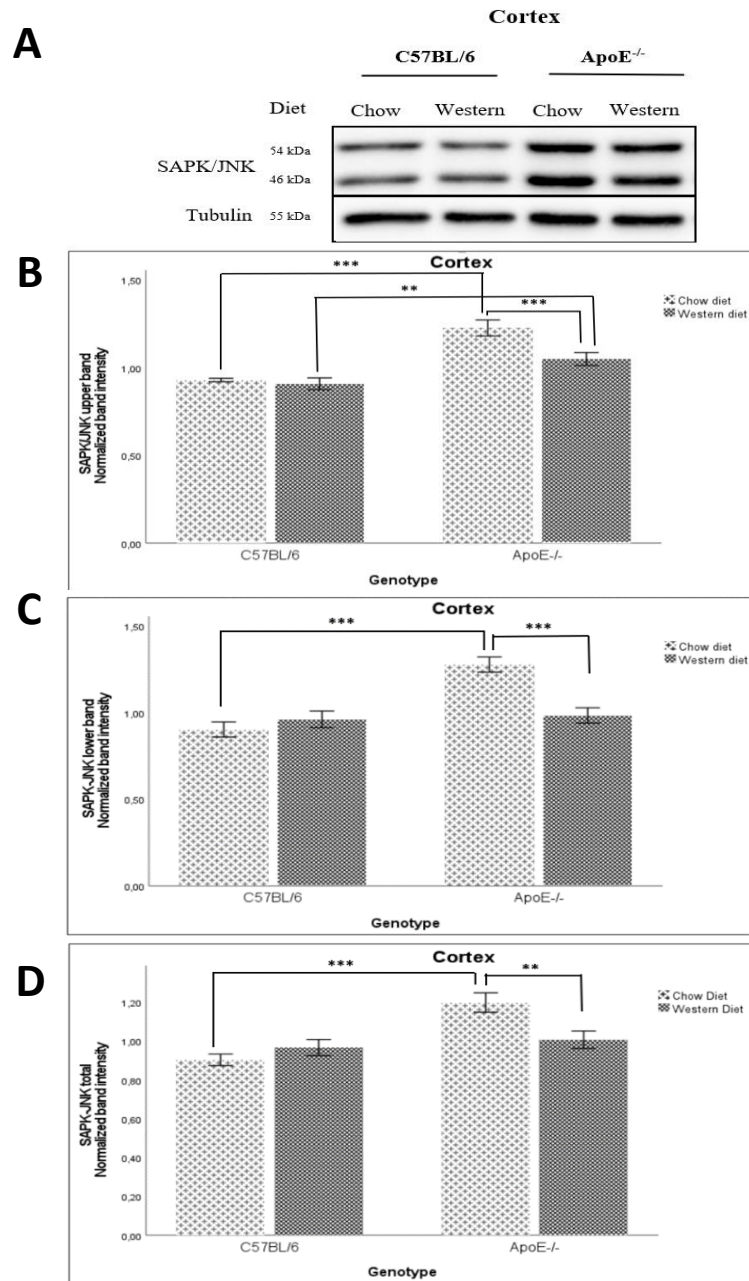


Figure 3.4. Western blot analysis of anti-SAPK/JNK in cerebral cortex. Effects of HF/HC diet on SAPK/JNK upper band, lower band, and total band protein levels were determined. 40 μ g protein samples were used. (A) Representative immunoblot images of anti-SAPK/JNK; the upper band were detected at 54 kDa, the lower band detected at 46 kDa and anti-tubulin at 55 kDa. The quantification of immunoblots (n=3, technical replicates) demonstrates protein level comparisons of (B) the SAPK/JNK upper band, (C) the SAPK/JNK lower band, and (D) total band of SAPK/JNK. Tubulin normalization was performed to calculate SAPK/JNK upper band, lower band, and total band protein levels separately in the cortex. Two-way ANOVA was used to determine significance values. Each bar indicates the mean \pm SEM, ** p <0.01, *** p <0.001.

3.5. Effect of high fat/high cholesterol diet on p-SAPK/JNK protein levels

Based on data obtained from Western blot results, the diet did not alter the protein levels of the p-SAPK/JNK upper band significantly in the cerebral cortex of C57BL/6 and ApoE^{-/-} groups. On the other hand, the main genotype had a significant impact on that protein levels (** $p < 0.01$). Pairwise comparisons indicated that the Western diet markedly increased the protein levels of p-SAPK/JNK upper band in the C57BL/6 mice compared to the chow diet-fed group ($p < 0.05$). However, the Western diet significantly decreased the p-SAPK/JNK upper band levels in ApoE^{-/-} group compared to the same genotype with the chow diet ($p < 0.05$). There was a statistically higher level of p-SAPK/JNK upper band proteins in ApoE^{-/-} mice fed with chow diet compared to C57BL/6 mice fed with chow diet (*** $p < 0.001$) (Figure 3.5B).

According to data, the main effect of diet (** $p < 0.01$) and genotype (** $p < 0.01$) were statistically significant on the p-SAPK/JNK lower band levels in the cerebral cortex. Pairwise comparisons showed that in C57BL/6 mice, the Western diet markedly increased the protein levels of the p-SAPK/JNK lower band compared to the chow diet (*** $p < 0.001$). On the other hand, there was no difference in ApoE^{-/-} mice between the chow and Western diet ($p > 0.05$). Furthermore, p-SAPK/JNK lower band expression level was significantly higher in the chow diet for ApoE^{-/-} mice than C57BL/6 mice (*** $p < 0.001$) (Figure 3.5C).

Western blot analysis showed that the main effect of diet on p-SAPK/JNK total protein levels was not significant ($p > 0.05$), whereas the main effect of genotype was significant (** $p < 0.01$). p-SAPK/JNK total protein levels were significantly higher in C57BL/6 mice on Western diet than on chow diet group ($p < 0.05$). However, there was no significant change between ApoE^{-/-} mice on chow and Western diet groups ($p > 0.05$). According to the pair-wise comparison results, there were markedly increased p-SAPK/JNK total protein levels in ApoE^{-/-} mice fed with chow diet compared to C57BL/6 mice with chow diet (*** $p < 0.001$). Although p-SAPK/JNK total protein level tended to decrease in ApoE^{-/-} mice fed with the Western diet, no

statistically significant result was obtained in ApoE^{-/-} mice based on the diet ($p>0.05$) (Figure 3.5D.). (The whole blot image could be seen in Appendix C, Figure C.4).

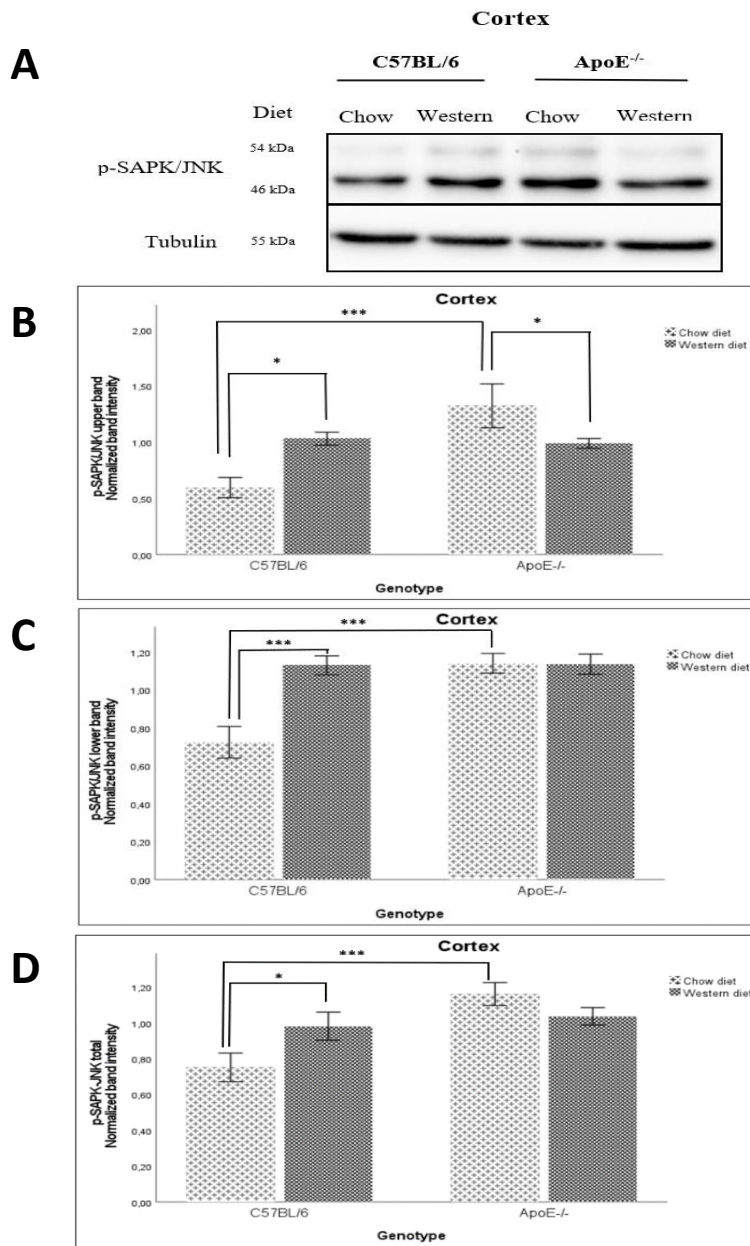


Figure 3.5. Western blot analysis of anti-p-SAPK-JNK in the cerebral cortex. Effects of HF/HC diet on p-SAPK/JNK upper band, lower band, and total band protein levels were determined. 40 μ g protein samples were loaded to each well. (A) Immunoblot image represented that anti-p-SAPK/JNK detected- upper bands at 54 kDa, lower bands at 46 kDa. As an internal control, anti-tubulin was used at 55 kDa. The quantification of immunoblots (n=3, technical replicates) demonstrates protein level comparison of (B) p-SAPK/JNK upper band, (C) lower band, and (D) total bands among the groups. Tubulin normalization was used to calculate p-SAPK/JNK upper band, lower band, and total band protein levels separately in the cortex. Two-way ANOVA was used to determine significance values. Each bar indicates the mean \pm SEM, * p <0,05, *** p <0.001.

3.6. Effect of high fat/high cholesterol diet on p-IRS-1 protein levels

The presence of insulin signaling impairment, p-IRS-1 protein levels were examined, and statistical analysis demonstrated that the main effect of diet on p-IRS-1 protein levels was not significant ($p>0.05$), whereas the main genotype had significantly impacted ($**p<0.01$). Although p-IRS-1 protein levels tended to increase in the Western diet of C57BL/6 group, there was no significant difference between chow and Western diet groups ($p>0.05$). Instead, lower level of p-IRS-1 in the ApoE^{-/-} Western diet group compared to the chow diet group ($**p<0.01$). In addition, p-IRS-1 protein levels were markedly increased in the ApoE^{-/-} chow diet group compared to the C57BL/6 chow diet group ($***p<0.001$) (Figure 3.6.) (The whole blot image could be seen in Appendix C, Figure C.5).

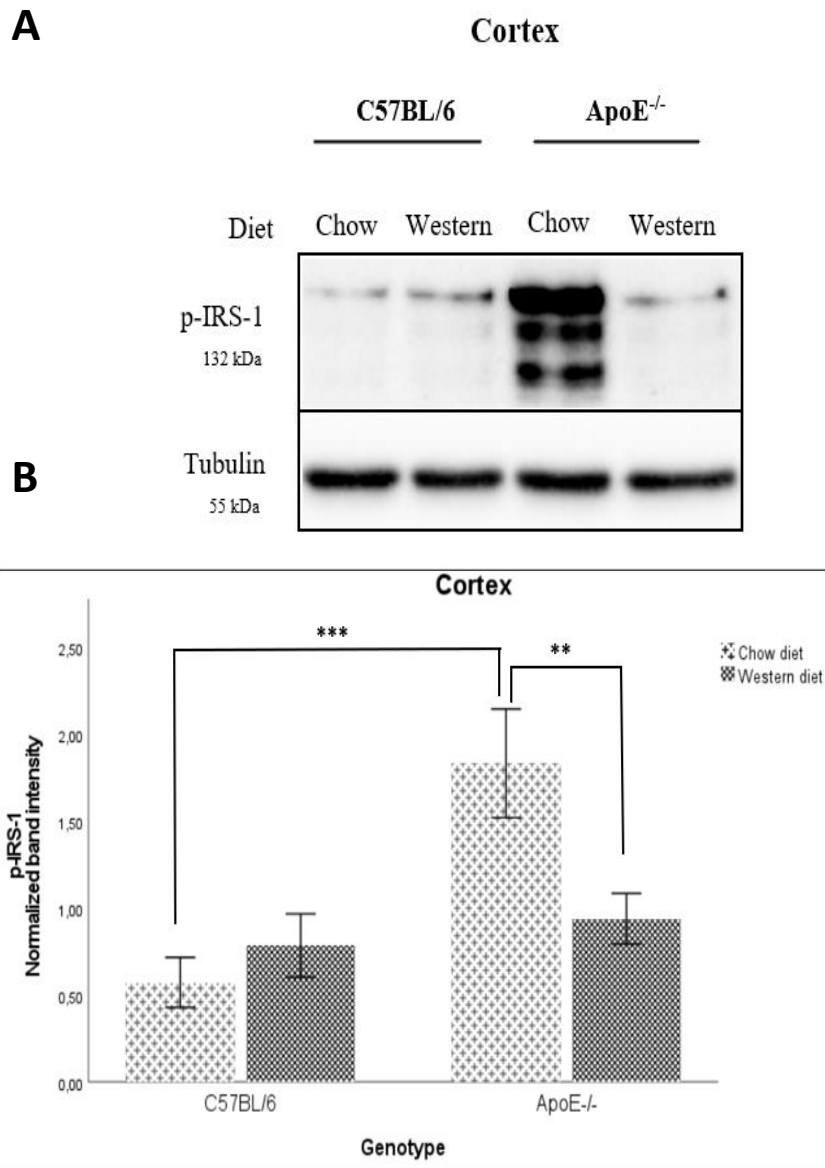


Figure 3.6. Western blot analysis of anti-p-IRS-1 levels in cerebral cortex. 40 μ g protein samples were used. (A) Representative immunoblot indicated that anti-p-IRS-1 bands were detected at 132 kDa and anti-tubulin at 55 kDa. (B) the quantification of immunoblots (n=3, technical replicates) demonstrates protein level comparison of anti-p-IRS-1 for the groups. Tubulin normalization was done to calculate p-IRS-1 protein levels in the cortex. Two-way ANOVA was used to determine significance values. Each bar indicates the mean \pm SEM, ** p <0.01, *** p <0.001.

3.7.Effect of high fat/high cholesterol diet on p-Akt protein levels

p-Akt protein levels were analyzed to further identify the insulin signaling impairment. Data showed that main diet did not make any effect on p-Akt levels ($p>0.05$), but the main genotype was significantly changed p-Akt levels ($***p<0.001$). Pair-wise analysis indicated that Western diet significantly increased the p-Akt levels in the C57BL/6 mice compared to chow diet ($*p\leq 0.05$). Oppositely, p-Akt protein level was significantly lower in the ApoE^{-/-} Western diet group compared to chow group ($**p<0.01$). The ApoE^{-/-} chow diet group had significantly higher p-Akt protein levels compared to the C57BL/6 chow diet group ($***p<0.001$). p-Akt levels tended to increase in ApoE^{-/-} Western diet group compared to C57BL/6 Western diet group ($p=0.053$) (Figure 3.7) (The whole blot image could be seen in Appendix C, Figure C.6).

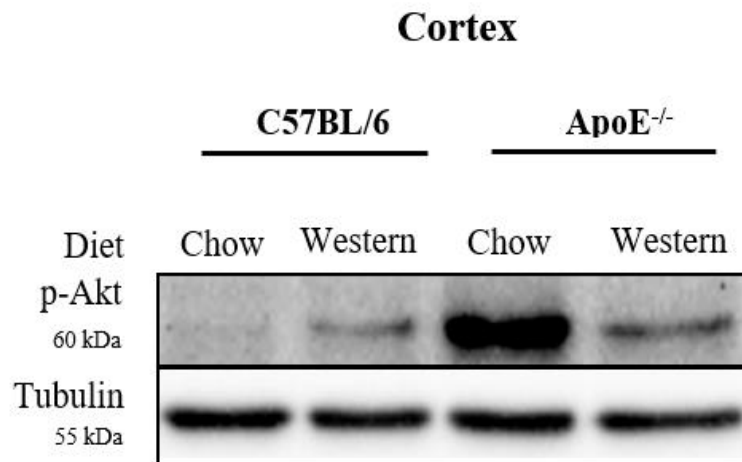
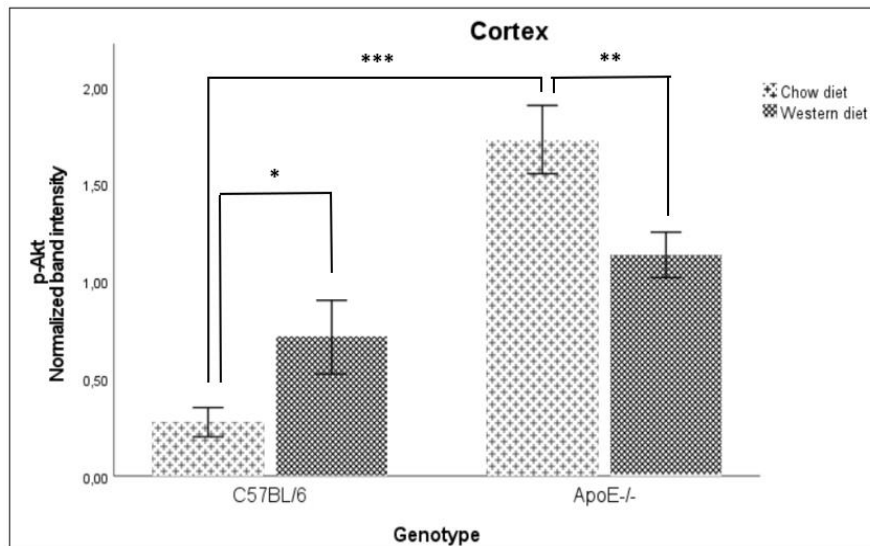
A**B**

Figure 3.7. Western blot analysis of anti-p-Akt protein levels in cerebral cortex. 40 μ g protein samples were used. (A) Representative immunoblot indicates that anti-p-Akt bands were detected at 60 kDa and anti-tubulin 55 kDa. (B) the quantification of immunoblots (n=2, technical replicates) demonstrates protein level comparison of p-Akt among the groups. Tubulin normalization was done to calculate p-Akt protein levels in the cortex. Two-way ANOVA was used to determine significance values. Each bar indicates the mean \pm SEM, * p <0,05 ** p <0.01, *** p <0.001.

3.8. The Working Model

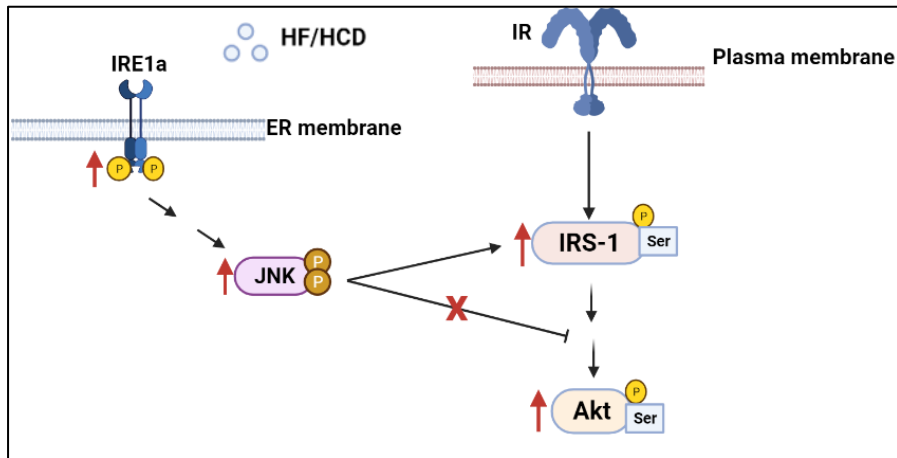


Figure 3.8. The Working model of this study.

CHAPTER 4

DISCUSSION

Due to the alteration in lifestyle and diet, obesity prevalence increases worldwide. HFD is the most crucial cause of obesity. High consumption of elevated FFAs in the bloodstream may induce low-grade inflammation and result in insulin resistance, insulin signaling impairment, and glucose homeostasis disruption (Gökhan S Hotamisligil, 2006). Significant studies showed that Western diet was linked to insulin resistance and T2DM (Gabbouj et al., 2019). CNS is one of the mostly affected parts of the body from obesity (Wotton & Goldacre, 2014). The cognitive decline was associated with obesity, yet its mechanisms have not been elucidated (Liang et al., 2015).

Hyperlipidemia has emerged with obesity, is the major risk for developing CVDs. One-third of the world's population has deceased from CVDs, and increasing population is suffering from it (Shattat, 2014). Therefore, mechanisms underlying hyperlipidemia needs to be clarified to prevent the development of the metabolic diseases via targeting the crucial molecules responsible for its progression. Cholesterol and lipid metabolism in the brain is crucial and tightly controlled with ApoE-mediated lipoprotein transport (Mahley, 2016). In addition to the inflammatory response to the raised amount of lipid molecules in the body, ROS are also produced and lead to ox-LDL molecules, which may lead to plaque formation, subsequently may result in CVDs (FERENCE et al., 2017). Therefore, it is clear that the brain is highly affected by lipid metabolism and more prone to develop neurodegenerative diseases.

Activation of cellular stress and inflammatory response in the cell are associated with obesity (Özcan et al., 2004). Although the origin of the stress has not been elucidated yet, ER is the critical organelle having a role in cellular stress response (Hampton, 2000). Glucose or nutrient privation, viral infections, lipids, risen synthesis of

secretory proteins, and accumulation of misfolded proteins are the several conditions that lead to ERS (Ma & Hendershot, 2001), which subsequently leads to UPR activation (Ron & Walter, 2007). Previous studies revealed that peripheral insulin resistance could be induced by ERS in the hypothalamus due to oxidative stress (X. Zhang et al., 2008) and leptin resistance (Lale Ozcan et al., 2009). Also, insulin receptor signaling was impaired by ERS-caused activation of JNK in the liver, and ERS and insulin receptor signaling interaction was demonstrated in the hippocampus and frontal cortex of the obese rats (Liang et al., 2015). However, this study was unique in terms of the animal model (ApoE^{-/-}) and the applied HF/HC diet. In our study, C57BL/6 (WT) and ApoE^{-/-} as transgenic mice were used and the effects of the HF/HC diet on the activation of IRE1 α arm of the ERS and insulin signaling pathway were investigated in the cerebral cortex.

It was also shown that LDL cholesterol and triglycerides as the marker for hyperlipidemia/hypercholesterolemia were increased in the blood levels of C57BL/6 mice fed with HFD (Thirumangalakudi et al., 2008). Whether this result was escorted with insulin resistance, they applied high fat/cholesterol (HFC) diet (21% fat and 1.25% cholesterol) to 4 months of C57BL/6 mice for two months. After two months when they did glucose tolerance test, they concluded that mice with HFC diet showed insulin intolerance which was the indicator for peripheral insulin resistance (Bhat & Thirumangalakudi, 2013). We performed the protein expression levels of IR- β in the cerebral cortex of C57BL/6 and ApoE^{-/-} mice fed with either standard chow or Western diet and showed no statistically significant change in the receptor expressions as expected. It was beneficial to determine the receptor expression levels since the downstream molecules (p-IRS-1 and p-Akt) in the insulin signaling pathway were investigated. When the insulin concentration increases, IR degradation is stimulated due to highly occupied receptors (Gavin et al., 1974). There was a slight decrease in IR- β levels of Western diet-fed mice groups. Therefore, for further studies, insulin levels may be tested in the cerebral cortex of these mice groups to have more consistent results. It is well-known that insulin can cross the BBB. However, the amount of

insulin that passes through the BBB strongly depends on the species (Stephen C Woods et al., 2003). For example, when rodents were given insulin peripherally, less than 1% of the insulin was detected in the CNS of these animals (STEPHEN C Woods & Porte Jr, 1977). It was shown that in the conditions of obesity, fasting, and aging, insulin transport to the CNS decreased, whereas, in some T2DM models, insulin transport was increased to the CNS. That is why, since little or no insulin is synthesized in the CNS, insulin levels in the brain may not reflect the peripheral conditions because of the unresolved molecular identity of this transport of insulin (Banks, 2004).

Previous studies showed that HFD (40% fat) induced a significant increase in PERK and downstream molecule eIF2 α phosphorylation in rats' hippocampus and frontal cortex (Liang et al., 2015). However, in our previous studies, there was no significant change in p-PERK and p-eIF2 α levels in the hippocampus but in the cerebral cortex of ApoE^{-/-} chow diet group significantly increased p-PERK protein levels were observed compared to C57BL/6 chow diet group (* $p < 0.05$). Also, in ApoE^{-/-} mice, p-eIF2 α levels were significantly increased in both diet types, suggesting that UPR was activated in the cortex of ApoE^{-/-} mice (Mengi, 2019). We studied another arm of the UPR in the ER, IRE1 α , which was not studied before in the literature with the animal groups in this study.

Previous studies revealed that ERS and subsequent activation of UPR had a major role in the development of obesity-caused insulin resistance and T2DM. However, ERS and UPR activation mechanisms in obesity have not been elucidated yet. According to the current evidence, excess nutrient exposure, FFAs, inflammatory cytokines, and mTOR pathway activation contribute to the ERS and UPR activation (Özcan et al., 2006). In a study, after showing the PERK activation, they wanted to test whether IRE1 α was activated in the hypothalamus of HFD (60% fat) fed mice, and they showed that there was significantly increased p-IRE1 α at Ser723 residue in the hypothalamus of HFD mice compared to the normal diet-fed group (Lale Ozcan et al., 2009). Also, it was shown that p-IRE1 α at Ser724 residue was markedly increased in the hippocampus and frontal cortex of HFD (40% energy from fat) rats in comparison with

control ones (Liang et al., 2015). In our study, a significant increase in p-IRE1 α (Ser724) level was demonstrated in the cerebral cortex of ApoE^{-/-} chow diet group in comparison to C57BL/6 mice. Yet, diet effect was not detected on the p-IRE1 α protein level, which was not expected. According to the literature, a chow diet was not enough to induce hyperlipidemia in C57BL/6 mice, so HF/HC diet like the Western diet was needed (Schreyer et al., 1998). It is because, with the help of HF/HC diet, circulation of FFAs is increasing in the bloodstream to induce ERS. Surprisingly, in C57BL/6 mice fed with chow diet, p-IRE1 α expression was approximately the same with the Western diet. It meant that there was no ERS and UPR activation with Western diet or there was already UPR activation in C57BL/6 mice fed with chow diet and increase in HF/HC effect was not effective on the p-IRE1 α expression. Another possibility was that diet duration was insufficient to induce IRE1 α activation in C57BL/6 Western diet group. The previous studies showed that, in ApoE^{-/-} mice fed with chow diet, the markedly increased level of p-IRE1 α may correspond to the impact of cholesterol in the blood. It is because in transgenic mice, plasma lipoprotein clearance was impaired (Plump & Breslow, 1995). Therefore, severe hypercholesterolemia, increased UPR activation and as a result increased p-IRE1 α expression in that group were hypothesized. Likewise, it was also expected even more p-IRE1 α levels in ApoE^{-/-} mice fed with Western diet because of accelerated cholesterol levels in the blood. However, ApoE^{-/-} Western diet group showed tendency towards decrease in p-IRE1 α levels, but decrease was not statistically significant. Maybe, the diet duration was excess (16 weeks), and the maximum tolerable ERS was seen in ApoE^{-/-} mice fed with the chow diet. Afterward, cells might have undergone apoptosis. Maybe, that is why the p-IRE1 α level was decreased. In our previous studies, apoptosis activation was tested by measuring the levels of CHOP in the same experimental setup but there was a tendency to decrease in CHOP levels in the cerebral cortex of ApoE^{-/-} Western group (Mengi, 2019). During transient stress, IRE1 α inhibits CHOP expression to support cell survival (Urano et al., 2000). However, based on the literature that prolonged IRE1 α is linked to apoptosis through TRAF2 and Ask1 interaction for the JNK activation and leading to NF- κ B expression and, in the end, TNF- α expression

(Estornes et al., 2014). To clarify this hypothesis, apoptosis markers induced by the IRE1 α pathway can be analyzed for further studies.

ER is the main site where sensing, integrating and transmitting metabolic signals take place in the cell. Those signals can be in the form of stress signals like JNK, IKK, and other pathways (Özcan et al., 2004). Moreover, cellular insulin resistance is induced by ERS through the IRE1 α -dependent activation of JNK (Sari et al., 2010). As mentioned before, IRE1 α can interact with TRAF2 and Ask1 to activate JNK (Estornes et al., 2014). Under pathological conditions, the function of JNK depends on the cell type and stimuli. For example, in neuronal cells, JNK activation can result in apoptosis (Xu et al., 2018). Therefore, in this study, the activation of JNK was tested. JNK had three isoforms which are JNK1, 2, and 3. JNK1 is also known as p46 (lower band), JNK2 is also known as p54 (upper band), and JNK3 is also known as p493F12 kinase (Gupta et al., 1996) (the name is coming from the monoclonal antibody which identifies JNK3 firstly (Mohit et al., 1995). Also, p46 JNK3 α 1 and p54 JNK3 α 2 forms of JNK3 are reported due to alternative splicing (Nakano et al., 2020).

The hippocampus and the frontal cortex of HFD fed rats that there was no significant change in JNK1 (p46, lower band) and JNK2 (p54, upper band) levels. However, in p-JNK1 (lower band) and p-JNK-2 (upper band) levels, there was a significant increase in HFD rats compared to control groups in both the hippocampus and the cortex (Liang et al., 2015). In this study, SAPK/JNK and p-SAPK/JNK markers were analyzed based on their upper (p54, JNK2), lower (p46, JNK1), and total band levels. It was expected to detect no significant differences between total SAPK/JNK protein levels in the upper, lower, and total band intensities in the C57BL/6 group compared to ApoE^{-/-} mice group since upper band (p54, JNK2) and lower band (p46, JNK1) was ubiquitously expressed throughout the body (Chang & Karin, 2001). Our data indicated that the diet and the genotype effects were significant on the expression of SAPK/JNK upper band levels. Also, a significant decrease in SAPK/JNK upper band was detected in the ApoE^{-/-} Western diet group compared to the chow diet group. There was also a significant increase in SAPK/JNK lower band level from C57BL/6 mice to

ApoE^{-/-} mice with chow diet, and a significant decrease in ApoE^{-/-} Western diet group compared to ApoE^{-/-} chow diet group. Lastly, both diet and genotype were effective on the SAPK/JNK total band protein levels, which were significantly increased from C57BL/6 chow diet group to ApoE^{-/-} chow diet group and significantly decreased in ApoE^{-/-} Western diet group compared to ApoE^{-/-} chow diet group. This difference might be caused by the effect of alternative splicing of JNK3, whose expression was restricted to the brain, testis, and pancreatic beta cells (Nakano et al., 2020). Maybe genotype and diet affected the expression level of JNK3 or its alternative splicing. Another hypothesis about the unexpected expression of SAPK/JNK upper, lower, and total protein levels might be caused by the time-dependent activation of JNK proteins as MAPKs. Activation of JNK and other MAPKs were tested in the hypothalamus of HFD fed Wistar rats in terms of their time-dependency. The experimental procedure was set up to have 6 different HFD groups, including 1 week 2 weeks, 3 weeks, 6 weeks, 10 weeks, 20 weeks, and 26 weeks of HFD durations compared to the control group. It was concluded that hippocampal JNK activation was observed at 1st week, 2nd week, 6th week, 10th week, and 26th week. On the other hand, there was no significant change in the protein expression of JNK at 3rd week and 20th week. It showed that SAPK/JNK activation might depend on the time interval (Abbasnejad et al., 2019). Maybe time dependent activation of JNK proteins were caused by total protein expression changes in time. Also, the diet types were important. It is because HFD composition was not the same in each study. For example, in our study, high cholesterol was added to diet which could change the fatty acid profile and that is why the result was different.

Overall, it was expected to detect an increased amount of p-SAPK/JNK (upper, lower, and total) in the C57BL/6 Western group, and in between C57BL/6 group and ApoE^{-/-} group since we increased the stress conditions. It was because our hypothesis was upon the IRE1 α -mediated activation of the JNK marker. In p-SAPK/JNK upper band (JNK2) levels, there were a significant increase in ApoE^{-/-} chow group compared to C57BL/6 chow group as it was expected. Moreover, there was a significant decrease

in the ApoE^{-/-} Western group compared to ApoE^{-/-} chow group, this pattern was like the p-IRE1 α result, but in the p-IRE1 α result, this decrease was not significant. Also, there was a significant increase between C57BL/6 chow and Western groups, which was not observed in the p-IRE1 α result.

In the lower band of p-SAPK/JNK (JNK1, p46), there was markedly increased expression from C57BL/6 chow group to both C57BL/6 Western group and ApoE^{-/-} chow group. This result was not expected because there should have been increased levels of lower band (JNK1) in phosphorylated p-SAPK/JNK from chow diet to Western diet. When the p-SAPK/JNK total band changes were analyzed, it was seen that the p-SAPK/JNK total band (JNK1 and 2) was significantly increased from C57BL/6 chow group to both C57BL/6 Western group and ApoE^{-/-} chow group. Like in the p-IRE1 α result, there was a downward trend of the total p-SAPK/JNK level in ApoE^{-/-} Western group compared to ApoE^{-/-} chow group. Different p-SAPK/JNK protein level patterns from the p-IRE1 α pattern might be caused by the differential expression and activation of total SAPK/JNK protein levels. Also, the upper band (JNK2) may have been more affected in SAPK/JNK activation (phosphorylation) from diet and genotype changes. Furthermore, JNKs were phosphorylated and activated by MKK4 and MKK7. Dual phosphorylation of Thr183 and Tyr185 residues was necessary for the JNK activation. Furthermore, the direct activator of p54 JNK3 α 2 is MKK4, whereas the JNK3 α 1 activation requires MKK4, MKK7, and MKK4/7. MKK4 regulates tyrosine phosphorylation of p46 JNK3 α 1, and MKK7 follows it by phosphorylating threonine residue (Nakano et al., 2020). Therefore, there could be an effect of these MAP2K on the expression of p-SAPK/JNK. To be able to have more consistent results, levels of MKK4 and MKK7 might be tested in future studies. Also, the time-dependent activation of SAPK/JNK might have affected the p-SAPK/JNK upper, lower, and total protein expressions.

After having results from SAPK/JNK and p-SAPK/JNK protein levels, it was meaningful to test the p-IRS-1 protein levels in the cerebral cortex of the animal groups. IRS-1 and IRS-2 are the substrates for the insulin receptor and JNK activation

impairs the insulin receptor signaling by phosphorylating serine residues of IRS-1. Because IRS-1, IRS-2, and Akt are the essential markers of insulin signaling (Y. H. Lee et al., 2003), their expression levels upon HF/HCD can show remarkable results. It was shown that p-IRS-1 (Ser307) protein levels were augmented in the hippocampus and the frontal cortex of HFD fed rats compared to chow diet group. Increased p-IRS-2 (Ser731) protein levels were observed only in the hippocampus of the HFD group but not changed in the frontal cortex. Insulin signaling impairment was primarily seen in the hippocampus, as it could be understood from the result of this study which was the indicator of the cognitive decline affecting the hippocampus because of disruption in insulin signaling (Liang et al., 2015). According to Liang et al, 2015, in the frontal cortex of the HFD fed rats, the significant change in p-IRS-2 levels was not observed, we only tested the p-IRS-1 protein level change in this study. Our results concluded that although there was an upward trend in the protein expression, no significant change in p-IRS-1 levels in the C57BL/6 Western group was observed compared to the chow group. This was not expected. It showed that the main diet was not effective on the protein level of p-IRS-1. Later, total and tyrosine-phosphorylated (for the proper functioning of IR signaling) protein expression of IRS-1 might be tested to have a better understanding. Also, no significant change was in p-IRE1 α protein levels in between chow and Western diet-fed C57BL/6 mice. It could be because of ERS activation in the cortex was not enough with only diet in C57BL/6 mice. On the other hand, in ApoE^{-/-} chow group, markedly increased p-IRS-1 protein levels were obtained compared to the C57BL/6 chow group which may have indicated the importance of the main genotype on the protein expression. Furthermore, there was a significant decrease in p-IRS-1 levels in the ApoE^{-/-} Western group compared to ApoE^{-/-} chow diet group. The apoptosis of the cells might cause this result upon prolonged expression of p-IRE1 α (Estornes et al., 2014). This possibility is consistent with the result of p-IRE1 α levels. Besides, time-dependent activation of SAPK/JNK proteins might have affected the p-IRS-1 (Ser307) activation. This hypothesis fits the result of the SAPK/JNK upper, lower, and total protein levels in C57BL/6 mice.

The last marker in the insulin signaling pathway was p-Akt, the downstream molecule of p-IRS-1 (Liang et al., 2015). It was expected the opposite expression pattern with p-IRS-1 in p-Akt protein expression. There was a significant increase in p-Akt protein expression from C57BL/6 chow group to both C57BL/6 Western group and ApoE^{-/-} chow group. In literature, p-Akt (Ser473) protein levels were significantly decreased in HFD rats compared to the control group, which showed insulin signaling impairment (Liang et al., 2015). In normal insulin signaling, when IRS-1 is activated from its tyrosine residue, PI3K recruitment occurs, and downstream signaling cascades including PDK1, Akt, and GSK-3 β are activated. GSK-3 β is responsible for glycogen synthesis and Tau phosphorylation. For the full activation of Akt, it should be first phosphorylated from its Thr308 by PDK1, then 'priming' phosphorylation should be carried out by mTOR from its Ser473 residue (Sarbasov et al., 2005). Next, activated Akt phosphorylates and negatively regulate GSK-3 β activity from its Ser9 residue. Also, GSK-3 β positive regulation is carried out through autophosphorylation at Tyr216 residue (Cole et al., 2004). In normal insulin signaling, GSK3 is kept inactive by Akt-dependent phosphorylation. It makes the reduced level of Tau hyperphosphorylation. In the impaired insulin signaling pathway, GSK3 control is disrupted, and there can be an increased risk for the development of AD (Hooper et al., 2008). In HF/HC diet-fed groups, there should have been lower levels of p-Akt, but the result was the opposite. In literature, it was shown that p-Akt activation could also be time-dependent. In that study, it was revealed that consuming HFD for 1, 2, 3, 6, 10, 20, and 26 weeks resulted in different activation states of p-Akt in the hippocampus of Wistar rats. For example, p-Akt expression was increased significantly on the 1st, 2nd, 20th and 26th weeks. Moreover, the expression was decreased on the 3rd week whereas not changed on the 6th and 10th weeks in the hypothalamus (Abbasnejad et al., 2019). Therefore, unexpected result might be caused by time-dependent activation of p-Akt, and type of our diet used in this study. Maybe significantly increased Akt activation would lead to inactivation of IRS-1 through negative feedback loop. Consequently, although impaired p-IRS-1 protein levels were

increased in in ApoE^{-/-} mice with chow diet, there was no direct result for the insulin signaling impairment because p-Akt at Ser473 residue still excessive.

Insulin have many functions like mitochondrial function, neuronal growth and synaptic plasticity in the brain. Cell maintenance and repair are also regulated by proper insulin signaling. If any disruption occurs in this pathway, accumulated damage due to non-replacable neuronal cells may increase the development of the neurodegenerative disorders in old age (Hölscher, 2019). In our previous studies, postsynaptic integrity of the neurons was tested by testing post-synaptic density 95 (PSD-95) protein levels in the cerebral cortex of the same experimental groups. From literature, it was expected to see lower amount of PSD-95 in the HFD applied mice group. Yet, in our results, there was significant increase in PSD-95 levels were observed in ApoE^{-/-} mice compared to C57BL/6 mice (Mengi, 2019). This difference from literature may be caused by the age of the subject. Therefore, in the future studies, HF/HC diet effect on ERS, insulin signaling impairment and synaptic integrity may be tested in older subjects.

Furthermore, in our previous studies, another pre-synaptic marker, synaptophysin levels were tested in both C57BL/6 and ApoE^{-/-} mice with either diet groups and it was concluded that in the cortex of ApoE^{-/-} Western group, there was a significant decrease in synaptophysin levels compared to chow group which might indicate synaptic impairment (Askin, 2019). According to the literature, inhibitory neurotransmission could be regulated by gephyrin, as a cytoplasmic protein at the post-synaptic sites (Tyagarajan & Fritschy, 2010). Our previous study showed that in ApoE^{-/-} Western group, the lowest amount of gephyrin in the cortex was obtained which might reflect the inhibitory control of food intake was impaired with HF/HCD (Askin, 2019). Synaptic integrity might be disrupted with abnormal activation of astrocytes which is induced by pro-inflammatory cytokines (Dossi et al., 2018). Our previous study demonstrated that there was increased astrocyte activation (glial fibrillary acidic protein (GFAP)) in ApoE^{-/-} mice of both diet groups accompanied with increased pro-inflammatory marker (IL-1 β) in the cortex (Askin, 2019). As a cumulative result,

HF/HCD led to ERS activation, inflammation, and synaptic impairment in the cerebral cortex of the transgenic mice. But, further studies were needed to clarify sub-specific regions of the brain.

CHAPTER 5

CONCLUSION AND FUTURE DIRECTION

This study tested the effect of HF/HC diet on ERS, insulin receptor, and insulin signaling pathway in the cerebral cortex of C57BL/6 (WT) and ApoE^{-/-} mice (as hyperlipidemic model). Eight-week-old male mice were used our study, and they were fed with either chow or Western diets for 16 weeks.

Based on the results, there was no statistically significant change in IR- β protein levels in between the groups in their cortex. Additionally, there was a significant effect of genotype but not diet on the expression of p-IRE1 α . Its level significantly increased in the ApoE^{-/-} chow group compared to C57BL/6 chow group. In SAPK/JNK upper (JNK2, p54), lower (JNK1, p46), and total protein levels, there was a marked increase from C57BL/6 chow group to ApoE^{-/-} chow group. Furthermore, a significant decrease in the Western diet was observed compared to the chow diet-fed ApoE^{-/-} mice in all upper, lower, and total band expressions. Only the upper band of SAPK/JNK significantly increased in ApoE^{-/-} Western group compared to C57BL/6 Western group. On the other hand, in p-SAPK/JNK upper (JNK2, p54), lower (JNK1, p46), and total band expressions, it was concluded that all of them were significantly increased in ApoE^{-/-} mice with chow diet compared to C57BL/6 mice with chow diet. Again, the same marked increase was revealed in between chow and Western diet groups of C57BL/6 mice. Also, in the only upper band of p-SAPK/JNK, there was a statistically significant decrease in ApoE^{-/-} mice's Western diet compared to the chow diet. As an important marker in the insulin signaling pathway, p-IRS-1 was remarkably increased in ApoE^{-/-} chow group compared to C57BL/6 chow group. Decreased levels of p-IRS-1 levels in ApoE^{-/-} Western group compared to ApoE^{-/-} chow group and increased p-Akt levels in C57BL/6 Western group and ApoE^{-/-} mice with chow diet compared to C57BL/6 chow diet group were observed. To sum up, the IRE1 α /JNK/IRS-1/Akt

pathway activation was raised in ApoE^{-/-} mice with chow diet. Even though IRE1 α activation and stress status of the cells increased with impaired IRS-1 activation in ApoE^{-/-} mice, there was no direct conclusion for the insulin signaling impairment.

In future studies, insulin levels from the periphery can be analyzed to have additional conclusive results. To confirm p-IRE1 α protein level change, p-IRE1 α -induced apoptosis markers might be studied. To be able to clarify p-SAPK/JNK and p-Akt protein level differences from literature, their time-dependent activations may be analyzed. Also, MKK4 and MKK7 protein levels would have provided a better understanding of the SAPK/JNK activation. Total and tyrosine-phosphorylated p-IRS-1 levels would give remarkable results for future studies.

Finally, the results of this study can be confirmed using immunohistochemistry (IHC) experiments. The effect of HF/HC diet on the ERS, insulin signaling impairment and subsequently synaptic integrity may be tested in older subjects.

REFERENCES

- Abbasnejad, Z., Nasser, B., Zardooz, H., & Ghasemi, R. (2019). Time-course study of high fat diet induced alterations in spatial memory, hippocampal JNK, P38, ERK and Akt activity. *Metabolic Brain Disease*, *34*(2), 659–673.
- Adamopoulos, C., Farmaki, E., Spilioti, E., Kiaris, H., Piperi, C., & Papavassiliou, A. G. (2014). Advanced glycation end-products induce endoplasmic reticulum stress in human aortic endothelial cells. *Clinical Chemistry and Laboratory Medicine*, *52*(1), 151–160.
- Adem, A., Jossan, S. S., d'Argy, R., Gillberg, P. G., Nordberg, A., Winblad, B., & Sara, V. (1989). Insulin-like growth factor 1 (IGF-1) receptors in the human brain: quantitative autoradiographic localization. *Brain Research*, *503*(2), 299–303.
- Agrawal, R., Reno, C. M., Sharma, S., Christensen, C., Huang, Y., & Fisher, S. J. (2021). Insulin Action in the Brain regulates both Central and Peripheral Functions. *American Journal of Physiology-Endocrinology and Metabolism*.
- Alessi, D. R., James, S. R., Downes, C. P., Holmes, A. B., Gaffney, P. R. J., Reese, C. B., & Cohen, P. (1997). Characterization of a 3-phosphoinositide-dependent protein kinase which phosphorylates and activates protein kinase Ba. *Current Biology*, *7*(4), 261–269.
- Almeida-Suhett, C. P., Scott, J. M., Graham, A., Chen, Y., & Deuster, P. A. (2019). Control diet in a high-fat diet study in mice: Regular chow and purified low-fat diet have similar effects on phenotypic, metabolic, and behavioral outcomes. *Nutritional Neuroscience*, *22*(1), 19–28. <https://doi.org/10.1080/1028415X.2017.1349359>
- Amuna, P., & Zotor, F. B. (2008). Epidemiological and nutrition transition in developing countries: impact on human health and development: The epidemiological and nutrition transition in developing countries: evolving trends and their impact in public health and human development. *Proceedings of the Nutrition Society*, *67*(1), 82–90.
- An, Y., Varma, V. R., Varma, S., Casanova, R., Dammer, E., Pletnikova, O., Chia, C. W., Egan, J. M., Ferrucci, L., & Troncoso, J. (2018). Evidence for brain glucose dysregulation in Alzheimer's disease. *Alzheimer's & Dementia*, *14*(3), 318–329.
- Apostolatos, A., Song, S., Acosta, S., Peart, M., Watson, J. E., Bickford, P., Cooper, D. R., & Patel, N. A. (2012). Insulin promotes neuronal survival via the alternatively spliced protein kinase CδII isoform. *Journal of Biological Chemistry*, *287*(12), 9299–9310.
- Arnold, S. E., Arvanitakis, Z., Macauley-Rambach, S. L., Koenig, A. M., Wang, H.-Y., Ahima, R. S., Craft, S., Gandy, S., Buettner, C., & Stoekel, L. E. (2018). Brain insulin resistance in type 2 diabetes and Alzheimer disease: concepts and conundrums. *Nature Reviews Neurology*, *14*(3), 168–181.
- Arruda, A. P., Pers, B. M., Parlakgöl, G., Güney, E., Inouye, K., & Hotamisligil, G.

- S. (2014). Chronic enrichment of hepatic endoplasmic reticulum–mitochondria contact leads to mitochondrial dysfunction in obesity. *Nature Medicine*, *20*(12), 1427–1435.
- Askin, B. (2019). *Assessment of the impacts of hyperlipidemia on brain and modulation of perk pathway against hyperlipidemia-induced synaptic impairment on hippocampus*.
- Back, S. H., & Kaufman, R. J. (2012). Endoplasmic reticulum stress and type 2 diabetes. *Annual Review of Biochemistry*, *81*, 767–793.
- Ballabh, P., Braun, A., & Nedergaard, M. (2004). The blood–brain barrier: an overview: structure, regulation, and clinical implications. *Neurobiology of Disease*, *16*(1), 1–13.
- Banks, W. A. (2004). The source of cerebral insulin. *European Journal of Pharmacology*, *490*(1–3), 5–12.
- Banks, W. A., Jaspán, J. B., Huang, W., & Kastin, A. J. (1997). Transport of insulin across the blood-brain barrier: saturability at euglycemic doses of insulin. *Peptides*, *18*(9), 1423–1429.
- Barter, P. J., Brewer Jr, H. B., Chapman, M. J., Hennekens, C. H., Rader, D. J., & Tall, A. R. (2003). Cholesteryl ester transfer protein: a novel target for raising HDL and inhibiting atherosclerosis. *Arteriosclerosis, Thrombosis, and Vascular Biology*, *23*(2), 160–167.
- Basseri, S., & Austin, R. C. (2012). Endoplasmic reticulum stress and lipid metabolism: mechanisms and therapeutic potential. *Biochemistry Research International*, *2012*.
- Beddows, C. A., & Dodd, G. T. (2021). Insulin on the brain: The role of central insulin signalling in energy and glucose homeostasis. *Journal of Neuroendocrinology*, *33*(4), e12947.
- Behrens, A., Sibilio, M., & Wagner, E. F. (1999). Amino-terminal phosphorylation of c-Jun regulates stress-induced apoptosis and cellular proliferation. *Nature Genetics*, *21*(3), 326–329.
- Belfiore, A., Malaguarnera, R., Vella, V., Lawrence, M. C., Sciacca, L., Frasca, F., Morrione, A., & Vigneri, R. (2017). Insulin receptor isoforms in physiology and disease: an updated view. *Endocrine Reviews*, *38*(5), 379–431.
- Bertolotti, A., Wang, X., Novoa, I., Jungreis, R., Schlessinger, K., Cho, J. H., West, A. B., & Ron, D. (2001). Increased sensitivity to dextran sodium sulfate colitis in IRE1 β -deficient mice. *The Journal of Clinical Investigation*, *107*(5), 585–593.
- Bhat, N. R., & Thirumangalakudi, L. (2013). Increased tau phosphorylation and impaired brain insulin/IGF signaling in mice fed a high fat/high cholesterol diet. *Journal of Alzheimer's Disease*, *36*(4), 781–789.
- Blasberg, R. G., Patlak, C. S., & Fenstermacher, J. D. (1983). Selection of experimental conditions for the accurate determination of blood–Brain transfer constants from single-time experiments: A theoretical analysis. *Journal of Cerebral Blood Flow & Metabolism*, *3*(2), 215–225.
- Borradaile, N. M., Han, X., Harp, J. D., Gale, S. E., Ory, D. S., & Schaffer, J. E.

- (2006). Disruption of endoplasmic reticulum structure and integrity in lipotoxic cell death. *Journal of Lipid Research*, 47(12), 2726–2737.
- Cai, W., Sakaguchi, M., Kleinridders, A., Gonzalez-Del Pino, G., Dreyfuss, J. M., O’Neill, B. T., Ramirez, A. K., Pan, H., Winnay, J. N., & Boucher, J. (2017). Domain-dependent effects of insulin and IGF-1 receptors on signalling and gene expression. *Nature Communications*, 8(1), 1–14.
- Carvalho, C., & Moreira, P. I. (2017). Isolation of Rodent Brain Vessels. *Bio-Protocol*, 7(17), e2535–e2535.
- Carvalho, F. A., Aitken, J. D., Vijay-Kumar, M., & Gewirtz, A. T. (2012). Toll-like receptor–gut microbiota interactions: perturb at your own risk! *Annual Review of Physiology*, 74, 177–198.
- Chang, L., & Karin, M. (2001). Mammalian MAP kinase signalling cascades. *Nature*, 410(6824), 37–40.
- Chatterjee, S., & Mudher, A. (2018). Alzheimer’s disease and type 2 diabetes: A critical assessment of the shared pathological traits. *Frontiers in Neuroscience*, 12, 383.
- Chen, W., Balland, E., & Cowley, M. A. (2017). Hypothalamic insulin resistance in obesity: effects on glucose homeostasis. *Neuroendocrinology*, 104(4), 364–381.
- Chen, X., Shen, J., & Prywes, R. (2002). The Luminal Domain of ATF6 Senses Endoplasmic Reticulum (ER) Stress and Causes Translocation of ATF6 from the ER to the Golgi*. *Journal of Biological Chemistry*, 277(15), 13045–13052.
- Cheng, H., Gang, X., Liu, Y., Wang, G., Zhao, X., & Wang, G. (2020). Mitochondrial dysfunction plays a key role in the development of neurodegenerative diseases in diabetes. *American Journal of Physiology-Endocrinology and Metabolism*, 318(5), E750–E764.
- Chua, L.-M., Lim, M.-L., Chong, P.-R., Hu, Z. P., Cheung, N. S., & Wong, B.-S. (2012). Impaired neuronal insulin signaling precedes A β 42 Accumulation in female A β PPsw/PS1 Δ E9 Mice. *Journal of Alzheimer’s Disease*, 29(4), 783–791.
- Cole, A., Frame, S., & Cohen, P. (2004). Further evidence that the tyrosine phosphorylation of glycogen synthase kinase-3 (GSK3) in mammalian cells is an autophosphorylation event. *Biochemical Journal*, 377(1), 249–255.
- Csajbók, É. A., & Tamás, G. (2016). Cerebral cortex: a target and source of insulin? *Diabetologia*, 59(8), 1609–1615.
- Dandekar, A., Mendez, R., & Zhang, K. (2015). Cross talk between ER stress, oxidative stress, and inflammation in health and disease. *Stress Responses*, 205–214.
- De Meyts, P., Roth, J., Neville Jr, D. M., Gavin III, J. R., & Lesniak, M. A. (1973). Insulin interactions with its receptors: experimental evidence for negative cooperativity. *Biochemical and Biophysical Research Communications*, 55(1), 154–161.
- Dietschy, J. M., & Turley, S. D. (2001). Cholesterol metabolism in the brain. *Current Opinion in Lipidology*, 12(2), 105–112.

- Dobrovolskaia, M. A., & Vogel, S. N. (2002). Toll receptors, CD14, and macrophage activation and deactivation by LPS. *Microbes and Infection*, 4(9), 903–914.
- Dodd, G. T., & Tiganis, T. (2017). Insulin action in the brain: Roles in energy and glucose homeostasis. *Journal of Neuroendocrinology*, 29(10), e12513.
- Dong, X., Park, S., Lin, X., Copps, K., Yi, X., & White, M. F. (2006). Irs1 and Irs2 signaling is essential for hepatic glucose homeostasis and systemic growth. *The Journal of Clinical Investigation*, 116(1), 101–114.
- Dossi, E., Vasile, F., & Rouach, N. (2018). Human astrocytes in the diseased brain. *Brain Research Bulletin*, 136, 139–156.
- Engin, A. B. (2017). What is lipotoxicity? *Obesity and Lipotoxicity*, 197–220.
- Engin, F., & Hotamisligil, G. S. (2010). Restoring endoplasmic reticulum function by chemical chaperones: an emerging therapeutic approach for metabolic diseases. *Diabetes, Obesity and Metabolism*, 12, 108–115.
- Estornes, Y., Aguilera, M. A., Dubuisson, C., De Keyser, J., Goossens, V., Kersse, K., Samali, A., Vandenabeele, P., & Bertrand, M. J. M. (2014). RIPK1 promotes death receptor-independent caspase-8-mediated apoptosis under unresolved ER stress conditions. *Cell Death & Disease*, 5(12), e1555–e1555.
- Feingold, K. R., & Grunfeld, C. (2015). *Introduction to lipids and lipoproteins*.
- Ference, B. A., Ginsberg, H. N., Graham, I., Ray, K. K., Packard, C. J., Bruckert, E., Hegele, R. A., Krauss, R. M., Raal, F. J., & Schunkert, H. (2017). Low-density lipoproteins cause atherosclerotic cardiovascular disease. 1. Evidence from genetic, epidemiologic, and clinical studies. A consensus statement from the European Atherosclerosis Society Consensus Panel. *European Heart Journal*, 38(32), 2459–2472.
- Fritsche, K. L. (2015). The science of fatty acids and inflammation. *Advances in Nutrition*, 6(3), 293S–301S.
- Gabbouj, S., Ryhänen, S., Marttinen, M., Wittrahm, R., Takalo, M., Kemppainen, S., Martiskainen, H., Tanila, H., Haapasalo, A., & Hiltunen, M. (2019). Altered insulin signaling in Alzheimer’s disease brain—special emphasis on PI3K-Akt pathway. *Frontiers in Neuroscience*, 13, 629.
- Gardner, B. M., & Walter, P. (2011). Unfolded proteins are Ire1-activating ligands that directly induce the unfolded protein response. *Science*, 333(6051), 1891–1894.
- Gavin, J. R., Roth, J., Neville, D. M., De Meyts, P., & Buell, D. N. (1974). Insulin-dependent regulation of insulin receptor concentrations: a direct demonstration in cell culture. *Proceedings of the National Academy of Sciences*, 71(1), 84–88.
- Ghemrawi, R., Battaglia-Hsu, S.-F., & Arnold, C. (2018). Endoplasmic reticulum stress in metabolic disorders. *Cells*, 7(6), 63.
- GOODNER, C. J., HOM, F. G., & BERRIE, M. A. N. N. (1980). Investigation of the effect of insulin upon regional brain glucose metabolism in the rat in vivo. *Endocrinology*, 107(6), 1827–1832.
- Graham, J. (2002). Homogenization of mammalian tissues. *TheScientificWorldJOURNAL*, 2, 1626–1629.
- Gray, S. M., & Barrett, E. J. (2018). Insulin transport into the brain. *American*

- Journal of Physiology-Cell Physiology*, 315(2), C125–C136.
- Grillo, C. A., Piroli, G. G., Kaigler, K. F., Wilson, S. P., Wilson, M. A., & Reagan, L. P. (2011). Downregulation of hypothalamic insulin receptor expression elicits depressive-like behaviors in rats. *Behavioural Brain Research*, 222(1), 230–235.
- Gual, P., Le Marchand-Brustel, Y., & Tanti, J.-F. (2005). Positive and negative regulation of insulin signaling through IRS-1 phosphorylation. *Biochimie*, 87(1), 99–109.
- Gupta, S., Barrett, T., Whitmarsh, A. J., Cavanagh, J., Sluss, H. K., Derijard, B., & Davis, R. J. (1996). Selective interaction of JNK protein kinase isoforms with transcription factors. *The EMBO Journal*, 15(11), 2760–2770.
- Haeusler, R. A., McGraw, T. E., & Accili, D. (2018). Biochemical and cellular properties of insulin receptor signalling. *Nature Reviews Molecular Cell Biology*, 19(1), 31–44.
- Hampton, R. Y. (2000). ER stress response: getting the UPR hand on misfolded proteins. *Current Biology*, 10(14), R518–R521.
- Hampton, R. Y. (2002). ER-associated degradation in protein quality control and cellular regulation. *Current Opinion in Cell Biology*, 14(4), 476–482.
- Hassler, J. R., Scheuner, D. L., Wang, S., Han, J., Kodali, V. K., Li, P., Nguyen, J., George, J. S., Davis, C., & Wu, S. P. (2015). The IRE1 α /XBP1s pathway is essential for the glucose response and protection of β cells. *PLoS Biology*, 13(10), e1002277.
- Havrankova, J., Roth, J., & BROWNSTEIN, M. (1978). Insulin receptors are widely distributed in the central nervous system of the rat. *Nature*, 272(5656), 827–829.
- Hawkins, B. T., & Davis, T. P. (2005). The blood-brain barrier/neurovascular unit in health and disease. *Pharmacological Reviews*, 57(2), 173–185.
- Hayashi, T, Rizzuto, R., Hajnoczky, G., & Tsung-ping, S. (2009). Mitochondria and the ER physically interact. *Trends in Cell Biology*, 19(2), 81–88.
- Hayashi, Teruo, & Fujimoto, M. (2010). Detergent-resistant microdomains determine the localization of σ -1 receptors to the endoplasmic reticulum-mitochondria junction. *Molecular Pharmacology*, 77(4), 517–528.
- Heni, M., Schöpfer, P., Peter, A., Sartorius, T., Fritsche, A., Synofzik, M., Häring, H.-U., Maetzler, W., & Hennige, A. M. (2014). Evidence for altered transport of insulin across the blood–brain barrier in insulin-resistant humans. *Acta Diabetologica*, 51(4), 679–681.
- Herzig, S. (2001). Long F, Jhala US, Hedrick S, Quinn R, Bauer A, Rudolph D, Schutz G, Yoon C, Puigserver P, Spiegelman B, Montminy M. *CREB Regulates Hepatic Gluconeogenesis through the Coactivator PGC-1*. *Nature*, 413, 179–183.
- Hibi, M., Lin, A., Smeal, T., Minden, A., & Karin, M. (1993). Identification of an oncoprotein-and UV-responsive protein kinase that binds and potentiates the c-Jun activation domain. *Genes & Development*, 7(11), 2135–2148.
- Hirosumi, J., Tuncman, G., Chang, L., Görgün, C. Z., Uysal, K. T., Maeda, K., Karin,

- M., & Hotamisligil, G. S. (2002). A central role for JNK in obesity and insulin resistance. *Nature*, *420*(6913), 333–336.
- Hölscher, C. (2019). Insulin signaling impairment in the brain as a risk factor in Alzheimer's disease. *Frontiers in Aging Neuroscience*, *11*, 88.
- Hooper, C., Killick, R., & Lovestone, S. (2008). The GSK3 hypothesis of Alzheimer's disease. *Journal of Neurochemistry*, *104*(6), 1433–1439.
- Hotamisligil, G S. (2008). Inflammation and endoplasmic reticulum stress in obesity and diabetes. *International Journal of Obesity*, *32*(7), S52–S54.
- Hotamisligil, Gökhan S. (2005). Role of endoplasmic reticulum stress and c-Jun NH2-terminal kinase pathways in inflammation and origin of obesity and diabetes. *Diabetes*, *54*(suppl 2), S73–S78.
- Hotamisligil, Gökhan S. (2006). Inflammation and metabolic disorders. *Nature*, *444*(7121), 860–867.
- Hotamisligil, Gökhan S, & Erbay, E. (2008). Nutrient sensing and inflammation in metabolic diseases. *Nature Reviews Immunology*, *8*(12), 923–934.
- Hotamisligil, Gökhan S, Peraldi, P., Budavari, A., Ellis, R., White, M. F., & Spiegelman, B. M. (1996). IRS-1-mediated inhibition of insulin receptor tyrosine kinase activity in TNF- α -and obesity-induced insulin resistance. *Science*, *271*(5249), 665–670.
- Hotamisligil, Gokhan S, Shargill, N. S., & Spiegelman, B. M. (1993). Adipose expression of tumor necrosis factor- α : direct role in obesity-linked insulin resistance. *Science*, *259*(5091), 87–91.
- Hu, M., Phan, F., Bourron, O., Ferré, P., & Foufelle, F. (2017). Steatosis and NASH in type 2 diabetes. *Biochimie*, *143*, 37–41.
- Hwang, D. H., Kim, J.-A., & Lee, J. Y. (2016). Mechanisms for the activation of Toll-like receptor 2/4 by saturated fatty acids and inhibition by docosahexaenoic acid. *European Journal of Pharmacology*, *785*, 24–35.
- Hwang, D., Huang, S., Rutkowsky, J. M., Snodgrass, R. G., Ono-Moore, K. D., Schneider, D. A., Newman, J. W., & Adams, S. H. (2012). *Saturated fatty acids activate TLR-mediated proinflammatory signaling pathways*. Wiley Online Library.
- Imagawa, Y., Hosoda, A., Sasaka, S., Tsuru, A., & Kohno, K. (2008). RNase domains determine the functional difference between IRE1 α and IRE1 β . *FEBS Letters*, *582*(5), 656–660.
- IS Sobczak, A., A Blindauer, C., & J Stewart, A. (2019). Changes in plasma free fatty acids associated with type-2 diabetes. *Nutrients*, *11*(9), 2022.
- Jørgensen, T., Capewell, S., Prescott, E., Allender, S., Sans, S., Zdrojewski, T., De Bacquer, D., De Sutter, J., Franco, O. H., & Løgstrup, S. (2013). Population-level changes to promote cardiovascular health. *European Journal of Preventive Cardiology*, *20*(3), 409–421.
- Kanekura, K., Ma, X., Murphy, J. T., Zhu, L. J., Diwan, A., & Urano, F. (2015). IRE1 prevents endoplasmic reticulum membrane permeabilization and cell death under pathological conditions. *Science Signaling*, *8*(382), ra62–ra62.
- Karmi, A., Iozzo, P., Viljanen, A., Hirvonen, J., Fielding, B. A., Virtanen, K.,

- Oikonen, V., Kemppainen, J., Viljanen, T., & Guiducci, L. (2010). Increased brain fatty acid uptake in metabolic syndrome. *Diabetes*, *59*(9), 2171–2177.
- Karoglu, E. T., Halim, D. O., Erkaya, B., Altaytas, F., Arslan-Ergul, A., Konu, O., & Adams, M. M. (2017). Aging alters the molecular dynamics of synapses in a sexually dimorphic pattern in zebrafish (*Danio rerio*). *Neurobiology of Aging*, *54*, 10–21.
- Kato, H., Nakajima, S., Saito, Y., Takahashi, S., Katoh, R., & Kitamura, M. (2012). mTORC1 serves ER stress-triggered apoptosis via selective activation of the IRE1–JNK pathway. *Cell Death & Differentiation*, *19*(2), 310–320.
- Kawaguchi, S., & Ng, D. T. W. (2011). Sensing ER stress. *Science*, *333*(6051), 1830–1831.
- Kelly, T., Yang, W., Chen, C.-S., Reynolds, K., & He, J. (2008). Global burden of obesity in 2005 and projections to 2030. *International Journal of Obesity*, *32*(9), 1431–1437.
- Kim, S., Joe, Y., Kim, H. J., Kim, Y.-S., Jeong, S. O., Pae, H.-O., Ryter, S. W., Surh, Y.-J., & Chung, H. T. (2015). Endoplasmic reticulum stress–induced IRE1 α activation mediates cross-talk of GSK-3 β and XBP-1 To regulate inflammatory cytokine production. *The Journal of Immunology*, *194*(9), 4498–4506.
- Kimata, Y., Oikawa, D., Shimizu, Y., Ishiwata-Kimata, Y., & Kohno, K. (2004). A role for BiP as an adjustor for the endoplasmic reticulum stress-sensing protein Ire1. *The Journal of Cell Biology*, *167*(3), 445–456.
- King, G. L., & Johnson, S. M. (1985). Receptor-mediated transport of insulin across endothelial cells. *Science*, *227*(4694), 1583–1586.
- Kleinridders, A. (2016). Deciphering brain insulin receptor and insulin-like growth factor 1 receptor signalling. *Journal of Neuroendocrinology*, *28*(11).
- Kleinridders, A., Ferris, H. A., Cai, W., & Kahn, C. R. (2014). Insulin action in brain regulates systemic metabolism and brain function. *Diabetes*, *63*(7), 2232–2243.
- Konishi, M., Sakaguchi, M., Lockhart, S. M., Cai, W., Li, M. E., Homan, E. P., Rask-Madsen, C., & Kahn, C. R. (2017). Endothelial insulin receptors differentially control insulin signaling kinetics in peripheral tissues and brain of mice. *Proceedings of the National Academy of Sciences*, *114*(40), E8478–E8487.
- Korinek, M., Gonzalez-Gonzalez, I. M., Smejkalova, T., Hajdukovic, D., Skrenkova, K., Krusek, J., Horak, M., & Vyklicky, L. (2020). Cholesterol modulates presynaptic and postsynaptic properties of excitatory synaptic transmission. *Scientific Reports*, *10*(1), 1–18.
- Kröger, J., Jacobs, S., Jansen, E. H. J. M., Fritsche, A., Boeing, H., & Schulze, M. B. (2015). Erythrocyte membrane fatty acid fluidity and risk of type 2 diabetes in the EPIC-Potsdam study. *Diabetologia*, *58*(2), 282–289.
- Kruse, K. B., Brodsky, J. L., & McCracken, A. A. (2006). Autophagy: an ER protein quality control process. *Autophagy*, *2*(2), 135–137.
- Kruzliak, P., Sabo, J., & Zulli, A. (2015). Endothelial endoplasmic reticulum and nitrate stress in endothelial dysfunction in the atherogenic rabbit model. *Acta Histochemica*, *117*(8), 762–766.
- Kullmann, S., Heni, M., Hallschmid, M., Fritsche, A., Preissl, H., & Häring, H.-U.

- (2016). Brain insulin resistance at the crossroads of metabolic and cognitive disorders in humans. *Physiological Reviews*, 96(4), 1169–1209.
- Kwon, H., & Pessin, J. E. (2020). Insulin-Mediated PI3K and AKT Signaling. *The Liver: Biology and Pathobiology*, 485–495.
- Lee, H.-M., Kim, J.-J., Kim, H. J., Shong, M., Ku, B. J., & Jo, E.-K. (2013). Upregulated NLRP3 inflammasome activation in patients with type 2 diabetes. *Diabetes*, 62(1), 194–204.
- Lee, Y. H., Giraud, J., Davis, R. J., & White, M. F. (2003). c-Jun N-terminal kinase (JNK) mediates feedback inhibition of the insulin signaling cascade. *Journal of Biological Chemistry*, 278(5), 2896–2902.
- Legrand-Poels, S., Esser, N., L'homme, L., Scheen, A., Paquot, N., & Piette, J. (2014). Free fatty acids as modulators of the NLRP3 inflammasome in obesity/type 2 diabetes. *Biochemical Pharmacology*, 92(1), 131–141.
- Lei, K., & Davis, R. J. (2003). JNK phosphorylation of Bim-related members of the Bcl2 family induces Bax-dependent apoptosis. *Proceedings of the National Academy of Sciences*, 100(5), 2432–2437.
- Li, H., Korennykh, A. V., Behrman, S. L., & Walter, P. (2010). Mammalian endoplasmic reticulum stress sensor IRE1 signals by dynamic clustering. *Proceedings of the National Academy of Sciences*, 107(37), 16113–16118.
- Liang, L., Chen, J., Zhan, L., Lu, X., Sun, X., Sui, H., Zheng, L., Xiang, H., & Zhang, F. (2015). Endoplasmic reticulum stress impairs insulin receptor signaling in the brains of obese rats. *PloS One*, 10(5), e0126384.
- Lipson, K. L., Fonseca, S. G., Ishigaki, S., Nguyen, L. X., Foss, E., Bortell, R., Rossini, A. A., & Urano, F. (2006). Regulation of insulin biosynthesis in pancreatic beta cells by an endoplasmic reticulum-resident protein kinase IRE1. *Cell Metabolism*, 4(3), 245–254.
- Liu, M., Spellberg, B., Phan, Q. T., Fu, Y., Fu, Y., Lee, A. S., Edwards, J. E., Filler, S. G., & Ibrahim, A. S. (2010). The endothelial cell receptor GRP78 is required for mucormycosis pathogenesis in diabetic mice. *The Journal of Clinical Investigation*, 120(6), 1914–1924.
- Lumeng, C. N., & Saltiel, A. R. (2011). Inflammatory links between obesity and metabolic disease. *The Journal of Clinical Investigation*, 121(6), 2111–2117.
- Ma, Y., & Hendershot, L. M. (2001). The unfolding tale of the unfolded protein response. *Cell*, 107(7), 827–830.
- Maganto-Garcia, E., Tarrío, M., & Lichtman, A. H. (2012). Mouse models of atherosclerosis. *Current Protocols in Immunology*, 96(1), 15–24.
- Mahley, R. W. (1988). Apolipoprotein E: cholesterol transport protein with expanding role in cell biology. *Science*, 240(4852), 622–630.
- Mahley, R. W. (2016). Central nervous system lipoproteins: ApoE and regulation of cholesterol metabolism. *Arteriosclerosis, Thrombosis, and Vascular Biology*, 36(7), 1305–1315.
- Mahmood, T., & Yang, P.-C. (2012). Western blot: technique, theory, and trouble shooting. *North American Journal of Medical Sciences*, 4(9), 429.
- Manning, B. D., & Cantley, L. C. (2007). AKT/PKB signaling: navigating

- downstream. *Cell*, 129(7), 1261–1274.
- Marchi, S., Marinello, M., Bononi, A., Bonora, M., Giorgi, C., Rimessi, A., & Pinton, P. (2012). Selective modulation of subtype III IP 3 R by Akt regulates ER Ca²⁺ release and apoptosis. *Cell Death & Disease*, 3(5), e304–e304.
- Martino, M. B., Jones, L., Brighton, B., Ehre, C., Abdulah, L., Davis, C. W., Ron, D., O’neal, W. K., & Ribeiro, C. M. P. (2013). The ER stress transducer IRE1 β is required for airway epithelial mucin production. *Mucosal Immunology*, 6(3), 639–654.
- Meijer, R. I., Gray, S. M., Aylor, K. W., & Barrett, E. J. (2016). Pathways for insulin access to the brain: the role of the microvascular endothelial cell. *American Journal of Physiology-Heart and Circulatory Physiology*, 311(5), H1132–H1138.
- Mengi, N. (2019). *The effects of high cholesterol/high fat diet on endoplasmic reticulum stress and neuronal dysfunction in the hippocampus and cerebral cortex of APOE^{-/-}MICE*. Middle East Technical University.
- Meyts, P. De. (1976). Cooperative properties of hormone receptors in cell membranes. *Journal of Supramolecular Structure*, 4(2), 241–258.
- Millington, G. W. M. (2007). The role of proopiomelanocortin (POMC) neurons in feeding behaviour. *Nutrition & Metabolism*, 4(1), 1–16.
- Milstein, J. L., & Ferris, H. A. (2021). The brain as an insulin-sensitive metabolic organ. *Molecular Metabolism*, 52(April), 101234. <https://doi.org/10.1016/j.molmet.2021.101234>
- Mishra, P. K., Ying, W., Nandi, S. S., Bandyopadhyay, G. K., Patel, K. K., & Mahata, S. K. (2017). Diabetic cardiomyopathy: an immunometabolic perspective. *Frontiers in Endocrinology*, 8, 72.
- Mohit, A. A., Martin, J. H., & Miller, C. A. (1995). p493F12 kinase: a novel MAP kinase expressed in a subset of neurons in the human nervous system. *Neuron*, 14(1), 67–78.
- Morse, S. M. J., Shaw, G., & Larner, S. F. (2006). Concurrent mRNA and protein extraction from the same experimental sample using a commercially available column-based RNA preparation kit. *BioTechniques*, 40(1), 54–58.
- Mukherjee, A., Morales-Scheihing, D., Butler, P. C., & Soto, C. (2015). Type 2 diabetes as a protein misfolding disease. *Trends in Molecular Medicine*, 21(7), 439–449.
- Mullier, A., Bouret, S. G., Prevot, V., & Dehouck, B. (2010). Differential distribution of tight junction proteins suggests a role for tanycytes in blood-hypothalamus barrier regulation in the adult mouse brain. *Journal of Comparative Neurology*, 518(7), 943–962.
- Mustapha, S., Mohammed, M., Azemi, A. K., Yunusa, I., Shehu, A., Mustapha, L., Wada, Y., Ahmad, M. H., Ahmad, W. A. N. W., & Rasool, A. H. G. (2021). Potential Roles of Endoplasmic Reticulum Stress and Cellular Proteins Implicated in Diabetes. *Oxidative Medicine and Cellular Longevity*, 2021.
- Nakagawa, T., Zhu, H., Morishima, N., Li, E., Xu, J., Yankner, B. A., & Yuan, J. (2000). Caspase-12 mediates endoplasmic-reticulum-specific apoptosis and

- cytotoxicity by amyloid- β . *Nature*, 403(6765), 98–103.
- Nakano, R., Nakayama, T., & Sugiya, H. (2020). Biological Properties of JNK3 and Its Function in Neurons, Astrocytes, Pancreatic β -Cells and Cardiovascular Cells. *Cells*, 9(8), 1802.
- Nelson, R. H. (2013). Hyperlipidemia as a risk factor for cardiovascular disease. *Primary Care: Clinics in Office Practice*, 40(1), 195–211.
- Nie, Y., Ma, R. C., Chan, J. C. N., Xu, H., & Xu, G. (2012). Glucose-dependent insulinotropic peptide impairs insulin signaling via inducing adipocyte inflammation in glucose-dependent insulinotropic peptide receptor-overexpressing adipocytes. *The FASEB Journal*, 26(6), 2383–2393.
- Nishitoh, H., Matsuzawa, A., Tobiume, K., Saegusa, K., Takeda, K., Inoue, K., Hori, S., Kakizuka, A., & Ichijo, H. (2002). ASK1 is essential for endoplasmic reticulum stress-induced neuronal cell death triggered by expanded polyglutamine repeats. *Genes & Development*, 16(11), 1345–1355.
- Okada, T., Kawano, Y., Sakakibara, T., Hazeki, O., & Ui, M. (1994). Essential role of phosphatidylinositol 3-kinase in insulin-induced glucose transport and antilipolysis in rat adipocytes. Studies with a selective inhibitor wortmannin. *Journal of Biological Chemistry*, 269(5), 3568–3573.
- Olefsky, J. M., & Glass, C. K. (2010). Macrophages, inflammation, and insulin resistance. *Annual Review of Physiology*, 72, 219–246.
- Organization, W. H. (2017). Cardiovascular disease. [Http://Www. Who. Int/Cardiovascular_diseases/En/](http://www.who.int/Cardiovascular_diseases/En/).
- Oyadomari, S., & Mori, M. (2004). Roles of CHOP/GADD153 in endoplasmic reticulum stress. *Cell Death & Differentiation*, 11(4), 381–389.
- Ozcan, L., & Tabas, I. (2016). Calcium signalling and ER stress in insulin resistance and atherosclerosis. *Journal of Internal Medicine*, 280(5), 457–464.
- Ozcan, L., Lale, Ergin, A. S., Lu, A., Chung, J., Sarkar, S., Nie, D., Myers Jr, M. G., & Ozcan, U. (2009). Endoplasmic reticulum stress plays a central role in development of leptin resistance. *Cell Metabolism*, 9(1), 35–51.
- Özcan, U., Cao, Q., Yilmaz, E., Lee, A.-H., Iwakoshi, N. N., Özdelen, E., Tuncman, G., Görgün, C., Glimcher, L. H., & Hotamisligil, G. S. (2004). Endoplasmic reticulum stress links obesity, insulin action, and type 2 diabetes. *Science*, 306(5695), 457–461.
- Özcan, U., Yilmaz, E., Özcan, L., Furuhashi, M., Vaillancourt, E., Smith, R. O., Görgün, C. Z., & Hotamisligil, G. S. (2006). Chemical chaperones reduce ER stress and restore glucose homeostasis in a mouse model of type 2 diabetes. *Science*, 313(5790), 1137–1140.
- Panuganti, K. K., Nguyen, M., Kshirsagar, R. K., & Doerr, C. (2021). *Obesity (Nursing)*.
- Pasinetti, G. M., & Eberstein, J. A. (2008). Metabolic syndrome and the role of dietary lifestyles in Alzheimer's disease. *Journal of Neurochemistry*, 106(4), 1503–1514.
- Patti, M.-E., Brambilla, E., Luzi, L., Landaker, E. J., & Kahn, C. R. (1998). Bidirectional modulation of insulin action by amino acids. *The Journal of*

- Clinical Investigation*, 101(7), 1519–1529.
- Petersen, M. C., & Shulman, G. I. (2018). Mechanisms of insulin action and insulin resistance. *Physiological Reviews*, 98(4), 2133–2223.
- Pilon, M. (2016). Revisiting the membrane-centric view of diabetes. *Lipids in Health and Disease*, 15(1), 1–6.
- Pilz, S., & März, W. (2008). Free fatty acids as a cardiovascular risk factor. *Clinical Chemistry and Laboratory Medicine*, 46(4), 429–434.
- Pincus, D., Chevalier, M. W., Aragón, T., Van Anken, E., Vidal, S. E., El-Samad, H., & Walter, P. (2010). BiP binding to the ER-stress sensor Ire1 tunes the homeostatic behavior of the unfolded protein response. *PLoS Biology*, 8(7), e1000415.
- Plump, A. S., & Breslow, J. L. (1995). Apolipoprotein E and the apolipoprotein E-deficient mouse. *Annual Review of Nutrition*, 15(1), 495–518.
- Plump, A. S., Smith, J. D., Hayek, T., Aalto-Setälä, K., Walsh, A., Verstuyft, J. G., Rubin, E. M., & Breslow, J. L. (1992). Severe hypercholesterolemia and atherosclerosis in apolipoprotein E-deficient mice created by homologous recombination in ES cells. *Cell*, 71(2), 343–353.
- Pomytkin, I., & Pinelis, V. (2021). Brain Insulin Resistance: Focus on Insulin Receptor-Mitochondria Interactions. *Life*, 11(3), 262.
- Prischi, F., Nowak, P. R., Carrara, M., & Ali, M. M. U. (2014). Phosphoregulation of Ire1 RNase splicing activity. *Nature Communications*, 5(1), 1–11.
- Pulverer, B. J., Kyriakis, J. M., Avruch, J., Nikolakaki, E., & Woodgett, J. R. (1991). Phosphorylation of c-jun mediated by MAP kinases. *Nature*, 353(6345), 670–674.
- Rai, S., Bhatia, V., & Bhatnagar, S. (2021). Drug repurposing for hyperlipidemia associated disorders: An integrative network biology and machine learning approach. *Computational Biology and Chemistry*, 92, 107505.
- Rask-Madsen, C., Buonomo, E., Li, Q., Park, K., Clermont, A. C., Yerokun, O., Rekhter, M., & King, G. L. (2012). Hyperinsulinemia does not change atherosclerosis development in apolipoprotein E null mice. *Arteriosclerosis, Thrombosis, and Vascular Biology*, 32(5), 1124–1131.
- Refolo, L. M., Pappolla, M. A., Malester, B., LaFrancois, J., Bryant-Thomas, T., Wang, R., Tint, G. S., Sambamurti, K., & Duff, K. (2000). Hypercholesterolemia accelerates the Alzheimer's amyloid pathology in a transgenic mouse model. *Neurobiology of Disease*, 7(4), 321–331.
- Riaz, T. A., Junjappa, R. P., Hadigund, M., Ferdous, J., Kim, H.-R., & Chae, H. (2020). Role of Endoplasmic Reticulum Stress Sensor IRE1 α . *Cell*, 9, 1–33.
- Riaz, T. A., Junjappa, R. P., Handigund, M., Ferdous, J., Kim, H.-R., & Chae, H.-J. (2020). Role of endoplasmic reticulum stress sensor IRE1 α in cellular physiology, calcium, ROS signaling, and metaflammation. *Cells*, 9(5), 1160.
- Rodríguez, E. M., Blázquez, J. L., Pastor, F. E., Peláez, B., Pena, P., Peruzzo, B., & Amat, P. (2005). Hypothalamic tanycytes: a key component of brain–endocrine interaction. *International Review of Cytology*, 247, 89–164.
- Rogero, M. M., & Calder, P. C. (2018). Obesity, inflammation, toll-like receptor 4

- and fatty acids. *Nutrients*, *10*(4), 432.
- Rojas-Rivera, D., Rodriguez, D. A., Sepulveda, D., & Hetz, C. (2018). ER stress sensing mechanism: Putting off the brake on UPR transducers. *Oncotarget*, *9*(28), 19461.
- Ron, D., & Walter, P. (2007). Signal integration in the endoplasmic reticulum unfolded protein response. *Nature Reviews Molecular Cell Biology*, *8*(7), 519–529.
- Russell, J. C., & Proctor, S. D. (2006). Small animal models of cardiovascular disease: tools for the study of the roles of metabolic syndrome, dyslipidemia, and atherosclerosis. *Cardiovascular Pathology*, *15*(6), 318–330.
- Rutkowski, D. T., & Kaufman, R. J. (2004). A trip to the ER: coping with stress. *Trends in Cell Biology*, *14*(1), 20–28.
- Saltiel, A. R. (2021). Insulin signaling in health and disease. *The Journal of Clinical Investigation*, *131*(1).
- Saltiel, A. R., & Olefsky, J. M. (2017). Inflammatory mechanisms linking obesity and metabolic disease. *The Journal of Clinical Investigation*, *127*(1), 1–4.
- Saponaro, C., Gaggini, M., Carli, F., & Gastaldelli, A. (2015). The subtle balance between lipolysis and lipogenesis: a critical point in metabolic homeostasis. *Nutrients*, *7*(11), 9453–9474.
- Sarbassov, D. D., Guertin, D. A., Ali, S. M., & Sabatini, D. M. (2005). Phosphorylation and regulation of Akt/PKB by the rictor-mTOR complex. *Science*, *307*(5712), 1098–1101.
- Sari, F. R., Watanabe, K., Thandavarayan, R. A., Harima, M., Zhang, S., Muslin, A. J., Kodama, M., & Aizawa, Y. (2010). 14-3-3 protein protects against cardiac endoplasmic reticulum stress (ERS) and ERS-initiated apoptosis in experimental diabetes. *Journal of Pharmacological Sciences*, *113*(4), 325–334.
- Schreyer, S. A., Wilson, D. L., & LeBoeuf, R. C. (1998). C57BL/6 mice fed high fat diets as models for diabetes-accelerated atherosclerosis. *Atherosclerosis*, *136*(1), 17–24.
- Schröder, M. (2008). Endoplasmic reticulum stress responses. *Cellular and Molecular Life Sciences*, *65*(6), 862–894.
- Schubert, M., Gautam, D., Surjo, D., Ueki, K., Baudler, S., Schubert, D., Kondo, T., Alber, J., Galldiks, N., & Küstermann, E. (2004). Role for neuronal insulin resistance in neurodegenerative diseases. *Proceedings of the National Academy of Sciences*, *101*(9), 3100–3105.
- Sears, B., & Perry, M. (2015). The role of fatty acids in insulin resistance. *Lipids in Health and Disease*, *14*(1), 1–9.
- Semenkovich, C. F. (2006). Insulin resistance and atherosclerosis. *The Journal of Clinical Investigation*, *116*(7), 1813–1822.
- Shattat, G. F. (2014). A review article on hyperlipidemia: Types, treatments and new drug targets. *Biomedical and Pharmacology Journal*, *7*(2), 399–409. <https://doi.org/10.13005/bpj/504>
- Shattat, G. F. (2015). A review article on hyperlipidemia: types, treatments and new drug targets. *Biomedical and Pharmacology Journal*, *7*(1), 399–409.

- Shaulian, E., & Karin, M. (2001). AP-1 in cell proliferation and survival. *Oncogene*, 20(19), 2390–2400.
- Shaw, L. M. (2011). The insulin receptor substrate (IRS) proteins: at the intersection of metabolism and cancer. *Cell Cycle*, 10(11), 1750–1756.
- Shibata, Y., Voeltz, G. K., & Rapoport, T. A. (2006). Rough sheets and smooth tubules. *Cell*, 126(3), 435–439.
- Siddle, K. (2011). Signalling by insulin and IGF receptors: supporting acts and new players. *Journal of Molecular Endocrinology*, 47(1), R1–R10.
- Slaaby, R., Schaffer, L., Lautrup-Larsen, I., Andersen, A. S., Shaw, A. C., Mathiasen, I. S., & Brandt, J. (2006). Hybrid receptors formed by insulin receptor (IR) and insulin-like growth factor I receptor (IGF-IR) have low insulin and high IGF-1 affinity irrespective of the IR splice variant. *Journal of Biological Chemistry*, 281(36), 25869–25874.
- Solinas, G., & Becattini, B. (2017). JNK at the crossroad of obesity, insulin resistance, and cell stress response. *Molecular Metabolism*, 6(2), 174–184.
- Solinas, G., & Karin, M. (2010). JNK1 and IKK β : molecular links between obesity and metabolic dysfunction. *The FASEB Journal*, 24(8), 2596–2611.
- Stranahan, A. M., Norman, E. D., Lee, K., Cutler, R. G., Telljohann, R. S., Egan, J. M., & Mattson, M. P. (2008). Diet-induced insulin resistance impairs hippocampal synaptic plasticity and cognition in middle-aged rats. *Hippocampus*, 18(11), 1085–1088.
- Sun, X. J., Crimmins, D. L., Myers Jr, M. G., Miralpeix, M., & White, M. F. (1993). Pleiotropic insulin signals are engaged by multisite phosphorylation of IRS-1. *Molecular and Cellular Biology*, 13(12), 7418–7428.
- Sun, X. J., Rothenberg, P., Kahn, C. R., Backer, J. M., Araki, E., Wilden, P. A., Cahill, D. A., Goldstein, B. J., & White, M. F. (1991). Structure of the insulin receptor substrate IRS-1 defines a unique signal transduction protein. *Nature*, 352(6330), 73–77.
- Suzuki, R., Lee, K., Jing, E., Biddinger, S. B., McDonald, J. G., Montine, T. J., Craft, S., & Kahn, C. R. (2010). Diabetes and insulin in regulation of brain cholesterol metabolism. *Cell Metabolism*, 12(6), 567–579.
- Tabas, I., & Bornfeldt, K. E. (2016). Macrophage phenotype and function in different stages of atherosclerosis. *Circulation Research*, 118(4), 653–667.
- Thévenin, A. F., Zony, C. L., Bahnson, B. J., & Colman, R. F. (2011). Activation by phosphorylation and purification of human c-Jun N-terminal kinase (JNK) isoforms in milligram amounts. *Protein Expression and Purification*, 75(2), 138–146.
- Thirumangalakudi, L., Prakasam, A., Zhang, R., Bimonte-Nelson, H., Sambamurti, K., Kindy, M. S., & Bhat, N. R. (2008). High cholesterol-induced neuroinflammation and amyloid precursor protein processing correlate with loss of working memory in mice. *Journal of Neurochemistry*, 106(1), 475–485.
- Tirasophon, W., Welihinda, A. A., & Kaufman, R. J. (1998). A stress response pathway from the endoplasmic reticulum to the nucleus requires a novel bifunctional protein kinase/endoribonuclease (Ire1p) in mammalian cells.

- Genes & Development*, 12(12), 1812–1824.
- Tyagarajan, S. K., & Fritschy, J. (2010). GABAA receptors, gephyrin and homeostatic synaptic plasticity. *The Journal of Physiology*, 588(1), 101–106.
- Urano, F., Wang, X., Bertolotti, A., Zhang, Y., Chung, P., Harding, H. P., & Ron, D. (2000). Coupling of stress in the ER to activation of JNK protein kinases by transmembrane protein kinase IRE1. *Science*, 287(5453), 664–666.
- Uysal, K. T., Wiesbrock, S. M., Marino, M. W., & Hotamisligil, G. S. (1997). Protection from obesity-induced insulin resistance in mice lacking TNF- α function. *Nature*, 389(6651), 610–614.
- Vance, J. E. (2012). Dysregulation of cholesterol balance in the brain: contribution to neurodegenerative diseases. *Disease Models & Mechanisms*, 5(6), 746–755.
- Varela, L., & Horvath, T. L. (2012). Leptin and insulin pathways in POMC and AgRP neurons that modulate energy balance and glucose homeostasis. *EMBO Reports*, 13(12), 1079–1086.
- Ventre, J., Doebber, T., Wu, M., MacNaul, K., Stevens, K., Pasparakis, M., Kollias, G., & Moller, D. E. (1997). Targeted disruption of the tumor necrosis factor- α gene: metabolic consequences in obese and nonobese mice. *Diabetes*, 46(9), 1526–1531.
- Vergeer, M., Holleboom, A. G., Kastelein, J. J. P., & Kuivenhoven, J. A. (2010). The HDL hypothesis: does high-density lipoprotein protect from atherosclerosis? *Journal of Lipid Research*, 51(8), 2058–2073.
- Voliiovitch, H., Schindler, D. G., Hadari, Y. R., Taylor, S. I., Accili, D., & Zick, Y. (1995). Tyrosine phosphorylation of insulin receptor substrate-1 in vivo depends upon the presence of its pleckstrin homology region. *Journal of Biological Chemistry*, 270(30), 18083–18087.
- Walter, P., & Ron, D. (2011). The unfolded protein response: from stress pathway to homeostatic regulation. *Science*, 334(6059), 1081–1086.
- Wang, Y., Li, G., Goode, J., Paz, J. C., Ouyang, K., Sreaton, R., Fischer, W. H., Chen, J., Tabas, I., & Montminy, M. (2012). Inositol-1, 4, 5-trisphosphate receptor regulates hepatic gluconeogenesis in fasting and diabetes. *Nature*, 485(7396), 128–132.
- Wellen, K. E. (2005). hotamisligil GS. *Inflammation, Stress, Diabetes. J Clin Invest*, 115, 1111–1119.
- White, M. F. (2002). IRS proteins and the common path to diabetes. *American Journal of Physiology-Endocrinology And Metabolism*, 283(3), E413–E422.
- White, M., & Kahn, C. R. (2021). Insulin action at a molecular level—100 Years of progress. *Molecular Metabolism*, 101304.
- Whitmer, R. A., Gustafson, D. R., Barrett-Connor, E., Haan, M. N., Gunderson, E. P., & Yaffe, K. (2008). Central obesity and increased risk of dementia more than three decades later. *Neurology*, 71(14), 1057–1064.
- Wilden, P. A., Kahn, C. R., Siddle, K., & White, M. F. (1992). Insulin receptor kinase domain autophosphorylation regulates receptor enzymatic function. *Journal of Biological Chemistry*, 267(23), 16660–16668.
- Winocur, G., & Greenwood, C. E. (2005). Studies of the effects of high fat diets on

- cognitive function in a rat model. *Neurobiology of Aging*, 26(1), 46–49.
- Wirhns, O. (2017). Extraction of Soluble and Insoluble Protein Fractions from Mouse Brains and Spinal Cords. *Bio-Protocol*, 7, e2422.
- Woods, STEPHEN C, & Porte Jr, D. (1977). Relationship between plasma and cerebrospinal fluid insulin levels of dogs. *American Journal of Physiology-Endocrinology And Metabolism*, 233(4), E331.
- Woods, Stephen C, Seeley, R. J., Baskin, D. G., & Schwartz, M. W. (2003). Insulin and the blood-brain barrier. *Current Pharmaceutical Design*, 9(10), 795.
- Wotton, C. J., & Goldacre, M. J. (2014). Age at obesity and association with subsequent dementia: record linkage study. *Postgraduate Medical Journal*, 90(1068), 547–551.
- Wozniak, M., Rydzewski, B., Baker, S. P., & Raizada, M. K. (1993). The cellular and physiological actions of insulin in the central nervous system. *Neurochemistry International*, 22(1), 1–10.
- Wu, A., Ying, Z., & Gomez-Pinilla, F. (2004). The interplay between oxidative stress and brain-derived neurotrophic factor modulates the outcome of a saturated fat diet on synaptic plasticity and cognition. *European Journal of Neuroscience*, 19(7), 1699–1707.
- Wu, J., Tseng, Y. D., Xu, C.-F., Neubert, T. A., White, M. F., & Hubbard, S. R. (2008). Structural and biochemical characterization of the KRLB region in insulin receptor substrate-2. *Nature Structural & Molecular Biology*, 15(3), 251–258.
- Xu, Q.-H., Song, B.-J., Liu, D., Chen, Y.-H., Zhou, Y., Liu, W.-B., Li, H., Long, T.-L., Zhang, R., & Liu, W. (2018). The MKK7 inhibitor peptide GADD45 β -I attenuates ER stress-induced mitochondrial dysfunction in HT22 cells: involvement of JNK-Wnt pathway. *Brain Research*, 1691, 1–8.
- Yang, S., Wu, M., Li, X., Zhao, R., Zhao, Y., Liu, L., & Wang, S. (2020). Role of endoplasmic reticulum stress in atherosclerosis and its potential as a therapeutic target. *Oxidative Medicine and Cellular Longevity*, 2020.
- Yoshida, H., Okada, T., Haze, K., Yanagi, H., Yura, T., Negishi, M., & Mori, K. (2000). ATF6 activated by proteolysis binds in the presence of NF-Y (CBF) directly to the cis-acting element responsible for the mammalian unfolded protein response. *Molecular and Cellular Biology*, 20(18), 6755–6767.
- YUKSEL, H. (n.d.). Social Determinants of Obesity: The Case of Turkey. *Süleyman Demirel Üniversitesi Fen-Edebiyat Fakültesi Sosyal Bilimler Dergisi*, 48, 15–33.
- Zaid, H., Antonescu, C. N., Randhawa, V. K., & Klip, A. (2008). Insulin action on glucose transporters through molecular switches, tracks and tethers. *Biochemical Journal*, 413(2), 201–215.
- Zhang, S. H., Reddick, R. L., Piedrahita, J. A., & Maeda, N. (1992). Spontaneous hypercholesterolemia and arterial lesions in mice lacking apolipoprotein E. *Science*, 258(5081), 468–471.
- Zhang, W., Patil, S., Chauhan, B., Guo, S., Powell, D. R., Le, J., Klotsas, A., Matika, R., Xiao, X., & Franks, R. (2006). FoxO1 regulates multiple metabolic

- pathways in the liver: effects on gluconeogenic, glycolytic, and lipogenic gene expression. *Journal of Biological Chemistry*, 281(15), 10105–10117.
- Zhang, X., Zhang, G., Zhang, H., Karin, M., Bai, H., & Cai, D. (2008). Hypothalamic IKK β /NF- κ B and ER stress link overnutrition to energy imbalance and obesity. *Cell*, 135(1), 61–73.
- Zhao, X., Han, Q., Gang, X., & Wang, G. (2018). Altered brain metabolites in patients with diabetes mellitus and related complications—evidence from 1H MRS study. *Bioscience Reports*, 38(5).

APPENDICES

A. Chemicals, Brands and Product Numbers

Table A.1. Chemical Names, Their Brands and Product Numbers

Chemicals	Brands and Product Numbers
Acrylamide/Bis Solution, 29:1 (40% w/v), 3.3 % C	Serva, 10680.01
Albumin Bovine, Modified Cohn Fraction V, pH 7.0 lyophil	Serva, 11943.01
Bromophenol blue	AppliChem, A2331
Clarity Western ECL Substrate	Bio-Rad, 170-5061
Glycerol, Biotechnology Grade	BioShop, Cas#56-81-5
Glycine, Analytical Grade, Ph. Eur., USP	Serva, Cas# 56-40-6
Methanol	Isolab, 947.046.2500
PageRuler Plus Prestained Protein Ladder	Thermo Scientific, 26619
2-propanol	Sigma Aldrich, 24137
Sodium Chloride	Isolab, 969.036.1000
Sodium Dodecyl Sulfate (SDS)	Sigma, L4390
TEMED	Bio-Rad, 161-0800
Trizma Base	Sigma, T1503

B. Solutions and Their Preparations for Western Blotting

10% (w/v) SDS: 5.0 grams of SDS was dissolved in 50 mL distilled water and it was stored at room temperature.

10% Ammonium PerSulphate (APS) (AppliChem, A2941): 0.1 gram of APS was dissolved in 1 mL distilled water, and it was aliquoted and stored at -20 degrees Celsius. It was used immediately and was not re-used.

1M Tris-HCl, pH 8.8: 48 g Tris-base was dissolved in 300 mL of distilled water. Then, pH was adjusted to 8.8 by using 6N HCl. When pH was adjusted, total volume was completed to 400 mL. It was stored at 4 degrees Celsius.

1M Tris-HCl, pH 6.8: 12 g Tris-base was dissolved in 50 mL of distilled water. Then, pH was adjusted to 6.8 by using 6N HCl. When pH was adjusted, total volume was completed to 100 mL. It was stored at 4 degrees Celsius.

1% (w/v) Bromophenol blue: 0.1 g of Bromophenol blue was dissolved in 10 mL of distilled water. It was stored at room temperature.

10% Resolving Gel Preparation: 3.54 mL distilled water; 2.5 mL 40% Acrylamide/Bis (29:1); 3.77 mL 1 M Tris-HCl, pH 8.8; 100 μ l 10% SDS was mixed first, then 100 μ l 10% APS and 10 μ l TEMED were freshly added and mixed well by vortexing (Without APS and TEMED, stock was stored at 4 degrees Celsius).

5% Stacking Gel Preparation: 3.770 mL distilled water; 0.5 mL 40% Acrylamide/Bis (29:1); 0.625 mL 1 M Tris-HCl, pH 6.8; 10% SDS was mixed first, then 50 μ l APS and 5 μ l TEMED were freshly added and mixed well by vortexing (Without APS and TEMED, stock was stored at 4 degrees Celsius).

2X Sample Loading Buffer Preparation: 1 mL 1M Tris-HCl, pH 6.8; 4 mL 10% SDS; 2 mL glycerol; 500 μ l 1% bromophenol blue were mixed and stored at room temperature in a foiled tube. 10% beta-mercaptoethanol was added to the required amount of mixture in 1:3 ratio before using (1 volume of beta-mercaptoethanol and 3 volumes of loading buffer should be mixed).

10X SDS-PAGE Running Buffer Preparation: Prepared by dissolving 30 g Tris-base (25 mM), 144 g glycine (192 mM), 10 g SDS (0.1%) in 1000 mL autoclaved distilled water. When preparing this buffer, SDS should be added last. It was stored at 4 degrees Celsius. Working concentration will be 1X.

10X Transfer Buffer Preparation: Prepared by dissolving 30 g Tris base and 144 g glycine in 1000 mL autoclaved distilled water and stored at 4 degrees Celsius.

1X Transfer Buffer: 100 mL of 10X transfer buffer, 700 mL autoclaved distilled water and 200 mL methanol were mixed, and it should be prepared at most one day before the experiment and stored at 4 degrees Celsius.

10X TBS: Prepared by dissolving 24.2 g Tris base (100 mM), 80 g NaCl (1500 mM) in 800 mL autoclaved distilled water and pH was adjusted to 7.6 by using 3 N NaOH or HCl. Then, total volume was completed to 1 L. It was stored at room temperature.

TST-T: Prepared by mixing 70 mL 10X TBS, 630 mL autoclaved distilled water and 700 μ l Tween-20.

C. Whole Western Blot Images for Each Marker

IR- β

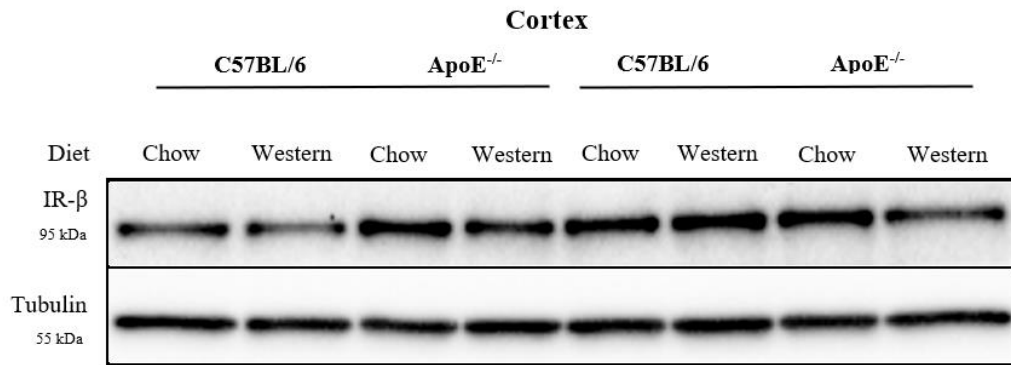


Figure C.1. Western blot image of anti-IR- β as whole blot

p-IRE1 α

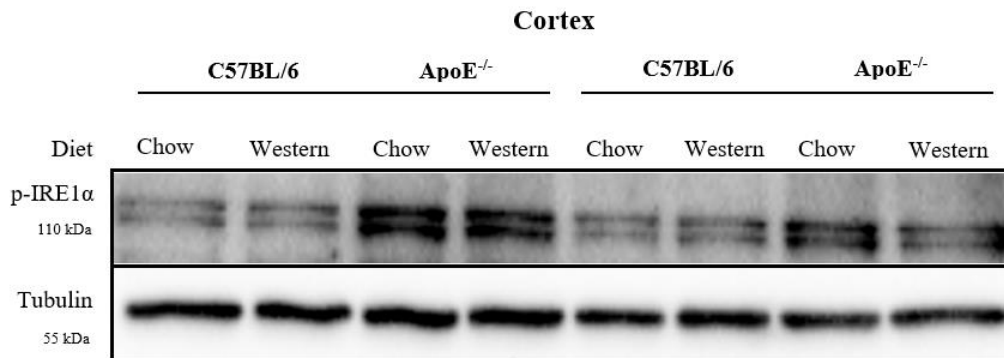


Figure C.2. Western blot image of anti-p-IRE1 α as whole blot

SAPK/JNK

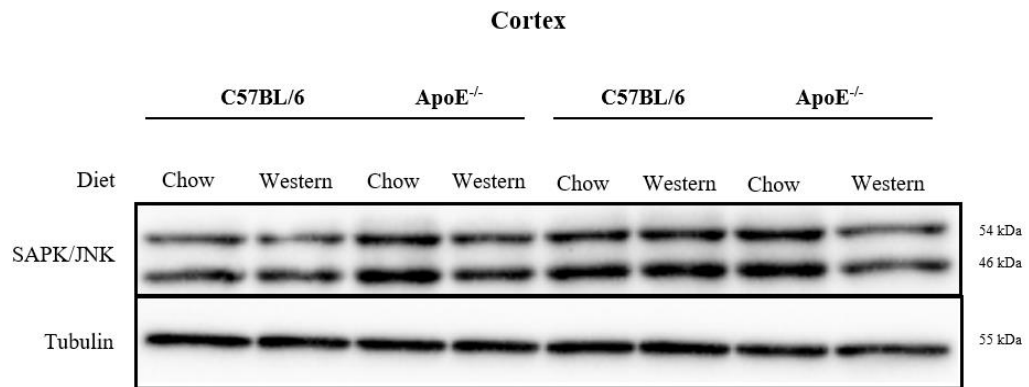


Figure C.3. Western blot image of anti-SAPK/JNK as whole blot

p-SAPK/JNK

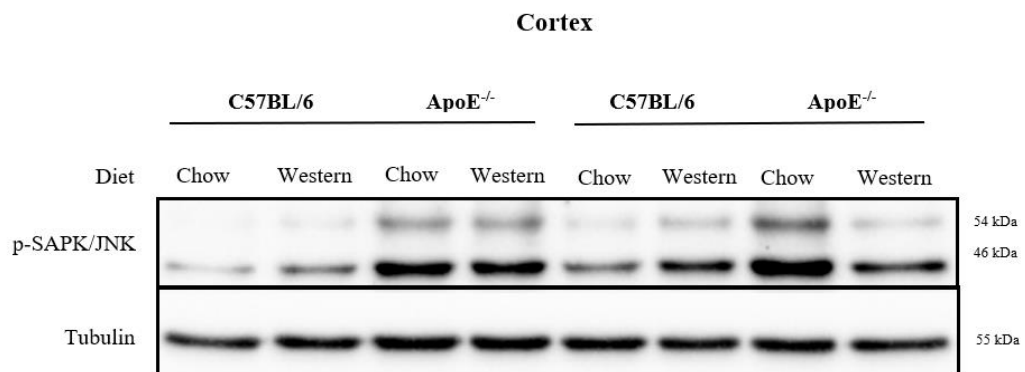


Figure C.4. Western blot image of anti-p-SAPK/JNK as whole blot

p-IRS-1

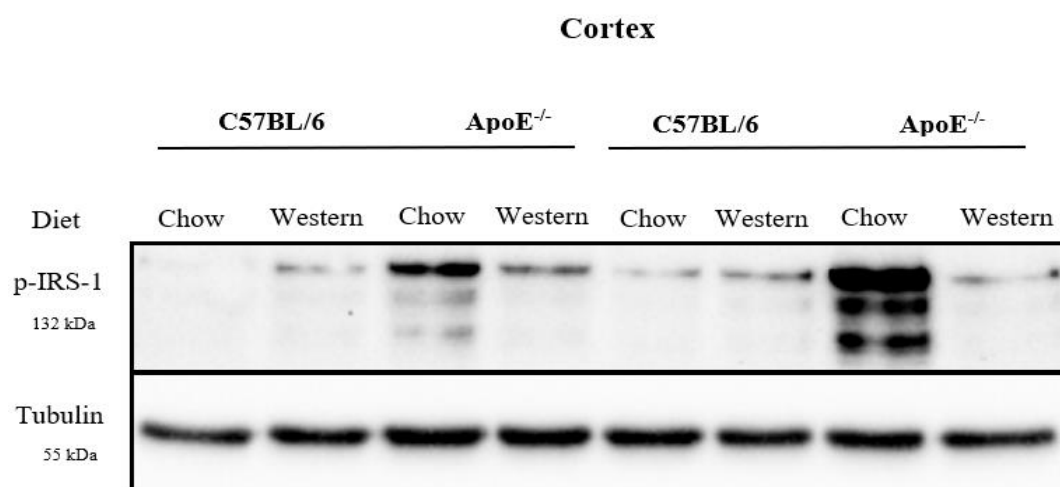


Figure C.5. Western blot image of anti-p-IRS-1 as whole blot

p-Akt

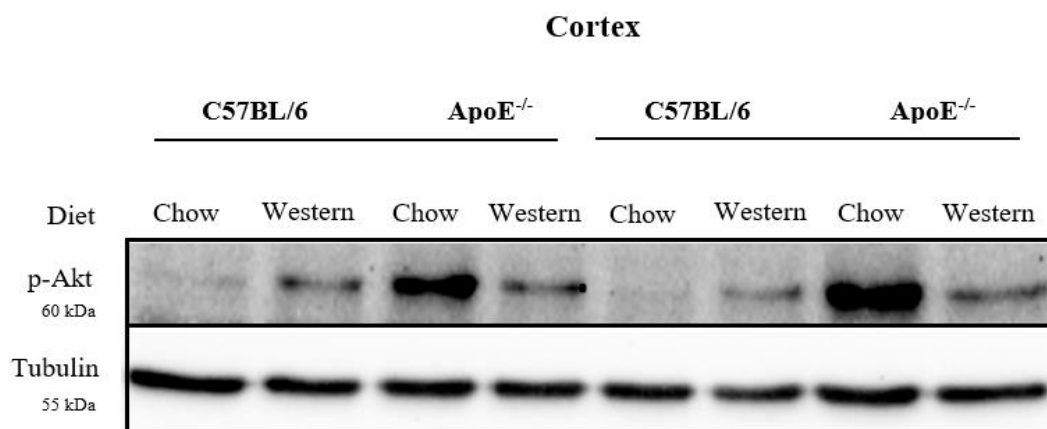


Figure C.6. Western blot image of anti-p-Akt as whole blot